



3 1293 00897 3178

This is to certify that the

thesis entitled


FUNCTIONAL GROUP EFFECTS IN THE CHEMISTRY
OF GAS-PHASE ALKALI IONS

presented by

Mary Louise Larrivee

has been accepted towards fulfillment
of the requirements for

M.S. degree in Chemistry


Major professor

Date May 3, 1990

**LIBRARY
Michigan State
University**

**PLACE IN RETURN BOX to remove this checkout from your record.
TO AVOID FINES return on or before date due.**

DATE DUE	DATE DUE	DATE DUE
SEP 6 1999 DATE 2 2000	_____	_____
_____	_____	_____
_____	_____	_____
_____	_____	_____
_____	_____	_____
_____	_____	_____
_____	_____	_____

MSU is An Affirmative Action/Equal Opportunity Institution

c:\circ\datedue.pm3-p.1

FUNCTIONAL GROUP EFFECTS IN THE CHEMISTRY
OF GAS-PHASE ALKALI IONS

BY

MARY LOUISE LARRIVEE

A THESIS

Submitted to
Michigan State University
in partial fulfillment of the requirement
for the degree of

MASTER OF SCIENCE

Department of Chemistry

1990

646-6456

ABSTRACT

FUNCTIONAL GROUP EFFECTS IN THE GAS-PHASE
CHEMISTRY OF ALKALI IONS

BY

Mary Louise Larrivee

The chemistry of alkali metal ions with organic molecules containing various functional groups has been studied in recent years. The observed products provide insights into basic questions of organometallic reactivity and mechanisms.

Two groups of organic compounds that have been studied are the alcohols and the alkyl halides. Alkali metal ions tend to induce

dehydrohalogenation and dehydration in alkyl halides and alcohols respectively.

This study involves the reactions of alkali metal ions, focusing on Li^+ , with various bromoalkanes and bifunctional molecules containing combinations of hydroxides and halides. Reaction products, as well as the determination of reactant-product relationships, are determined by Ion Cyclotron Resonance (ICR) Mass Spectrometry, using a frequency scanned detector (FSD).

This is dedicated to my parents
for all their prayers and continual support.
They give me the courage and the ambition
to not be a quitter.

ACKNOWLEDGMENTS

I would like to extend a very special thank-you to Dr. John Allison for all his guidance, time and especially his patience. The knowledge and the experience that I have gained by learning from him is a precious resource that I will use to further my academic and professional careers.

I would also like to thank Dr. Watson, Dr. Nocera, and Dr. Morrisey for serving on my committee. Their comments were most helpful.

I would finally like to thank "Bruno", the Ion Cyclotron Resonance Mass Spectrometer at MSU for holding out, and not dying before I was able to finish my research. Dr. Allison was right, research can still be accomplished with you.

TABLE OF CONTENTS

SECTION	PAGE
A. Theory of Ion Cyclotron Resonance Mass Spectrometry	1
1. Introduction	1
2. Non-resonant Ion Dynamics	1
3. Resonant Ion Dynamics	4
4. ICR Experimental Setup	6
5. Obtaining a Spectrum	12
B. Experiments Requiring Double Resonance	17
1. Excited States of Ni ⁺	17
2. Double Resonance	20
3. Resolution	24
C. Chemistry With Metal Ions	37
1. Benefits of Studying Gas/Phase Chemistry	37
2. Typical Reactions and Mechanisms	37
3. The Chemistry	41
a. Purpose	41
b. Experimental Methods	48
c. Experimental Results with the Indium Emitter	50
d. Discussion of the Results From the Indium Emitter	51
e. Experimental Results for Reactions of Li ⁺	55
f. Discussion of the Monofunctional Compounds with Lithium	65
g. Chemistry of Li ⁺ with Chloroalkanes	65
h. Monofunctional Alcohols Reacting with Li ⁺	79

i. Chemistry of Li ⁺ with Bromoalkanes	84
j. Chemistry of Li ⁺ With Bifunctional Molecules	92
k. Chemistry of Li ⁺ With α,ω -bromo, chloroalkanes	94
l. Chemistry of Li ⁺ With α,ω -bromo-alcolols	110
m. Chemistry of Li ⁺ With α,ω -chloro-alcolols	116
n. Conclusions	124
APPENDIX A	126
APPENDIX B	136
APPENDIX C	138
ADDENDIX D	141
List of References	149

LIST OF TABLES

TABLE	PAGE
Table 1 Reactions of Ni^+ from 3 compounds with various organic molecules	18
Table 2a Compilation of successful reactions involving Li^+ , and Na^+	42
Table 2b Compilation of unsuccessful reactions involving Li^+ , and Na^+	44
Table 3 Estimated ionic radius of various metal ions	55
Table 4 Compilation of reactions, and branching ratios	56
Table 5 List of the alkyl and alkali cations, and their chloride affinities	68
Table 6 List of the alkyl and alkali cations, and their hydroxide affinities	80
Table 7 List of the alkyl and alkali cations, and their bromide affinities	86
Table 8 Previous work with bifunctional molecules, and alkali metal ions	93

LIST OF FIGURES

Figure	Page
Figure 1 Relationship of drift velocity, magnetic field, and electric field	3
Figure 2 Ion motion through a cell for resonant ions, $\omega_1 = \omega_c$	5
Figure 3 Ion motion through a cell for non-resonant ions, $\omega_1 \neq \omega_c$	5
Figure 4 Block diagram of an ICR experimental setup	7
Figure 5 Cutaway View of an ICR cell	8
Figure 6 Circuitry diagram for the Frequency Scanned Detector	10
Figure 7 Various powers used to irradiate an ion	15
Figure 8 Double resonance spectra of $\text{Co}(\text{CO})_3\text{NO}$	22
Figure 9 First derivative spike as a result of mismatched peaks	25
Figure 10 Effects of mismatched peaks	25
Figure 11 Voltage incrementation vs. time	27

Figure 12	Frequency incrementation vs. time	27
Figure 13	Actual stepping of frequency in time vs. theoretical stepping	29
Figure 14	Actual peak shape vs. an ideal gaussian peak shape	30
Figure 15	A peak obtained with a normal frequency range	32
Figure 16	A peak obtained with the frequency range decreased by one third	32
Figure 17	Plot resulting from $m/z=87$ being irradiated	35
Figure 18a	Potential energy surface with no barrier	54
Figure 18b	Potential energy surface with a barrier	54
Figure 19	Chloride affinities	71
Figure 20	Bromide affinities	73
Figure 21	Hydroxide affinities	74
Figure 22	Potential energy diagram for Li^+ and isopropyl chloride	77
Figure 23	Potential energy diagram for Li^+ and t-butanol	83
Figure 24	Potential energy diagram for Li^+ and isopropyl bromide	87
Figure 25	Potential energy diagram for Li^+ and t-butyl bromide	90
Figure 26	Potential energy diagram for Li^+ and α,ω -chloro,bromobutane	95
Figure 27	Various ways to represent the early stages of a reaction	99

Figure 28	Potential energy diagram for Li^+ , and α,ω -bromobutanol	115
Figure 29	Potential energy diagram for Li^+ , and α,ω -chlorobutanol	120
Figure 30	Spectra of Li^+ and 4-bromo-1-butanol	137

LIST OF SCHEME

SCHEME	PAGE
Scheme 1	41
Scheme 2	66
Scheme 3	70

A. THEORY OF ION CYCLOTRON RESONANCE MASS SPECTROMETRY

1. INTRODUCTION

Ion cyclotron resonance (ICR) spectrometry is a widely accepted experimental technique for the study of gaseous ion/molecule reactions. Varian Associates in 1966 built the first ion cyclotron mass spectrometer, based on the work of Hipple, Sommer, and Thomas, who built an omegatron in 1949. The omegatron was used to determine the mass-to-charge ratio of the proton¹, and also was used as a residual gas analyzer. This relatively new technique has been extensively reviewed in the literature²⁻⁶. This technique allows ion/molecule reactions to be studied, by measuring the frequency of ion motion in a magnetic field. Ion/molecule reactions occur because the ions are trapped in the reaction region of a cell for several milliseconds, thereby providing the opportunity for many collisions between ions and molecules. Through the use of experiments such as ion ejection and double resonance, the user is able to obtain information such as precursor-product relationships.

2. NON-RESONANT ION DYNAMICS

ICR is based on the behavior of a charged particle in a magnetic field (\mathbf{B}), and electric fields (\mathbf{E})⁶. Vectors will be expressed in **bold**. A free charged particle in a uniform magnetic

field is confined to a circular orbit with a precessing frequency, ω_c , in a plane normal to \mathbf{B} . The motion of the particle is unrestricted in the dimension (or coordinate) parallel to \mathbf{B} . Ions, in the presence of a perpendicular electric and magnetic fields, experience a force which causes them to move in a direction perpendicular to both the electric and the magnetic fields, through the cell with a velocity v_d , given as:

$$v_d = l/\partial = E/B$$

where l is the length of the analyzer region, and ∂ is the time spent in the analyzer region³. The relationship between the three vectors can be seen in Figure 1.

The force can be expressed as follows:

$$F = (q/c)(v \times B) = qvB/c$$

where v is the velocity component of the ion normal to \mathbf{B} , \mathbf{B} is the uniform magnetic field, v is the speed of the ion, c is the speed of light, q is the charge of the particle, and B is the magnetic flux density. This force will move a particle, in a circular motion, in a plane normal to the magnetic and electric fields, so it follows that:

$$mv^2/r = qvB/c$$

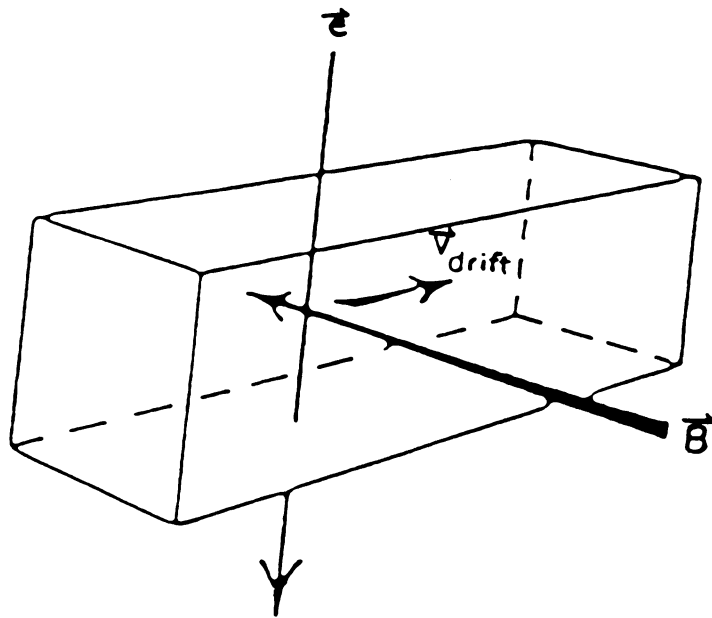


Figure 1 Relationship of drift velocity, magnetic field, and electric field

where mv^2/r is the centrifugal force on the ion, and r is the radius of the orbit. If the above equation is rearranged, it follows that the cyclotron frequency is given by:

$$\omega_c = v/r = qB/mc$$

where m is the mass of a particle, and ω_c is the natural cyclotron frequency of an ion in the presence of a particular B . The circular motion that the ions traverse in the cell is due to the cyclotron frequency (expressed above in radians/sec). This motion is normal to the magnetic field².

3. RESONANT ION DYNAMICS

Ions of a particular m/z will absorb energy when radio-frequency radiation with a frequency, ω_1 , is applied to the drift plates of the cell, and it is equal to ω_c of that ion. When $\omega_1 = \omega_c$ the ions absorb energy from the radio-frequency radiation and gain kinetic energy. This power absorption causes the ions to become accelerated to larger velocities and therefore, larger orbital radii. The path that these ions take can be seen in Figure 2. This energy absorption can be large enough to cause the ions to be swept out of the cell, i.e., to collide with the walls of the cell.

When $\omega_1 \neq \omega_c$, as is the case for non-resonant ions, no power absorption occurs and the ions follow the path shown in Figure 3. The absorption of power from radio-frequency radiation by the ions

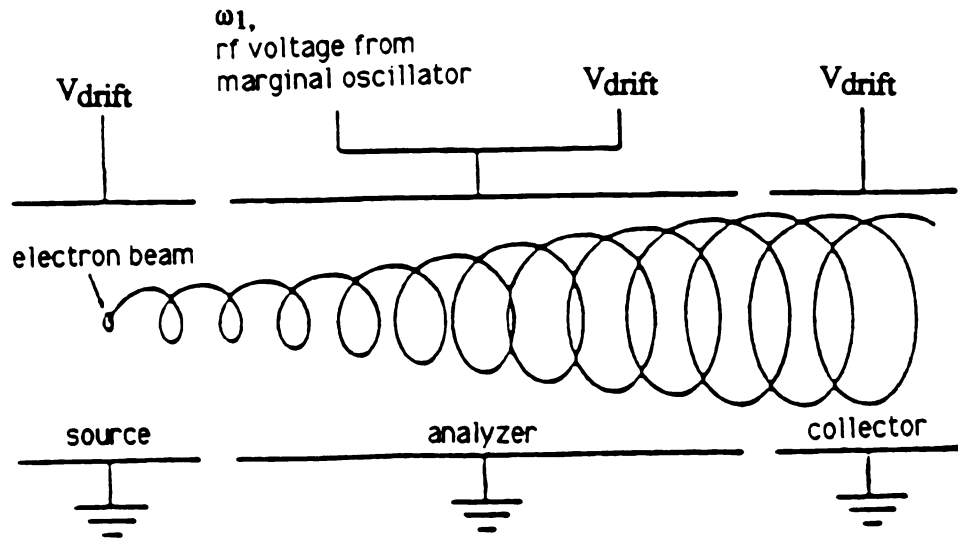


Figure 2 Ion motion through a cell for resonant ions, $\omega_1 = \omega_c$

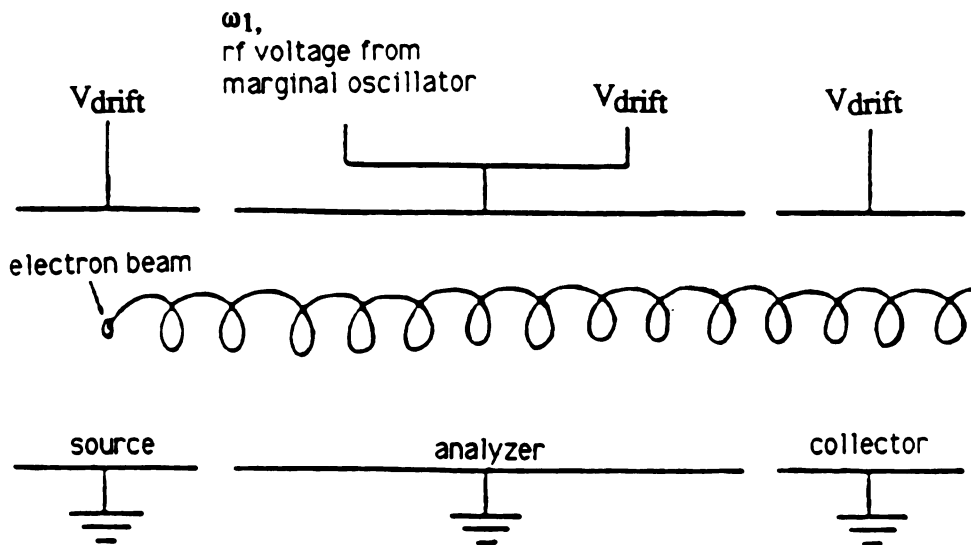


Figure 3 Ion motion through a cell for non-resonant ions, $\omega_1 \neq \omega_c$

causes the power from the energy source to change; this change can then be detected, as will be discussed later, through the use of a phase sensitive detector, the ratio of the signal-to-noise for this measurement can be enhanced⁷.

4. ICR EXPERIMENTAL SETUP

Figure 4 shows a block diagram of the ICR's experimental setup which includes the frequency scanned detector (FSD). It can be noted from Figure 4 that the ICR cell is placed between the two polecaps of an electromagnet. This cell is seated in a stainless steel canister, in which the base pressure is approximately 10^{-7} torr.

The ICR cell is shown in Figure 5⁸. A typical ICR cell has three sections to it. There is a source region, an analyzer region, and a collector region. Electrons are emitted from a rhenium wire filament when the filament is heated. The filament current is controlled from outside of the cell, and can be varied from 0-5 amperes. The electrons are collimated into a beam by the influence of the magnetic field. The electrons are accelerated towards the collector plate by imposing a negative potential on the filament. The number of electrons hitting the collector is measured as the emission current. This current is part of a feedback loop which allows for the electron current to be held at a constant value. When a neutral molecule interacts with this electron beam, it causes some of the molecules to become ionized such that:

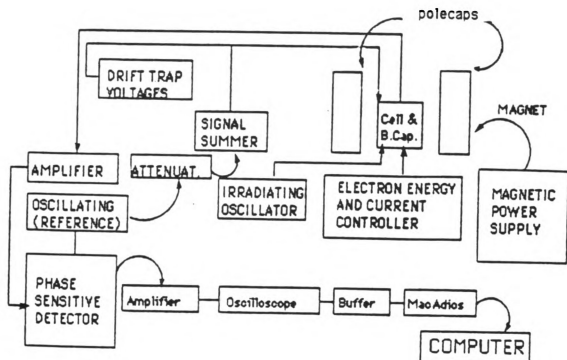


Figure 4 Block diagram of an ICR experimental setup

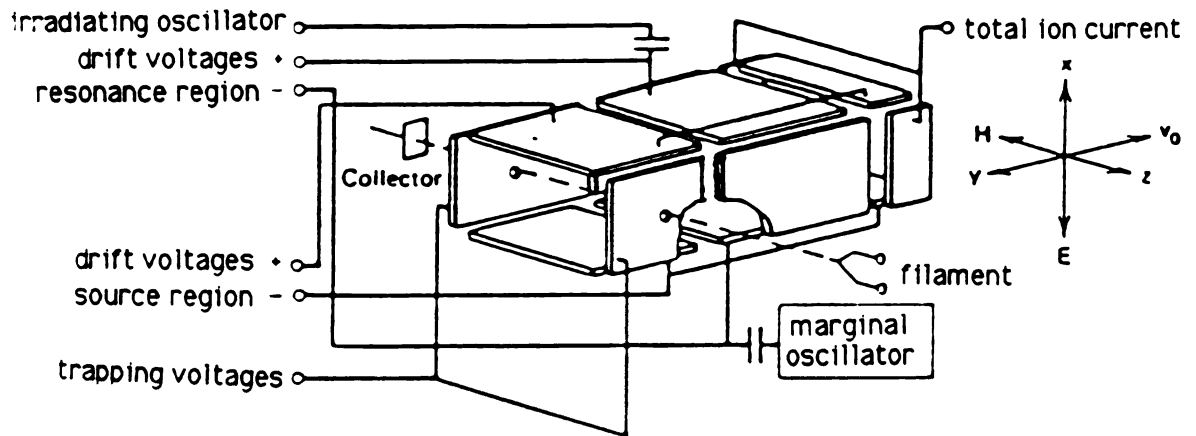


Figure 5 Cutaway View of an ICR cell



Once ionized, the ions will drift in a cycloidal path through the cell. To keep the ions from colliding with the sides of the cell, a trapping potential is applied. A trapping potential is a positive potential, $< .5$ volts. It has the same sign as the charge on the ions, and it is applied to the trapping plates during the ion's cycloidal path. An oscillating electric field, w_1 , is then applied to either the source, or the analyzer region. An alternating electric field is applied to the cell. As energy is absorbed from this field, when $w_1 = w_c$, this power loss is detected by the frequency-scanned detector.

Frequency-scanned detection (FSD) has been used by Wobschall as early as 1963⁹. The FSD used in our laboratory was built by Dr. John Wronka⁹. Figure 6 provides the FSD's circuit diagram. Figure 4 shows the block diagram for the experimental setup using the FSD. The following describes how a FSD works.

In this experiment a fixed magnetic field is used. A radio-frequency (rf) source, such as a function generator, generates a sine wave. This sine wave goes to a signal summer where it is split into two equal intensity, but 180°-out-of-phase, sine waves. One of these sine waves is then sent into the ICR cell, and the complementary signal goes through the balance capacitor. The two sine waves are joined once again at a null point, which acts to compare the two sine waves. When $w_1 = w_c$ (i.e, the frequency of a

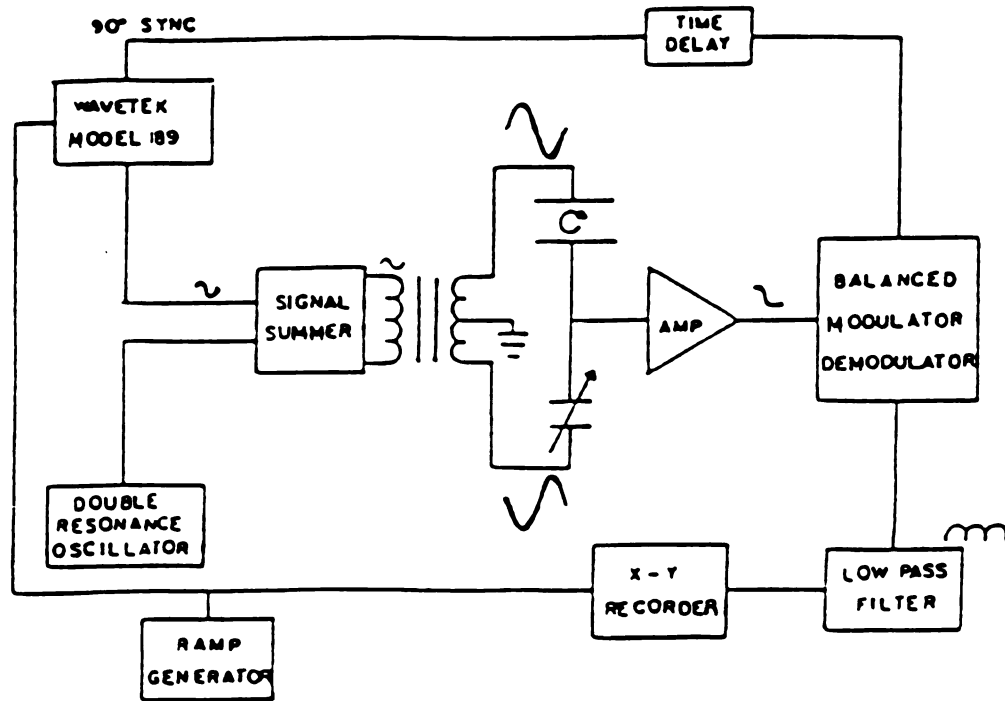


Figure 6 Circuitry diagram for the Frequency-Scanned Detector

precessing ion matches the frequency of the rf source) power absorption will affect the balance of this bridge and a voltage at the cyclotron frequency will be developed at the null point, since power was absorbed from the rf field¹⁰. From here, the signal is amplified 101 times by the preamplifier and sent to the phase-sensitive detector, which compares the signal to a reference signal of the same frequency as the excitation source. The generated information is in the form of power absorption vs. frequency. At resonance, the peak height is proportional to the power absorption as follows:

$$A(\omega_C) = \frac{1e^2 E^2 \partial^2}{8m}$$

where m/e is the mass-to-charge ratio, l is the number of ions, of a particular m/e value, in the analyzer region, ∂ is the number of ions entering or leaving the analyzer region, and E is the radio-frequency field strength³. Therefore, a mass spectrum resulting as a plot of the intensity of the power absorbed vs. frequency. The resolution in an ICR mass spectrum can be determined as follows:

$$R = \omega_C / \Delta \omega_{1/2}$$

where ω_C is the cyclotron resonance frequency, and $\Delta \omega_{1/2}$ is the half-width of the peak in frequency units at half of the maximum height. This equation has been shown to approximately equal $2.78/\partial$, where ∂ is the time during which the ions absorb energy. If ∂ is the time for the ions to traverse the analyzer region of the cell, it follows that:

$$R = w_C / \Delta w_{1/2} = \partial Be / 2.78m = 1B^2e / 2.78Em$$

since $w_C = eB/m$, and $v_d = 1/\partial = E/B$.

5. OBTAINING A SPECTRUM

All of the components of the ICR mass spectrometer must be turned on, and operating correctly at their appropriate settings. The block diagram in Figure 4 shows how all of the components of the ICR are to be connected. A mass range of interest is set by choosing the appropriate frequency range with the start and stop controls of the function generator. Generally, a mass range of 50 a.m.u. to 250 a.m.u. provides a useful range for many of the ion/molecule reactions studied by ICR. This corresponds to a frequency range of 115 kHz to 576 kHz, at a constant magnetic field of 18.80 kilogauss. The spectrum should be observed on the oscilloscope, when the sweep time/cm is set on channel B, at a scan rate of 0.1 second.

A gas sample is admitted into the cell by leak valves. The amount of gas that enters the cell can be monitored with the Veeco RG1000 Ionization Gauge located on the control panel. A good pressure to achieve with one gas being admitted is 5.0×10^{-6} Torr. With a mixture of gases being admitted, the total pressure should not exceed 1.0×10^{-5} Torr. The filament is turned on by flipping the appropriately labeled switches on the control panels. A current of 0-3 amperes, depending on the diameter of the rhenium wire being used, can be passed through the filament by turning the knob under

the current meter. Peaks may, or may not, be seen at this point. In either case, tuning up is required. Tuning up means that the voltages on the cell's plates are adjusted until the peaks are optimized in shape and intensity, and a good quality spectrum is obtained. In general, the trapping plates voltage are held at approximately 2 volts and the drift plates should be under .5 volts.

For a single resonance mass spectrum, data can be collected in arrays called "waves". The single resonance program "Sires", is selected by double clicking on it, with the computer's mouse. I wrote "Siress" to facilitate data collection. This will automatically start the program. "Siress" is listed in Appendix A. To make sure that the program is in fact collecting data, the transfer light on the digital-to-analog converter will flash to signify that data are being collected. When the program is completed, signified with a beep, the spectrum is ready to be displayed on the monitor. The MacManager 411 software does have graphic capabilities, so this mode should be opened by double clicking on "MM411". The spectrum is loaded from MicroSoft Basic onto the view-four window where it can be manipulated, and printed.

Taking a double resonance spectrum is only a little different. Double resonance is a technique used to obtain a precursor-product relationship between the ions in a spectrum. A second frequency source is used to eject a precursor, or reactant ions from the cell, so that its effect on the product distribution can be observed. This technique will be discussed in much more detail later. Before doing

a double resonance experiment, it is necessary to make sure that the Wavetek's main frequency dial is set to the frequency correlating to the mass to be irradiated. To do this take 1530, (a constant associated with the irradiating frequency source and the magnet), and multiply it by the magnetic field. This product number is then divided by the mass to be irradiated. The equation is as follows:

$$1530 \times (B) / (m/z) = \nu$$

This resulting number is the frequency related to the mass of interest. The Wavetek can be placed on "Continuous" mode to make sure that the power "blip" is sitting on top of the desired peak, which will correspond to the frequency that was just calculated. If the "blip" is not completely covering the peak, it is necessary to adjust the power to change its amplitude, so that all the ions of a particular mass interest are completely removed from the cell. For a further explanation, see Figure 7. The top spectrum, 7a, displays a mass spectrum which will represent the peak of interest to be irradiated. The middle spectrum, 7b, shows a peak not completely irradiated, due to insufficient power. Spectrum 7c shows a peak with sufficient power to be irradiated completely. Turn the Wavetek from the "continuous" mode back to the "gated" mode. In this mode, the computer will control the Wavetek. This allows the user to obtain two spectra in two separate sweeps. One sweep will be taken when no peaks are irradiated, and the other sweep will be taken when an ion of interest will be irradiated. The program that

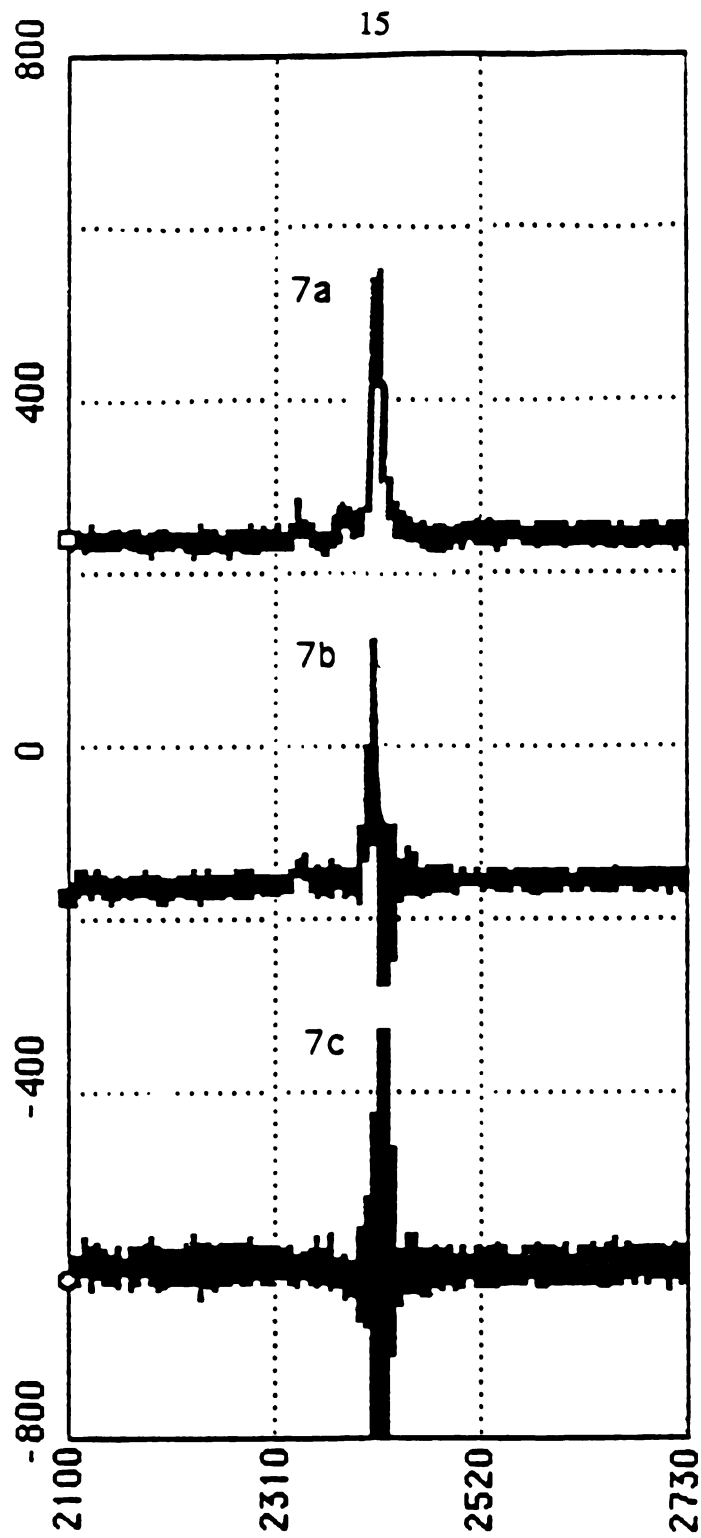


Figure 7 Various powers used to irradiate an ion

collects double resonance data, is started by double clicking on "Doubres". "Doubres" was written by me, and I have provided a listing of the program in Appendix A. Data transfer can be confirmed by making sure that the transfer light is blinking on the digital to analog converter. Quit MicroSoft Basic when the program is completed, and open MacManager 411 to display the spectrum in MM411's graphics window, View 4.

B. EXPERIMENTS REQUIRING DOUBLE RESONANCE

1. EXCITED STATES of Ni⁺

My original project was to investigate state-specific reactions of nickel ions. There is strong evidence to suggest that it is possible to create different excited states of Ni⁺, by using electron impact on different compounds that contain nickel. Preliminary work done in this lab¹¹ suggests that different metal compounds could produce metal ions in different states. This study observed the products when Ni⁺ from three different compounds, Ni(CO)₄, Ni(PF₃)₄, and NiCpNO, was reacted with organic compounds such as iodobenzene, benzyl alcohol, methyl benzyl alcohol, and nitrobenzene. The results are listed in Table 1.

It appears that Ni⁺ from both Ni(CO)₄ and Ni(PF₃)₄ is able to react with C₆H₅I to produce NiC₆H₄⁺ and NiC₆H₅⁺ in similar ratios. Note, however, that when Ni(CO)₄ was the nickel ion source, only NiC₆H₅I⁺ was produced. Also studied were the reactions of the three nickel ions with nitrobenzene and methyl benzyl alcohol. It became clear that, although the same products were produced when Ni(CO)₄ was the metal ion source, the products were not present in the same ratio as those produced by Ni(PF₃)₄, and NiCpNO. It was also shown that, when the three nickel ions reacted with benzyl alcohol, one of the products was NiC₆H₅CHO⁺. Note, however, that

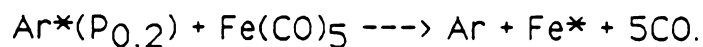
Table 1 Reactions of Ni⁺ from 3 compounds with various organic molecules

	<u>Ni⁺ from Ni(CO)₄</u>	<u>Ni⁺ from Ni(PF₃)₄</u>	<u>Ni⁺ from NiCoNO</u>
C ₆ H ₅ I	NiC ₆ H ₄ ⁺ (45%) NiC ₆ H ₅ ⁺ (55%)	NiC ₆ H ₄ ⁺ (37%) NiC ₆ H ₅ ⁺ (63%)	NiP ⁺ (100%)
PhNO ₂	NiC ₅ H ₅ ⁺ (84%) NiC ₆ H ₅ O ⁺ (16%)	NiC ₅ H ₅ ⁺ (86%) NiC ₆ H ₅ O ⁺ (14%)	NiC ₅ H ₅ ⁺ (52%) NiC ₆ H ₅ O ⁺ (26%) NiP ⁺ (21%)
PhCH ₂ OH	C ₇ H ₇ ⁺ (75%) NiPhCHO ⁺ (25%)	C ₇ H ₇ ⁺ (85%) NiPhCHO ⁺ (15%)	NiPhCHO ⁺ (100%)
PhCHOHCH ₃	NiPhCH ₃ ⁺ (69%) NiPhCHCH ₂ ⁺ (31%)	NiPhCH ₃ ⁺ (52%) NiPhCHCH ₂ ⁺ (48%)	NiPhCH ₃ ⁺ (24%) NiPhCHCH ₂ ⁺ (76%)

the Ni^+ from $\text{Ni}(\text{CO})_4$ formed 100% of $\text{NiC}_6\text{H}_5\text{CHO}^+$. The other two sources of nickel ions produced only small amounts of this product. The second product that was formed more substantially by Ni^+ from $\text{Ni}(\text{PF}_3)_4$ and NiCpNO was C_7H_7^+ .

Due to the different products and the different ratios of products that were formed, it is apparent that the nickel ions produced by electron impact were different, depending on the compound that produced them. These results suggest that a means to explore state-specific reactions involving nickel ions is warranted. If the Ni^+ ions were in the same electronic state, then the same products and the same ratios should have been observed.

A publication by Hartman and Winn, in 1978¹², provides the first evidence that a metal-containing compound can produce different states of a metal in addition to that of the ground state. This paper reports the first chemiluminescence, which resulted from collisional electronic energy transfer to a metal carbonyl, $\text{Fe}(\text{CO})_5$. The following reaction was observed:



The results showed that when all of the carbonyl ligands were removed from iron pentacarbonyl, many excited states of the iron atom resulted. This publication suggests that nickel compounds would react in a similar manner, in that different nickel compounds

would give different states of the nickel ion, but further work was necessary to prove this.

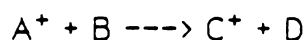
To determine which state the nickel ion is in, the ionization potential (I.P.) of the various excited states of the nickel ion needed to be obtained, as well as the I.P. for various compounds. The compounds need to be chosen so that they range in I.P. from below that of the lowest excited state of Ni^+ to above the I.P. of the highest excited state of Ni^+ under consideration. To determine the state of the Ni^+ , a charge transfer reaction is employed. A given charge transfer reaction will occur, when the Ni^+ is reacted with the neutral molecule, if the I.P. of the Ni^+ is larger than the I.P. of the compound in question. Likewise, no charge transfer reaction will occur if the I.P. of the compound employed is larger than that of the Ni^+ . Therefore, by charge transfer reactions, it is possible to determine the state of the nickel ion.

To determine if a charge transfer reaction occurred, the technique of double resonance would be employed.

2. DOUBLE RESONANCE

Double resonance is a technique used to study ion/molecule reactions. This allows the user to establish a reactant ion/product ion relationship³. Beauchamp and Armstrong showed that if a radio frequency field is applied to the trapping plates of the ICR cell at

the cyclotron frequency of a particular reactant ion, those ions can be ejected from the ICR cell. If a reactant ion A^+ is ejected, by supplying the ion with rf power at its cyclotron frequency, ω_C , then a change will occur in the concentration of the product ion C^+ if it is coupled to A^+ through a chemical reaction:



The intensity of the peak that represents C^+ will then undergo a decrease in intensity, which relates to the amount contributed from the reactant ion, A^+ . Therefore, complete elimination of a reactant ion, of a specific m/z , from the cell will allow one to determine the effect of this specific reactant on the product distribution. Not only does double resonance provide information into reaction pathways, reaction rates may also be determined by observing the intensity of the product ions⁴.

The following is an example of a double resonance experiment performed with the ICR mass spectrometer at MSU. The compound employed was $\text{Co}(\text{CO})_3\text{NO}$, and the ion of $m/z=87$, $\text{Co}(\text{CO})^+$, was irradiated and ejected. A spectrum of $\text{Co}(\text{CO})_3\text{NO}$ is first taken by single resonance methods. This spectrum can be seen in Figure 8a. Next, 8b shows a spectrum that was obtained while the fixed oscillator was set to irradiate $m/z=87$. These two spectra are then subtracted by a subtraction program on the Macintosh computer. The results can be viewed in Figure 8c. The net spectrum reveals all of

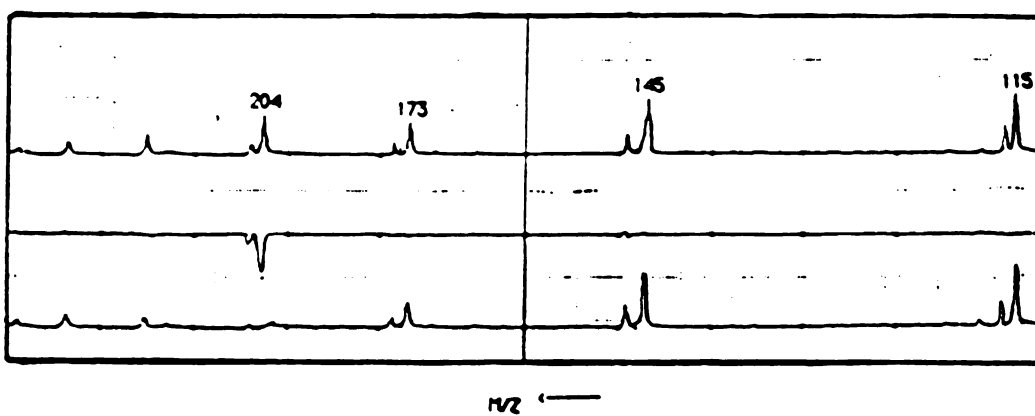
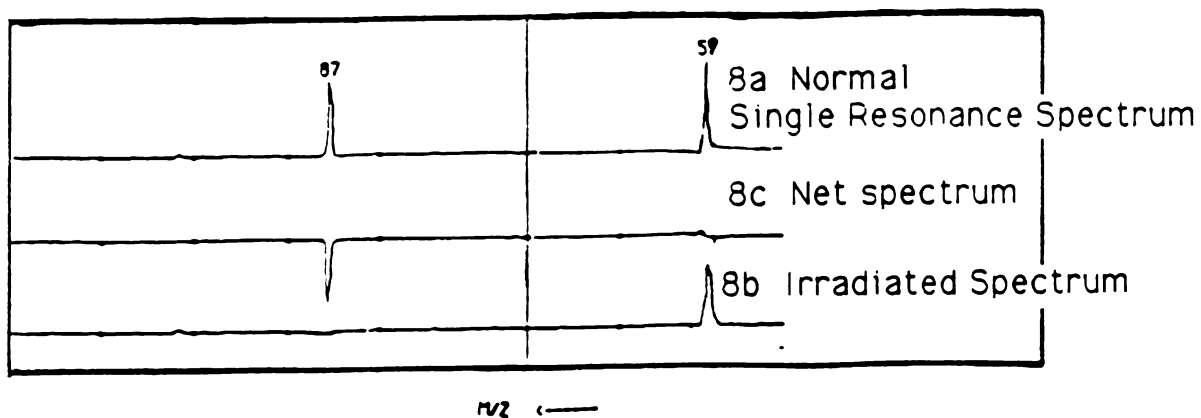


Figure 8 Double resonance spectra of $\text{Co}(\text{CO})_3\text{NO}$
 8a Normal Single Resonance Spectra
 8b Irradiated Spectra
 8c Net spectrum

the products of the irradiated ion. The intensity of the subtracted peak indicated how much of each product peak is a result of the ion irradiated. It is possible, to have more than one reactant ion produce a particular product ion. For example, it is known that both $m/z=115$, ($\text{Co(CO)}^+ + \text{Co(CO)}_3\text{NO} \rightarrow \text{Co(CO)}_2^+ + \text{Co(CO)}_2\text{NO}$), and $m/z=143$, ($\text{Co(CO)}^+ + \text{Co(CO)}_3\text{NO} \rightarrow \text{Co(CO)}_3^+ + \text{Co(CO)NO}$), are formed by $m/z=59$. To determine if they are solely a product of $m/z=59$, or a product of two or more reactants, observe the net spectra to provide this information. An analysis of the difference in the peak area between the single resonance mass spectra, and the net spectra, would provide information about the actual percentage of the product formed from the reactant under investigation. If the intensity of the subtracted peaks in the net spectrum are smaller than their respective peaks in the mass spectrum, then they are formed from more than one reactant peak.

As explained, a qualitative, and semi-quantitative study of ion/molecule reactions can be easily conducted using double resonance. This is possible since translational energies of reactant ions are only slightly in excess of thermal energy, so only the products of thermoneutral and exothermic ion/molecule reactions are observed. Because of this, it is easy to obtain data of thermodynamic interest such as proton affinities, hydrogen affinities, relative gas phase acidities, and electron affinities³.

In theory, with the computer software, and the necessary instrumentation available to do double resonance, the actual data accumulation should be trivial. However, when the actual data were being collected, many problems to be discussed in the next section arose, which prevented the experiments, as planned, to be performed successfully.

3. RESOLUTION

The software first employed to conduct double resonance experiments was the program "scanner" written by Richard Stepnowski. This method of data collection proved unsuccessful for three reasons: The first two were that the resolution, and the peak shape, of a spectrum needed to be improved. The third reason, was that when trying to do double resonance experiments the subtracted net spectra contained many first derivative-like responses as a result of mismatched peaks. Mismatched peaks can be shown in Figure 9. Figure 10 contains an actual mass spectrum, where the effect of mismatched peaks can be observed. Scan three is subtracted from scan one, and the resulting subtracted spectra, with the first derivative-like spikes are seen in scan two. Appendix A contains the program "scanner", as well as a listing of the program. The following is an example of how the experiments were set up.

The MacAdios has 12-bit analog inputs, and outputs, and a range of -10 to +10 Volts. The MacAdios steps along this 20 volt

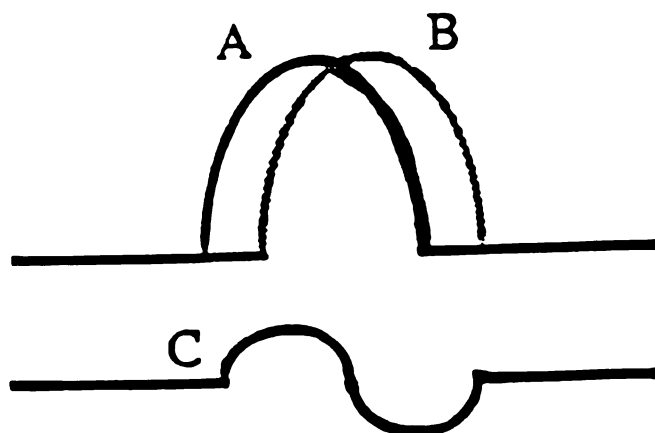


Figure 9 First derivative spike as a result of mismatched peaks
First Derivative Spike=C; Mismatched Peaks=(A & B)

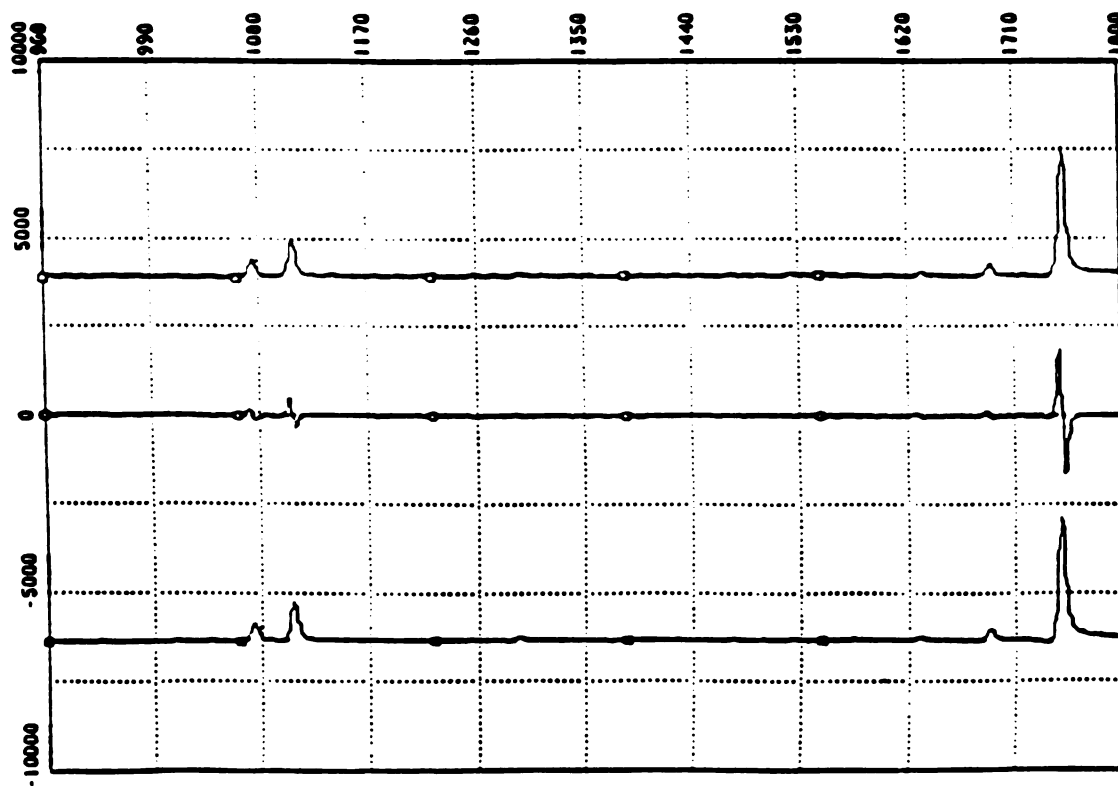


Figure 10 Effects of mismatched peaks

range in increments of 4.88 millivolts. See Figure 11 for an example of how incrementation occurs. Scanner was generally used with a 15 volt range. This means that only 3150 points were available to represent an entire spectrum, which represents a frequency range of approximately 500 kHz. Since both the voltage range, and the 4.88 millivolt increment, are inherent to the MacAdios, the maximum number of points could never exceed 4096 points. Therefore, to improve resolution and peak shape, a viable solution does not include obtaining a spectrum with more points, as long as the spectrum was being collected with the MacAdios.

The program "scanner" contained an integration step, to account for the low resolution which resulted because the computer only collected 3150 points. To maximize the signal-to-noise, the solution first employed was to vary the number of points integrated. The integration step in the program "scanner" collected twelve points at each frequency step, and averaged them to represent a single point. The number of points were varied from six to eighteen, and the signal-to-noise ratio was calculated. Since there was not much difference in the results, the twelve-point integration step was retained. The way the integration step works is as follows: When the MacAdios does a 4.88 millivolt step, it causes a step in frequency to occur also. See Figure 12. Once a step in the voltage, and frequency occurred, twelve points are sampled and averaged to represent one point in the spectrum. Part of the problem was that there is a time lag associated with this voltage step, so that all

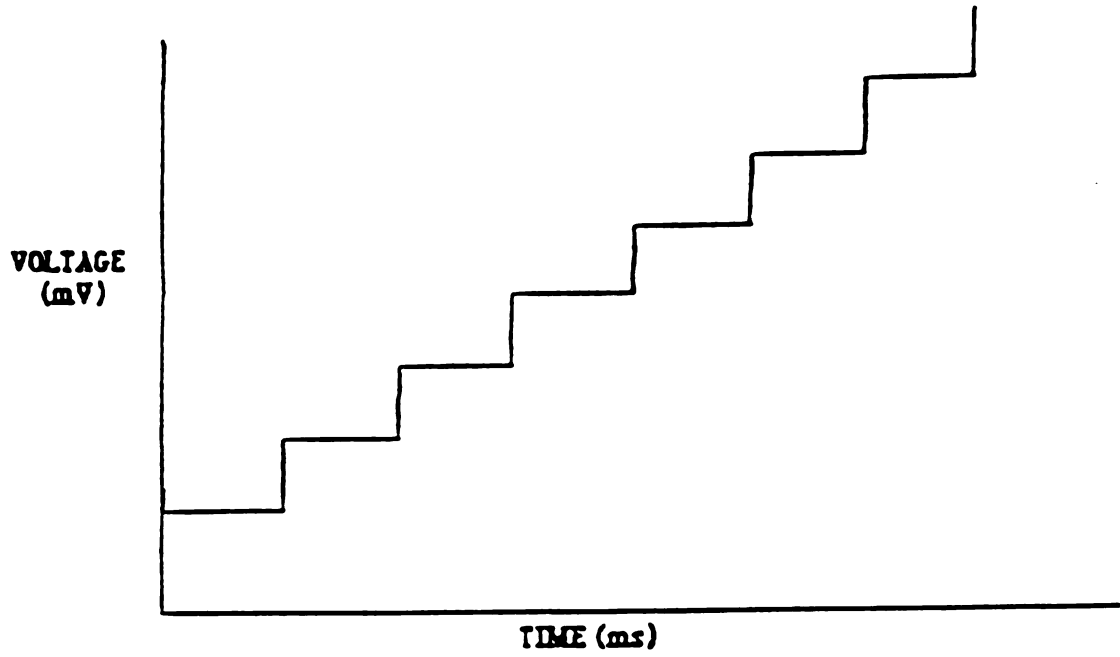


Figure 11 Voltage incrementation vs. time

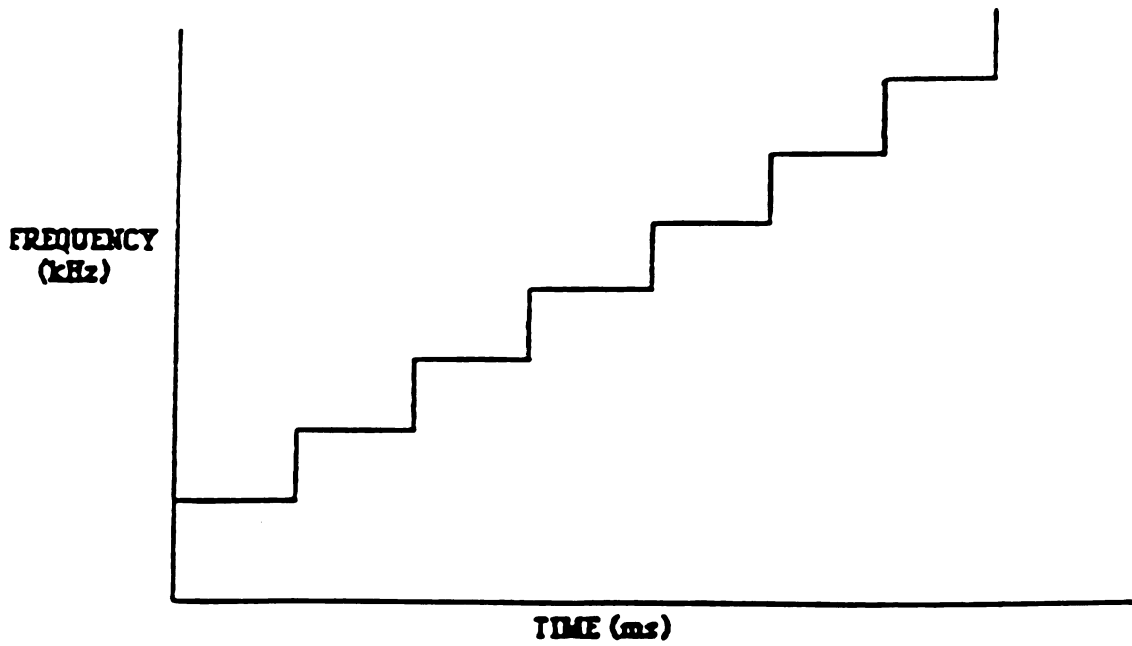


Figure 12 Frequency incrementation vs. time

twelve points are not taken at the same frequency. Therefore, when subtraction on offset peaks was attempted, first derivative responses were observed. See Figure 13. A solution to this problem would seem to be solved by adding a delay that would allow the voltage, and therefore the frequency, to reach one constant, desired value. This time delay yielded some improvement, but never seemed to eliminate the problem of mismatched peaks, even when quite lengthy delays were implemented.

The problem of distorted, broad peaks still existed. Instead of obtaining smooth gaussian peaks, peak distortion was apparent when there was a 4.88 mv step in the voltage, and a step in the frequency. See Figure 14. To help eliminate this problem, a convolution step was utilized. (Refer to the program scanner.) "Convolve" is a MacAdios command capable of peak smoothing. The problem with this solution, was that convolving acts to decrease the peak intensity, while having little effect on noise reduction. Therefore, there is a trade off between increasing resolution and obtaining Gaussian peak shapes. With the convolve placed in the program, peak shapes did improve slightly. It was obvious that the only way to improve the peak shapes was to acquire more points per mass spectral peak.

Another means was also examined to increase resolution, so that double resonance would function correctly. Resolution was observed as a function of pressure, and the number of ions in the

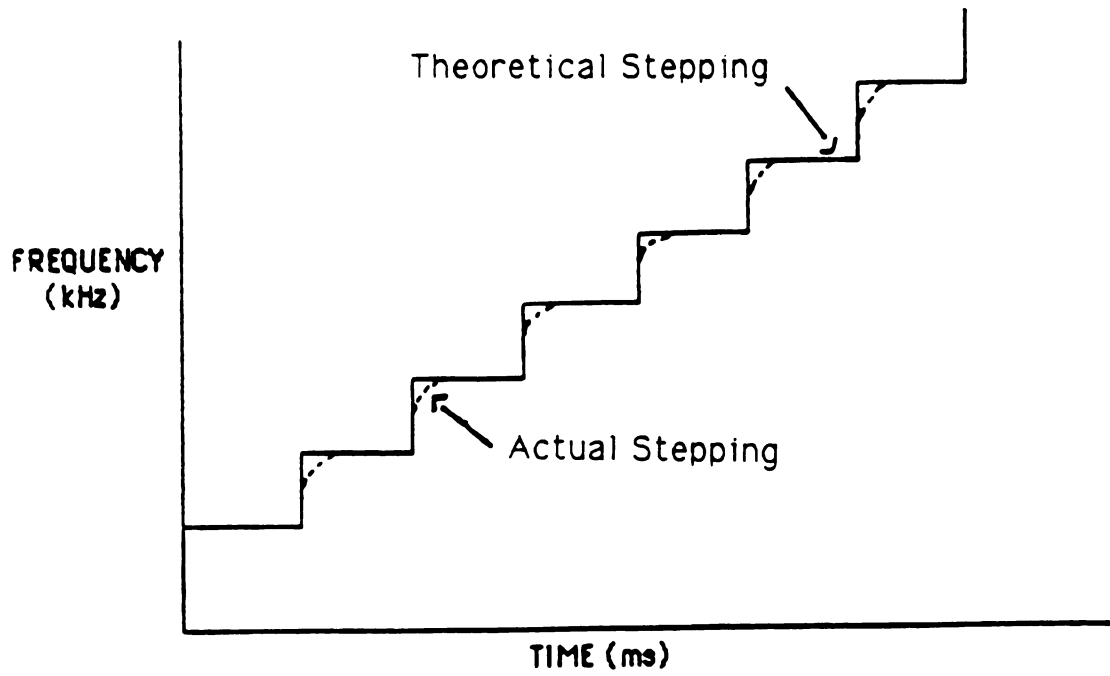


Figure 13 Actual stepping of frequency in time vs. theoretical stepping

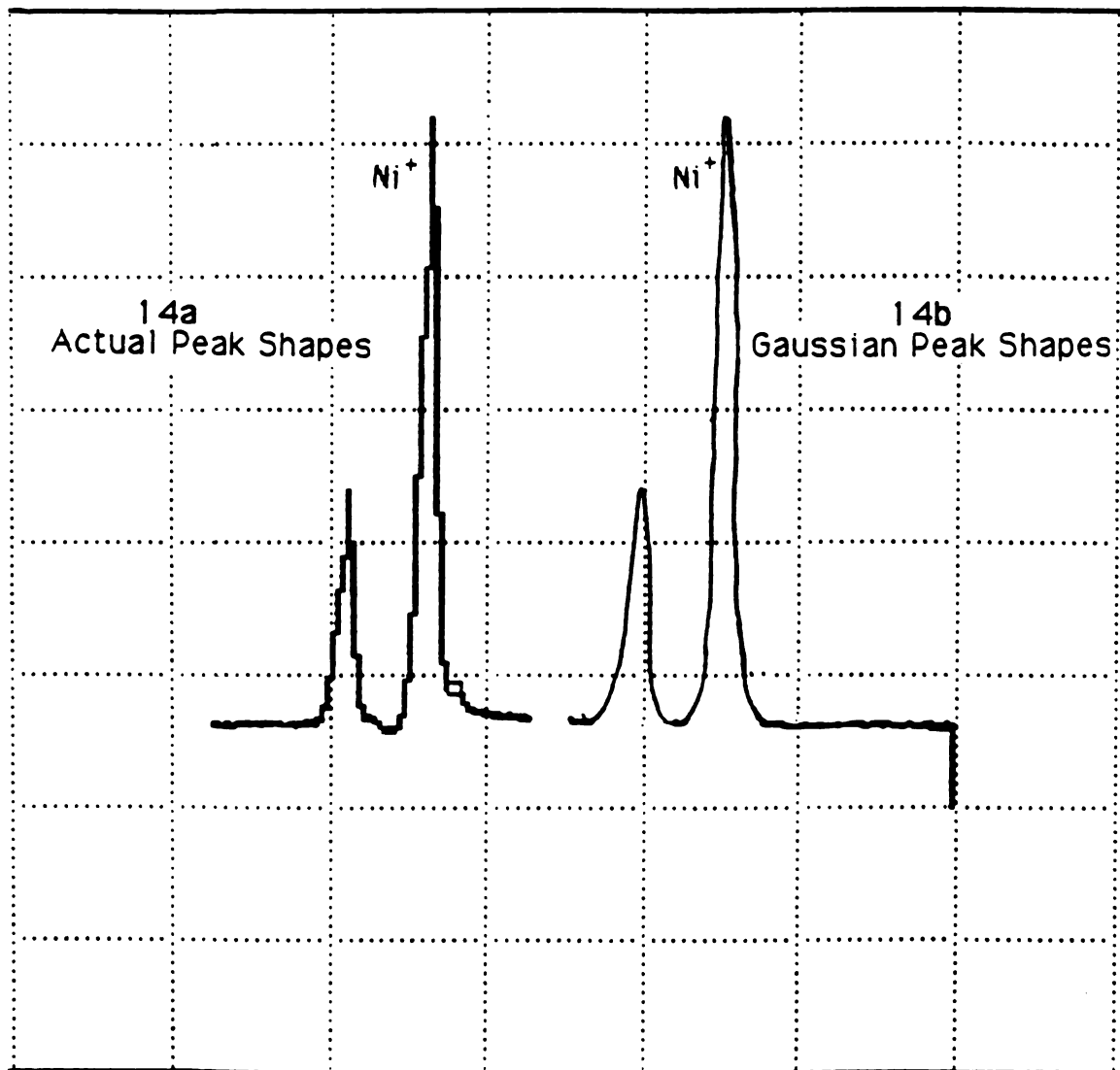


Figure 14 Actual peak shape vs. an ideal gaussian peak shape

14a Actual Peak Shape

14b Gaussian Peak Shape

cell. It was believed that if the number of ions was reduced, i.e., the number of electrons was reduced, then the effect of too many ions, i.e., the space-charge effect, would be reduced, and double resonance would work. So, the current supplied to the filament was cut in half and the pressure was cut to half. The resolution was only marginally improved.

The solution to the resolution, and peak shape dilemma became quite obvious after a test experiment was performed. The experiment was done to see if the resolution, and the peak shape, would actually improve if more points were available. The end result would permit double resonance with no mismatched peaks. To test this solution, the frequency range was cut down to one third of the original range, such that three times as many points were concentrated into this region. The results are provided in Figure 15 and 16. When three times the number of points were available, the resolution improved drastically. It can be observed, that a small indistinguishable peak in Figure 15 became quite obvious in Figure 16 when more points were available. The solution to the problem seemed to depend on the ability to obtain spectra with more points. The MacAdios was the limiting factor in the maximum number of points that were obtainable.

The key to increasing the number of points became apparent when an oscilloscope trace of the spectrum was observed. This spectrum is triggered by a 10-volt ramp generated from the function

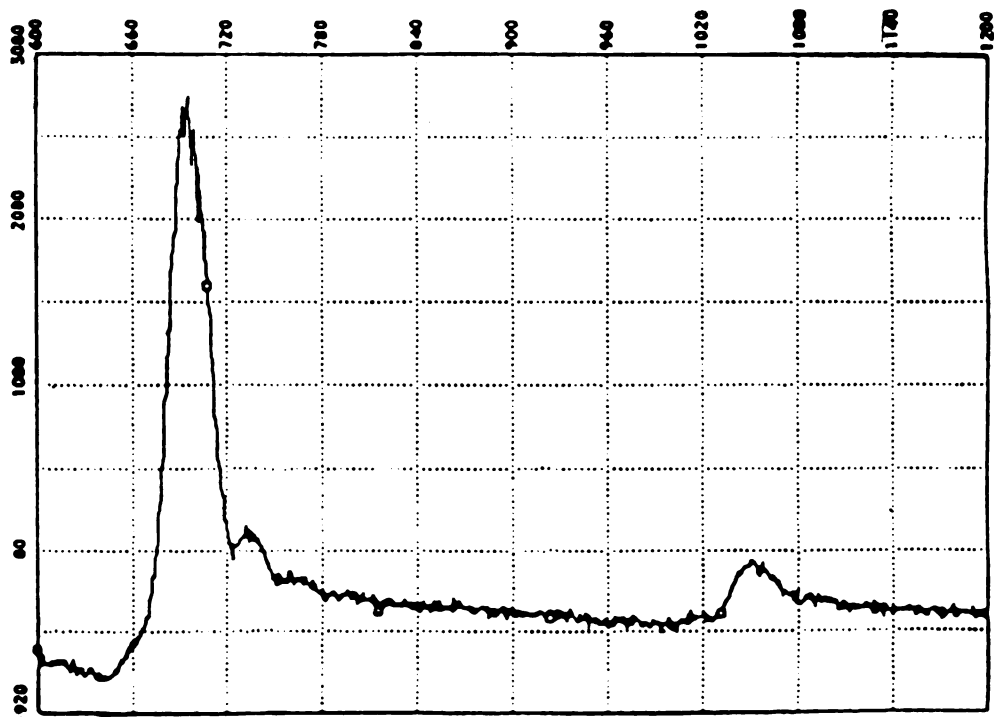


Figure 15 A peak obtained with a normal frequency range

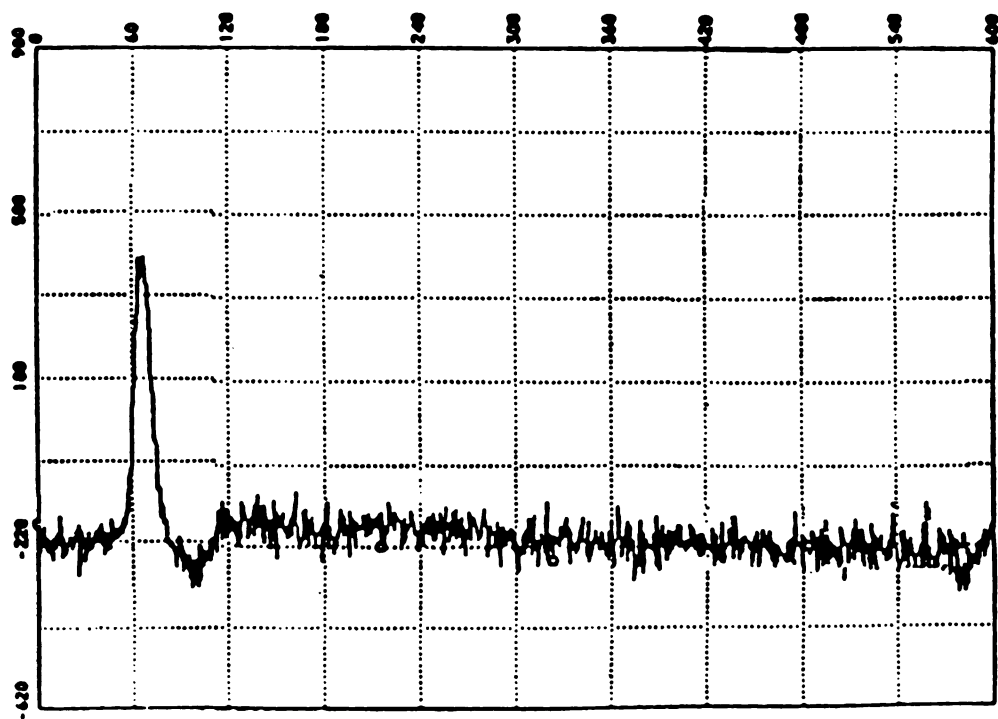


Figure 16 A peak obtained with the frequency range decreased by one third

generator's linear sweep output, and therefore it always starts in the same place, and is very stable. Therefore, the function generator and not the Macintosh would be used to generate the voltage ramp. Each 10-volt ramp corresponded to one scan of the frequency range set by the start, and the stop, on the frequency dial. The rate at which this spectrum is displayed, depends on the scan rate set by the sweep duration. One end of a BNC connector is hooked into the linear sweep output of the function generator, and the other end to the input channel B, of the MacAdios. When the voltage equals .025 volts, the MacAdios is triggered to start the scan and collect data. The maximum number of points that it can handle is 10,000. Due to the memory, this limit is internal to the MacAdios for analog waveforms. All experimental programs were written to obtain 9,000 data points since the time required to collect these points correlated well with a frequency scan of 10 seconds. It should be noted, that the MacAdios designates the rate at which data are collected and no matter if one point, or thousands of points are collected, the rate that data are collected is the same. The only imposition to this method of data collection is correlating the number of points that are to be taken during a scan of a particular designated speed. This is remedied by increasing the scan rate, if too few points are collected for a scan speed, or reducing the scan speed if the scan is completed before all the points have not yet been collected. Another solution is to add more points, or to decrease the number of points to fit the particular scan speed chosen. For the experimental setup, refer to Figure 4.

New programs were needed to obtain data when the function generator's linear sweep output was supplying the voltage ramp, which controlled the number of points that could be collected. A program called "Siress" was written to collect single resonance spectra. This program is listed in Appendix A, and is explained according to the line number. A double resonance experiment can be performed by employing the program "Doubres", which stands for double resonance. "Doubres" is also listed, and explained in Appendix A.

With the function generator's linear sweep output controlling the number of points being collected, the resolution improved drastically. However, double resonance experiments were still not successful. Mismatched peaks were no longer a problem, but another problem arose. Refer back to the double resonance spectrum experiment done with $\text{Co}(\text{CO})_3\text{NO}$, when $m/z=87$ was irradiated. The peak at $m/z=204$ is the only reaction product. It appears that when the ion $m/z=87$ was irradiated, peaks such as $m/z=59$, and $m/z=115$, and $m/z=204$ would be subtracted. This suggests that all of these are products of $m/z=87$. Therefore, an inaccurate precursor/product relationship was being obtained. See Figure 17. Spectrum 17a shows $m/z=87$ being irradiated. spectrum 17b is a spectrum obtained when $m/z=87$, and its products were removed from the cell. The spectrum i 17c is the net spectrum obtained when 17a, and 17b were subtracted. It is obvious that $m/z=59$ is not a product of $m/z=87$, but another reactant ion. Double resonance was ineffective.

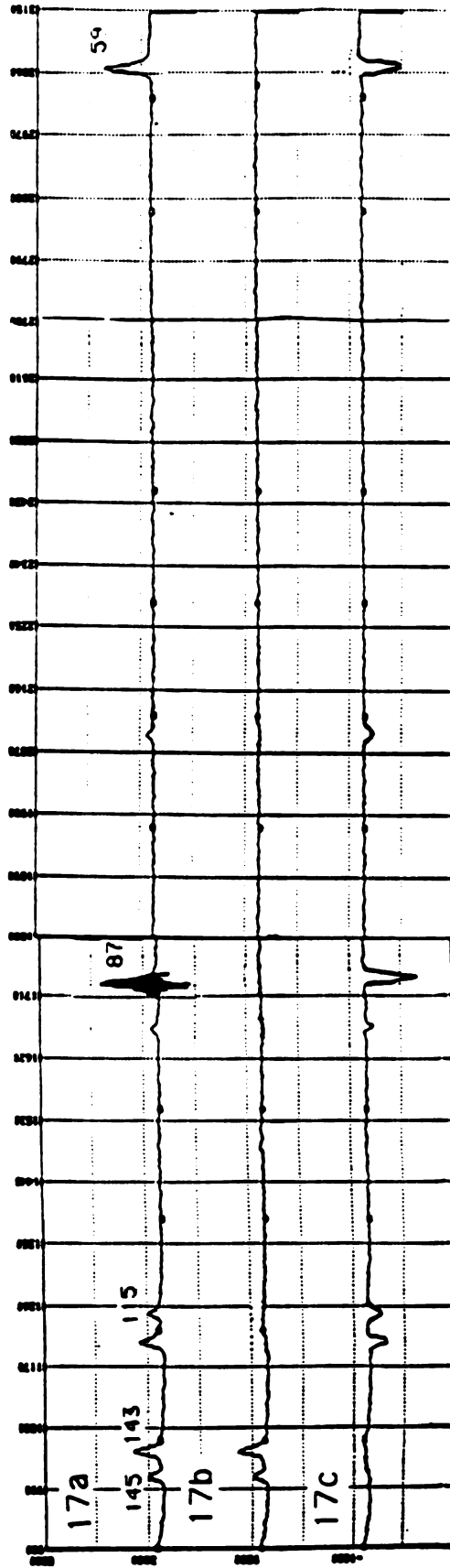


Figure 17 Plot resulting from $m/z=87$ being irradiated

17a Normal Mass Spectra

17b Mass Spectra with $m/z=87$ irradiated

17c Net spectrum

It was hoped, that too much power was causing a frequency shift in the ions. However, repetitive experiments where $m/z=87$ was irradiated with different amounts of power did not produce reproducible results. To solve this problem, the power used to irradiate ions was varied from 4.0 to 0.1 volts.

Double resonance seemed futile, and the limitations to performing the experiments were placed on the detector system. A new project was necessary. The project would have to limit the number of different reactant ions being produced, to simplify this situation. A precursor-product relationship would need to be obtained from the oscilloscope directly. Thermionic emitters seem to be the obvious solution because they produce only one metal ion, which is the only reactant observed, and all other ions are products of that ion, and they can be observed on the oscilloscope.

C. CHEMISTRY WITH METAL IONS

1. BENEFITS OF STUDYING GAS PHASE CHEMISTRY

Most of the understanding that scientists have about reactions involving ions and molecules has been obtained from studying the chemistry of these two species in solution¹³. It should be noted, however, that in the condensed phase, solvent molecules can greatly influence (i) the extent at which the reaction occurs; (ii) the rate, by orders of magnitude; (iii) the nature of the products; and (iv) the equilibria between reaction intermediates and products. Ions in solution are always under the solvent's influence¹³. It thus seems logical that chemists could benefit from the study of reactions between ions and molecules in the absence of a solvent.

There are a number of very good reasons, in addition to solvent effects, why gas/phase ion/molecule reactions should be studied. These are: (i) ions are both easy to make and to detect in the gas-phase; (ii) to study fundamental chemistry; (iii) thermodynamics can be determined; (iv) kinetics can be obtained.

2. TYPICAL REACTIONS AND MECHANISMS

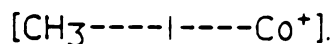
The area that has attracted the most attention in gas/phase chemistry employing ICR are the reactions between transition metal ions and organic molecules such as alkyl halides, alkenes, alcohols, amines, aldehydes, ketones, carboxylic acid, esters, ethers, sulfides, and mercaptans¹⁴. These reactions all seem to proceed by the same metal insertion, β -hydride shift, competitive ligand loss mechanism.

One of the first studies of gas/phase transition metal ion chemistry was conducted in 1975 by Allison and Ridge^{15,16}. Typical reactions studied by Allison and Ridge by ion cyclotron

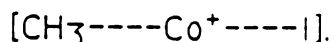
resonance (ICR) were those involving transition metals reacting with organic molecules, such as alkyl halides. Allison and Ridge generated this information to investigate bond energies, rate constants, and mechanisms. In this study, Allison and Ridge examined how a transition metal ion (Co^+) reacted with a methyl halide (CH_3I). The reaction was found to yield only two products:



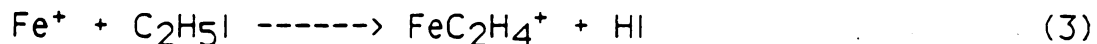
To propose a viable mechanism, an intermediate was first sought. Allison and Ridge considered that if the positive metal ion attacked the electronegative end of a methyl iodide molecule, one would expect an intermediate such as:



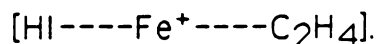
This intermediate explains only the products of reaction (2). Therefore, they proposed an alternative intermediate, which suggested that the metal ion inserts into the C--I bond to form the following intermediate:



When the alkyl halide contained a β -hydrogen¹⁵, products other than those indicative of only simple insertion were observed:



The nature of the intermediate that dissociates to yield the observed products is:

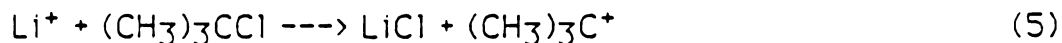


This intermediate was formed by a metal insertion followed by a β -hydrogen atom shift. The distribution of the final products were then determined by the relative binding energies of the two ligands, HI and C_2H_4 , to the metal¹⁶. This mechanism was significant since most transition metal ions reacting with organic molecules appear to follow this mechanism.

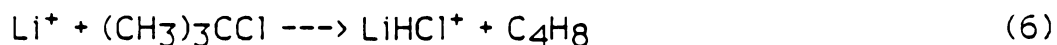
Other ions explored in the gas/phase with an ICR were the alkali metal ions^{5,17-24}. The experiments reported will now be discussed. Work has been done to determine the gas/phase binding energies of simple Lewis bases¹⁷, π -donor, and n -donor bases²³, with lithium ions as the reference acid. From this information, free energies could be derived¹⁷. Also, the mechanism of reaction for lithium ions with alkyl halides has suggested that these reactions provide a useful means of producing carbonium ions with relative ease. Producing carbonium ions is limited in solution¹⁸. Carbonium ions were generated when an alkali ion was reacted with an organic molecule, to form an activated species which then could be dissociated to form a carbonium ion, and an alkyl halide¹⁸. Another study by Beauchamp, Staley, and Wieting, conducted similar experiments by observing bromide transfer reactions with alkali ions, alkyl carbenium ions, acyl cations, and cyclic halonium ions²⁴. These data are practical and useful in that they can be used to make predictions for general theories about acid-base interactions in the gas phase. These generalizations can then be used to make comparisons with reactions in solution. Yet another study by Weddle, Allison, and Ridge, reported an experiment performed to observe the bond strength between various $\text{Li}^+ \text{-L}$ complexes, by observing various ligand substitution reactions¹⁹. Photodissociation spectra have been obtained to observe the excitation of lithium complexes of benzaldehyde, nitrobenzene, cyanobenzene, and aniline²¹. Molecular beam scattering experiments were performed to observe the reaction pathway

observed when cesium ions were reacted with ortho-, meta-, and para-chlorotoluenes²², as well as benzyl chloride²⁵. However, the work most pertinent to this study was conducted in 1979^{15,26} when Allison and Ridge conducted experiments to observe how various alkali metal ions reacted with monofunctional compounds such as alkyl halides, and alcohols.

The experiments performed by Allison and Ridge in the gas/phase by ICR allowed them to propose a mechanism for the observed dehydrohalogenation and dehydration reaction products that had been observed¹⁵. They expected to see the following reaction when a lithium ion was reacted to t-butyl chloride^{15,26}:



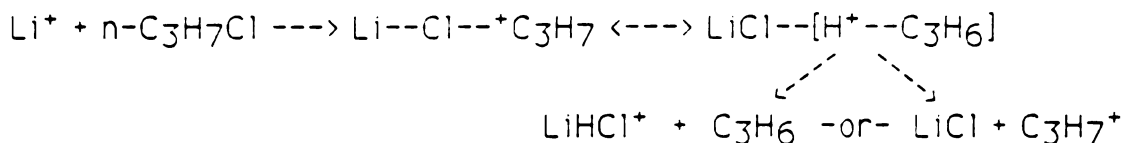
Instead, the following reactions resulted:



These results motivated the study of other systems, such as alkyl halides and alcohols, with alkali ions to observe the generalities of the reaction products with these monofunctional groups. It appeared from the observed products of the reaction between the alkali ion and the organic molecules, RH and ROH, that the alkali metal ions were not reacting as did the transition metal ions, that would insert into a molecule, followed by a β -hydrogen shift, and competitive ligand loss. What was suggested by the observed products can be denoted in Scheme 1. The alkali ion interacted with the electronegative end of the molecule which causes a positive charge to then be localized on the alkyl group. Whether this actually occurs will depend on whether the lithium ion, or the alkyl cation has a stronger affinity for the anion in question. At this point a resonance structure can be drawn for the molecule, in which the

alkyl group is considered as a protonated olefin. Whether the alkali halide portion, or the alkyl portion, obtains the proton and then fragments to form products seems to depend on which species has the larger proton affinity.

Scheme 1.



It was found that lithium ions unexpectedly caused dehydration from various alcohols, and dehalogenation, from various alkyl halides^{15,26}, as do the transition metals, but not by the same mechanism. Staley and Beauchamp^{23,24} were the first to report reactions typical of lithium ions and discuss a mechanism of formation of an intermediate $\text{Li}^+(\text{HX})(\text{olefin})$, but did not speculate on details of the mechanism.

Table 2a is a compilation of all of the reaction involving Li^+ , and Na^+ , in the gas/phase that yielded products, and Table 2b is a compilation of reactants that were unsuccessful, i.e., formed no products, or mere addition products, when reacted with Li^+ , and Na^+ .

3. THE CHEMISTRY

a. PURPOSE

The primary focus of this research is to extend the work conducted by Allison in 1978. Included will be experiments to see if indium ions, a group IIIA element, is reactive with simple organic molecules, as is aluminum. Also, lithium was known to react with

Table 2b (cont'd)

	n=1	2	3n	3i	3t	4n	4i	4t	5	7	10
$\text{Li}^+ + \text{C}_n\text{H}_{4n}\text{O}^+ \rightarrow \text{Li}(\text{C}_n\text{H}_{2n})^+ + \text{H}_2\text{O}$	X										
$\quad \rightarrow \text{Li}(\text{H}_2\text{O})^+ + \text{C}_n\text{H}_{2n}$	X										
$\text{Li}^+ + \text{Fe}(\text{CO})_n \rightarrow \text{LiFe}(\text{CO})_{n-1}^+ + \text{CO}$										X	
$\quad \rightarrow \text{Li}(\text{CO})^+ + \text{Fe}(\text{CO})_{n-1}$										X	
$\text{Li}^+ + \text{C}_n\text{H}_{2n+1}\text{I} \rightarrow \text{Li}(\text{C}_n\text{H}_{2n})^+ + \text{HI}$											X
$\quad \rightarrow \text{Li}(\text{HI})^+ + \text{C}_n\text{H}_{2n}$											X
$\text{Li}^+ + \text{C}_n\text{H}_{n+2}\text{I} \rightarrow \text{Li}(\text{C}_n\text{H}_{n+1})^+ + \text{HI}$	X										
$\quad \rightarrow \text{Li}(\text{HI})^+ + (\text{C}_n\text{H}_{n+1})$	X										
$\text{Li}^+ + \text{CF}_n \rightarrow \text{LiF} + \text{CF}_{n-1}^+$											X
$\text{Li}^+ + \text{N}_n\text{O} \rightarrow \text{No reaction}$											X
$\text{Li}^+ + \text{CF}_n\text{Cl}_n \rightarrow \text{LiCl} + \text{CF}_n\text{Cl}_{n-1}^+$											X
$\quad \rightarrow \text{LiF} + \text{CF}_{n-1}\text{Cl}_n^+$											X
$\text{Li}^+ + \text{C}_n\text{H}_{2n+1}\text{Cl} \rightarrow \text{Li}(\text{C}_n\text{H}_{2n})^+ + \text{HCl}$											X
$\quad \rightarrow \text{Li}(\text{HCl})^+ + \text{C}_n\text{H}_{2n}$											X
$\text{Li}^+ + \text{C}_n\text{H}_{n+1}\text{OBr} \rightarrow (\text{C}_n\text{H}_{n+1}\text{O})^+ + \text{LiBr}$											X
$\text{Li}^+ + \text{C}_n\text{H}_{2n+2}\text{O} \rightarrow \text{Li}(\text{C}_n\text{H}_{2n})^+ + \text{H}_2\text{O}$										X	X X X
$\quad \rightarrow \text{Li}(\text{H}_2\text{O})^+ + \text{C}_n\text{H}_{2n}$										X	X X X

Table 2b (cont'd)

	n=2	3n	3i	3t	4n	4i	4t	5	7	10
$\text{Li}^+ + \text{C}_n\text{H}_{n+5}\text{Br} \longrightarrow \text{C}_n\text{H}_{n+5}^+ + \text{LiBr}$										X
$\text{Na}^+ + \text{C}_n\text{H}_n\text{Cl} \longrightarrow \text{NaCl} + \text{C}_n\text{H}_n^+$										X
$\text{Na}^+ + \text{C}_n\text{H}_{2n+1}\text{I} \longrightarrow \text{Na}(\text{C}_n\text{H}_{2n})^+ + \text{HI}$							X			
$\quad \quad \quad \longrightarrow \text{Na}(\text{HI})^+ + \text{C}_n\text{H}_{2n}$							X			

both alcohols and chloroalkanes^{15,26}. It was desirable to see what sort of products would result when lithium ions react with various bromoalkanes, not yet considered, and bifunctional compounds composed of the halide, and hydroxide functionalities. When lithium ions were reacted with the bifunctional compounds, it was supposed that any one of the following may be observed:

- 1) Products would represent both those of an alcohol, and those typical of an alkyl halide reaction, if the bifunctional compound contained a hydroxide, and an alcohol.
- 2) Products typical of one of the functional groups would be formed and not the other, meaning that Li^+ would show a preference for one type of functional group over another.
- 3) Products unique to this combination of functional groups would be formed.

To extend this work, it was advantageous to react a variety of bromoalkanes and bisubstituted n-alkanes with lithium ions, to see if the proposed mechanism for predicting products held correct. Experiments were conducted on bifunctional molecules with two to five carbons in a chain. Yet, it was of particular interest to observe the bisubstituted n-butanes, and n-pentanes. These long chain alkanes would be helpful to predict whether Li^+ preferred one group over the other group, since having four to five carbons in a molecule may cause it to be too long for both groups to easily interact with the alkali metal simultaneously.

In Allison's studies^{15,26}, it was found that chloroethane and ethanol would not undergo typical dehydrohalogenation and dehydration reactions with lithium, as would other alkyl halides and alcohols with longer chains. It is assumed, that the first step of the mechanism, used to explain these products, is an ion/molecule interaction. It is supposed, that if this interaction does not produce much energy, a barrier to the rest of the reaction is encountered.

Therefore, it can be determined, that the first step of the lithium ion and the chloroethane interaction, or the lithium ion and the ethanol interaction does not produce sufficient energy to overcome early reaction barriers.

It is of great interest to do an experiment to observe if bifunctional molecules, such as chloroethanol, will form a strong enough interaction with the lithium ion to overcome the reaction barrier, and produce products where none were observed before. This sort of scenario could be imagined if the following were possible. Suppose for instance, that the lithium ion interaction with ethanol releases -38 kcal/mol, and the interaction between the lithium ion and chloroethane was approximately -34 kcal/mol. It is possible, that the interactions would be additive when the lithium ion reacted with chloroethanol to have a combined interaction energy of -72 kcal/mol. This combined interaction may be enough to induce some chemistry, and therefore warrants further investigation.

b. EXPERIMENTAL METHODS

All experiments were performed on an ion cyclotron resonance (ICR) mass spectrometer that has been described previously. All samples were degassed by multiple freeze-pump-thaw cycles. The sample was not used until it was determined that the compound was pure. Purity was determined by comparing the electron impact spectrum of the various compounds, with a literature spectrum²⁷, as well as performing gas chromatography / mass spectrometry on the compound. For impure compounds, further purification was generally completed through distillation. The instrument was run in the "drift mode." Pressures for the experiments were on the order of 5×10^{-6} to 3×10^{-5} Torr. In the instance that a precursor of a product needed to be determined, double resonance techniques were employed to determine this information.

A lithium emitter is made by making up a β -Eucryptite, $1\text{Li}_2\text{O}:2\text{Al}(\text{NO}_3)_2:2\text{SiO}_2$, powder, and the indium emitter is made from $1\text{In}_2\text{O}_3:\text{Al}_2\text{O}_3:2\text{SiO}_2$. Then, the powdery mixture, of the emitter desired, is placed on a piece of platinum metal and heated in an acetylene-oxygen flame to approximately 1700°C until it formed a melt. Once a slurry forms, the rhenium wire which is shaped in the form of a loop is pulled through the melt in order to form a bead on the tip of the loop.

If a melt was hard to achieve, as was the case with Indium, an alternate method had to be performed. Instead of trying to melt the mixture, the loop was placed right into the powdery mixture. Once there was some powder suspended on the loop, the loop was placed in the flame just long enough to form a solid coating. This method could be repeated many times until the bead was of sufficient size.

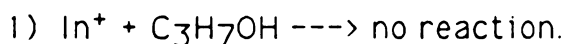
Once a filament is made, it is mounted inside the source region of the cell. In order to cause alkali ions to be emitted, a current of 1.0-1.5 amps, and a positive bias of 3-5 volts, is placed on the filament. The first ions that are observed are from sodium, and potassium. These two ions arise as impurities in the β -eucryptite mixture, and they are seen before the lithium ion peak since they have a lower ionization energy. The appearance, and amounts of the sodium and potassium ion peaks depend on the age of the filament, and the temperature. Generally, sodium ions are only seen for the first couple of hours that the filament is used, but it can be observed for the lifetime of the filament. After approximately eight hours, lithium ions predominate the mass spectra.

With the indium emitter, indium ions are noted right away. There are however, rubidium and cesium ions which appear in the spectrum, as well as sodium and potassium ions due to impurities in the mixture. Cesium was very small relative to the abundance of the other ions. The presence of these metal ion impurities allows the chemistry of these ions to be studied in addition to the chemistry of the indium ion.

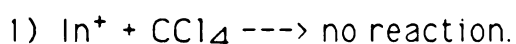
c. EXPERIMENTAL RESULTS WITH THE INDIUM EMITTER

1) 1-Propanol

There were no reactions observed with 1-propanol and In^+ .

**2) Carbon Tetrachloride**

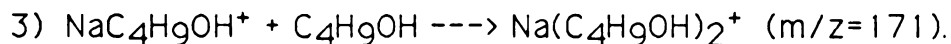
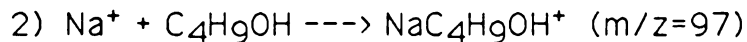
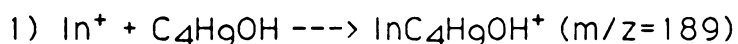
There were no reactions observed with carbon tetrachloride and In^+ .

**3) Cyclohexane**

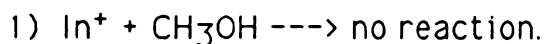
There were no observed reactions with cyclohexane and In^+ .

**4) 1-Butanol**

Indium showed addition to the parent molecule. Sodium also showed addition to 1-butanol

**5) Methanol**

There were no observed reactions with methanol and In^+ .

**6) 3-Chloropropane**

There were no observed reactions with 3-chloropropane and In^+ .

1) $\text{In}^+ + \text{C}_3\text{H}_7\text{Cl} \rightarrow$ no reaction.

7) Propylamine

Indium showed addition to the parent molecule. Also, the impurities in the emitter, such as sodium, potassium, and rubidium also showed addition to propylamine.

1) $\text{In}^+ + \text{C}_3\text{H}_9\text{N} \rightarrow \text{InC}_3\text{H}_9\text{N}^+$ ($m/z=174$)

2) $\text{Na}^+ + \text{C}_3\text{H}_9\text{N} \rightarrow \text{NaC}_3\text{H}_9\text{N}^+$ ($m/z=82$)

3) $\text{Rb}^+ + \text{C}_3\text{H}_9\text{N} \rightarrow \text{RbC}_3\text{H}_9\text{N}^+$ ($m/z=144$)

4) $\text{K}^+ + \text{C}_3\text{H}_9\text{N} \rightarrow \text{KC}_3\text{H}_9\text{N}^+$ ($m/z=98$).

8) Tricarbonylnitrosyl Cobalt(0)

Indium ions showed no reaction with the parent molecule, however, sodium ions did form an addition product.

1) $\text{In}^+ + \text{Co}(\text{CO})_3\text{NO} \rightarrow$ no reaction

2) $\text{Na}^+ + \text{Co}(\text{CO})_3\text{NO} \rightarrow \text{NaCo}(\text{CO})_3\text{NO}^+$ ($m/z=196$).

d. DISCUSSION OF THE RESULTS FROM THE INDIUM EMITTER

The focus of this part of the thesis is on the experiments performed with indium, to determine how this metal ion, not previously studied in the gas phase, reacted with various organic molecules. In order to observe how this ion reacted with various compounds in the gas phase, organic molecules with various functionalities were examined. Therefore, the alcohols, amines, carbonyls, aromatics, and halogens were examined. The results show that the indium ion is virtually non-reactive, aside from some addition products that were observed. These results were not expected since Indium is in group 111A as is aluminum, and was

therefore expected to undergo the same sort of reactions, as have been reported for Al^+ .

Gas/phase studies employing aluminum ions have been reported²⁸⁻³¹. The aluminum ion, Al^+ , resembles the alkali metal ions, which have a noble gas configuration, since it has a filled subshell, $[\text{Ne}]3s^2$. Therefore, the reactivity would be expected to be similar. To test if the aluminum ions reacted similarly to the alkali metal ions, various studies have been done^{28,31}. Since it is well known that alkali metal ions dehydrohalogenate, and dehydrogenate alcohols, the type of reactions that would occur when these components react with aluminum ions, needed to be examined. One study found that there were three types of reactions observed when aluminum ions react with alkyl halides: (1) halide transfer, (2) dehydrohalogenation, and (3) oxidation. The study concluded that reaction thermodynamics, and collision energy determined if halide transfer, or dehydrohalogenation occurred²⁸. When aluminum ions react with alcohols, it was found that they form two products due to: (1) hydroxide transfer, and (2) dehydration.

Since indium is a group IIIA element, as is aluminum, it was hoped that the indium ion would induce similar reaction products as reported above when reacted with alkyl halides, and alcohols. Also, as the aluminum ion, the indium ion has a filled subshell $[\text{Kr}]4d^{10}5s^2$, and therefore resembles the alkali metal ions with their noble gas configuration. This was the basis for suggesting that indium would be reactive with alkyl halides, and alcohols. However, as mentioned, not only was no reactivity observed with these two groups, but no reactivity was observed with other functional groups either.

The reactivity of indium ions could be limited for various reasons. A study conducted by Beauchamp and Schilling suggests that the reactivity could be inhibited by the size of the metal ion. Their study³² was performed on the lanthanide ions Pr^+ , Eu^+ , Gd^+ , with various alkanes, and cycloalkanes. In this work it was

suggested that the large size of an atomic ion could inhibit a strong ion-neutral interaction, since this complex is held together by the force due to a permanent dipole, or an induced dipole.

Beauchamp and Schilling also suggested³² that the first step in a gas/phase ion/molecule reaction is the formation of a weak collision complex. If this first step does not produce enough energy, earlier barriers to the reaction cannot be overcome. If this is the case, it is understandable, why the reaction would not occur.

To obtain a better understanding about the energetics, consider Figure 18a. E_1 is the binding energy released when the ion and the molecule come together and interact electrostatically. E_2 is the energy available for step II, which is the barrier to the reaction. E_2 is the energy available when E_b has been subtracted from E_1 . Therefore, if E_1 was large, indicating a strong ion/molecule interaction, and E_b is small, then E_2 is "pulled down" to a lower energy, and there is no barrier to the reaction. Note Figure 18b. If E_1 is small, indicating a weak ion/molecule interaction, then E_2 will be higher on the energy scale, and above the zero line. The zero line is a barrier to the reaction products. Therefore, it can be seen why the first step of the reaction can be the limiting factor.

To further support the postulated theory of why the indium ion will not react due to size is the study conducted by Dzidic and Kebarle²⁰. Their work reports the binding energies, ΔH^0 , for various alkali metal ions to water. As the alkali metal ions increase in size from the lithium ion to the cesium ion, the binding energies can be observed to decrease from 34 kcal/mol to 13.7 kcal/mol, respectively. This is yet more evidence to support the theory that as size increases, ion/molecule interactions, and therefore the binding energies, decrease.

To give an idea of the difference in the ionic radius of the metal ions that would react, and the indium ion, Table 3 was

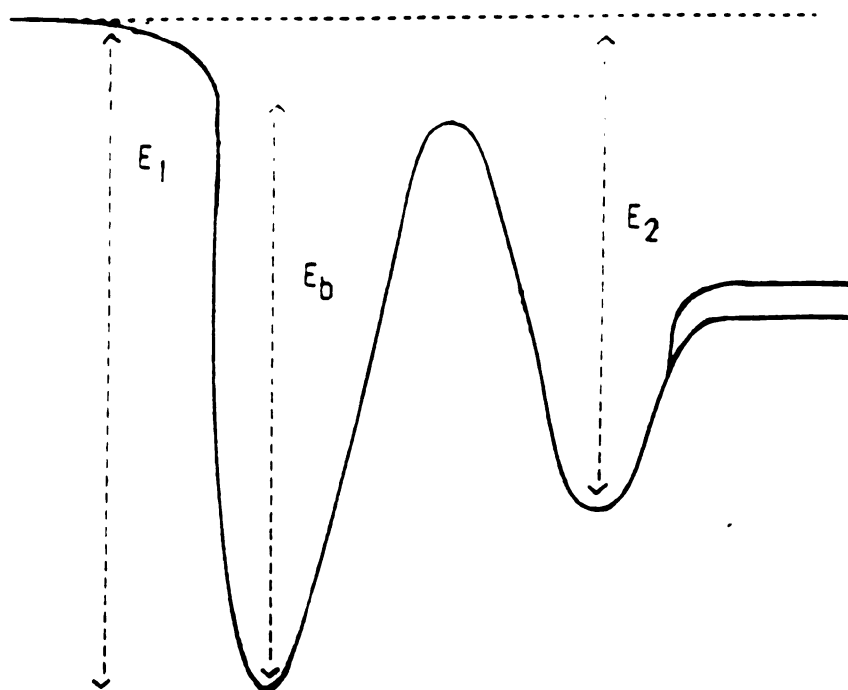


Figure 18a Potential energy surface with no barrier

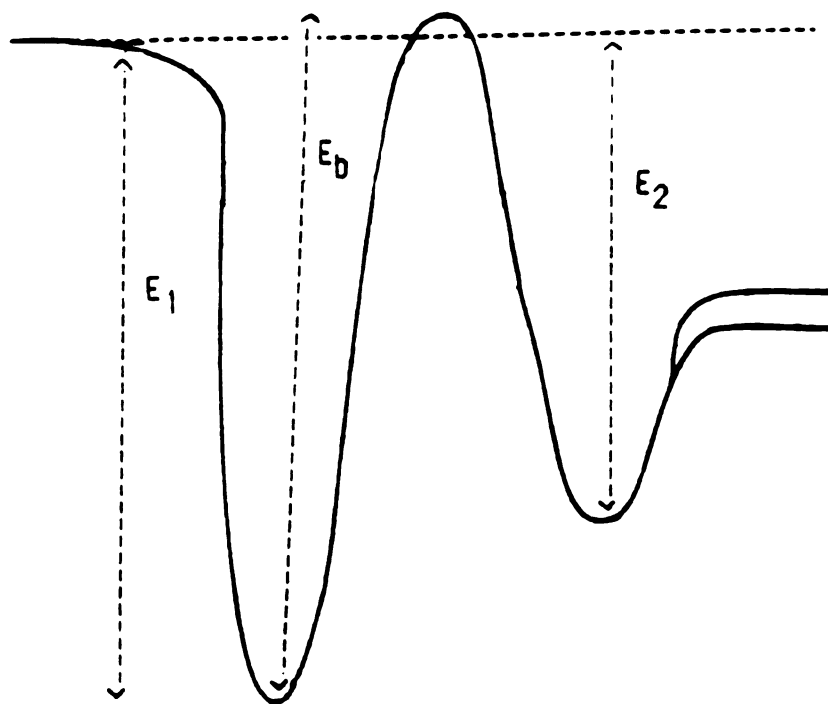


Figure 18b Potential energy surface with a barrier

provided. Note, that all of the metal ions listed, with the exception of In^+ , are known to react with alkyl halides and alcohols.

TABLE 3. ESTIMATED IONIC RADIUS OF VARIOUS METAL IONS

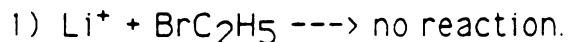
<u>METAL</u>	<u>ION</u>	<u>IONIC</u>	<u>RADIUS (A)</u>
Co	$^+$	>.72	
Li	$^+$.76	
Al	$^+$	>.51	
In	$^+$	>.81	

e. EXPERIMENTAL RESULTS FOR REACTIONS OF Li^+

The results below include all the reactions that occurred between the lithium ion and the various organic molecules employed. It should be noted, that other metal ions were present as impurities in the emitter, and when a reaction occurred with one of these, it was noted in the results. The branching ratios for the reactions observed are listed in Table 4. An example of how the branching ratios were calculated is provided in Appendix B.

1) Bromoethane

There were no reactions observed with bromoethane and Li^+ .



2) 2-Chloroethanol

The following processes were observed when Li^+ was reacted with $\text{ClC}_2\text{H}_4\text{OH}$:

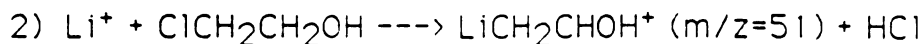
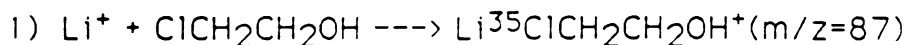


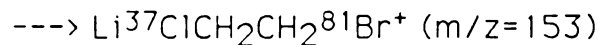
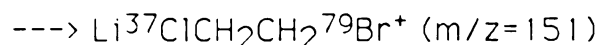
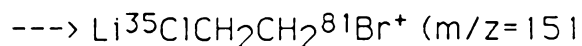
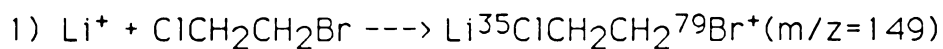
Table 4 Compilation of Reactions, and Branching Ratios

Reaction	n=2	n=3	n=4	n=5
$\text{Li}^+ + \text{C}_n\text{H}_{2n+1}\text{Br} \text{ ---} \rightarrow \text{HBr} + \text{LiC}_n\text{H}_{2n}^+$ $\text{---} \rightarrow \text{LiHBr}^+ + \text{C}_n\text{H}_{2n}$		100%	100%	100%
$\text{Li}^+ + \text{C}_n\text{H}_{2n+1}\text{Cl} \text{ ---} \rightarrow \text{HCl} + \text{LiC}_n\text{H}_{2n}^+$ $\text{---} \rightarrow \text{LiHCl}^+ + \text{C}_n\text{H}_{2n}$				100%
$\text{Li}^+ + \text{ClC}_n\text{H}_{2n}\text{Br} \text{ ---} \rightarrow \text{HCl} + \text{LiC}_n\text{H}_{2n-1}\text{Br}^+$ $\text{---} \rightarrow \text{HBr} + \text{LiC}_n\text{H}_{2n-1}\text{Cl}^+$ $\text{---} \rightarrow \text{HCl} + \text{HBr} + \text{LiC}_n\text{H}_{2n-2}^+$ $\text{---} \rightarrow (\text{cyclo-C}_n\text{H}_{2n}\text{Br}^+) + \text{LiCl}$ $\text{---} \rightarrow (\text{cyclo-C}_n\text{H}_{2n}\text{Cl}^+) + \text{LiBr}$		100%	87% 2% 3% 85% 3%	12% 5% 7% 74% 2%
$\text{Li}^+ + \text{ClC}_n\text{H}_{2n}\text{OH} \text{ ---} \rightarrow \text{LiH}_2\text{O}^+ + \text{ClC}_n\text{H}_{2n-1}$ $\text{---} \rightarrow \text{LiHCl}^+ + \text{C}_n\text{H}_{2n-1}\text{OH}$ $\text{---} \rightarrow \text{LiC}_n\text{H}_{2n-1}\text{OH}^+ + \text{HCl}$ $\text{---} \rightarrow \text{LiClC}_n\text{H}_{2n-1}^+ + \text{H}_2\text{O}$ $\text{---} \rightarrow \text{LiC}_n\text{H}_{2n-2}^+ + \text{HCl} + \text{H}_2\text{O}$ $\text{---} \rightarrow \text{LiOH} + (\text{cyclo-C}_n\text{H}_{2n}\text{Cl}^+)$			1% 1% 64% 15% 4% 16%	1% 91% 5% 3%
$\text{Li}^+ + \text{BrC}_n\text{H}_{2n}\text{OH} \text{ ---} \rightarrow \text{LiH}_2\text{O}^+ + \text{BrC}_n\text{H}_{2n-1}$ $\text{---} \rightarrow \text{LiHBr}^+ + \text{C}_n\text{H}_{2n-1}\text{OH}$ $\text{---} \rightarrow \text{LiC}_n\text{H}_{2n-1}\text{OH}^+ + \text{HBr}$ $\text{---} \rightarrow \text{LiBrC}_n\text{H}_{2n-1}^+ + \text{H}_2\text{O}$ $\text{---} \rightarrow \text{LiC}_n\text{H}_{2n-2}^+ + \text{HBr} + \text{H}_2\text{O}$ $\text{---} \rightarrow \text{LiOH} + (\text{cyclo-BrC}_n\text{H}_{2n}^+)$		95% 5%	100% 17% 4% 2% 77%	

Lithium ions react by dehydrohalogenation. Also, addition to the chloroethanol molecule is observed.

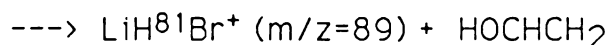
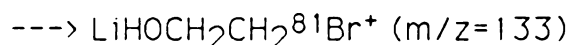
3) 1-Chloro-2-Bromoethane

The addition of Li^+ to the parent molecule was the only observed reaction to occur:



4) 2-Bromoethanol

The processes that occur when lithium ions react with the molecule are as follows:

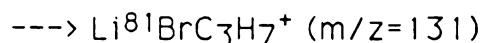


Lithium ions react by dehydrohalogenation of the molecule, as well as addition to the alkyl halide. It should be noted that an ion at $\text{m/z}=95$ kept appearing in the mass spectrum of this compound when it was reacted with the lithium ions. By running an NMR of the compound it was determined that the impurity could be due to dioxane. This was concluded because the difference between the

literature NMR spectrum of 2-bromoethanol and an NMR spectrum obtained from a sample of the 2-bromoethanol used in the experiment was a singlet at 3.7 ppm. The NMR literature spectrum reported for dioxane contains only one peak at 3.7 ppm. Room temperature distillation was used to try to remove this decomposition product of 2-bromoethanol. Further evidence to support the conclusion that the impurity was in fact dioxane came from a mass spectrum that resulted when dioxane was reacted with the lithium ions. The only reaction product that was observed appeared at $m/z=95$, $[\text{Li}^+-\text{dioxane}]$.

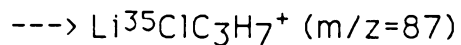
5) 1-Bromopropane

This compound showed addition to the lithium ion and a loss of HBr:



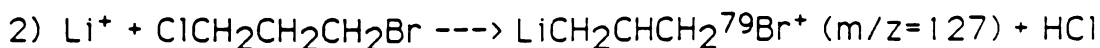
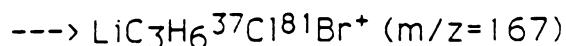
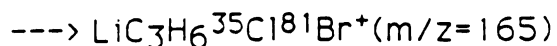
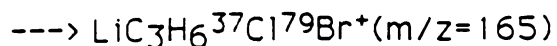
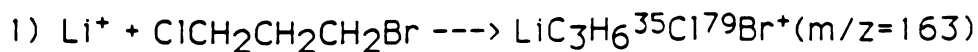
6) 1-Chloropropane

This compound showed addition to the lithium ion, as well as dehydrohalogenation.



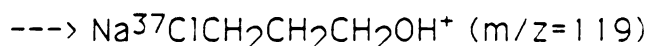
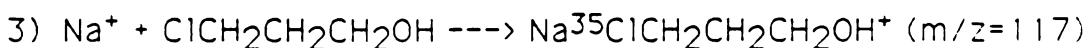
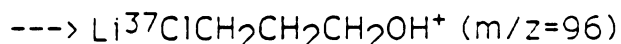
7) 1-Chloro-3-Bromopropane

When Li^+ reacts with 1-chloro-3-bromopropane, the products resulted from addition, and dehydrohalogenation of the parent molecule to form the following products:



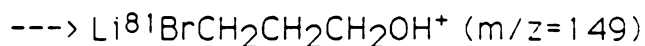
8) 3-Chloropropanol

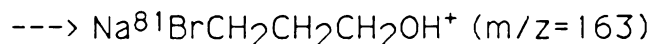
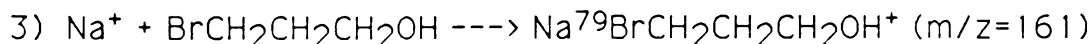
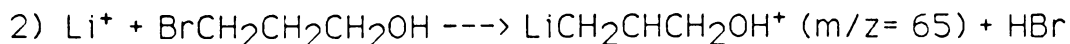
When lithium ions react with 3-chloropropanol, an addition product, and a dehydrohalogenation product are formed.



9) 3-Bromopropanol

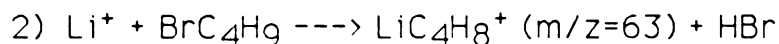
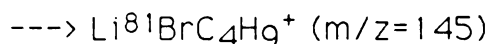
Lithium ions and sodium ions both added to the 3-bromopropanol. Besides these addition products, hydrogen bromide was eliminated to form a lithium-olefin ion.





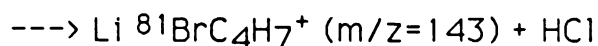
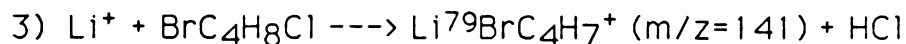
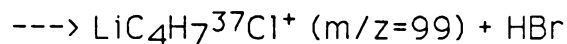
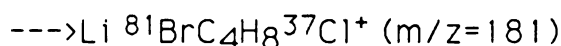
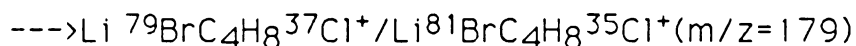
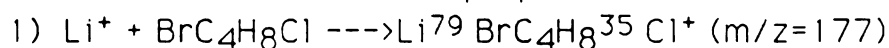
10) 1-Bromobutane

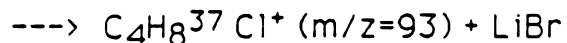
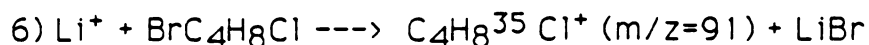
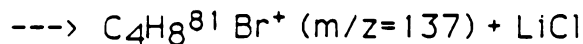
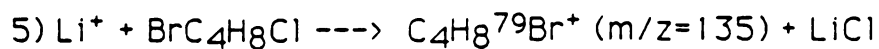
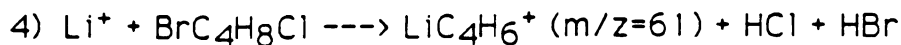
This compound showed addition to the lithium ion and a loss of HBr.



11) 1-Chloro-4-Bromobutane

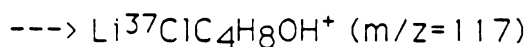
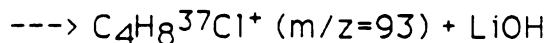
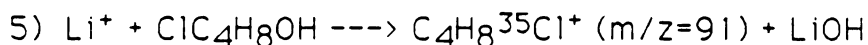
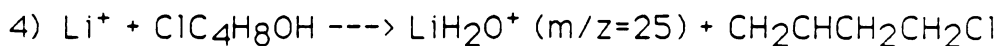
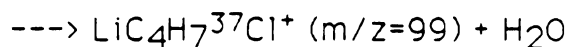
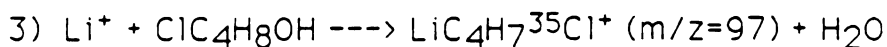
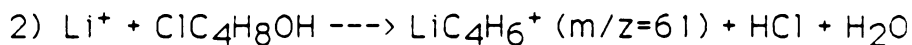
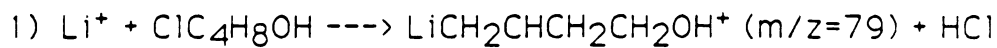
When this molecule reacts with lithium ions, addition to the molecule is observed as well as HBr, and HCl elimination. It should also be noted that HBr and HCl are lost at the same time, as well as the formation of two alkyl ion products, which were not seen with the 1-bromo-3-chloropropane.





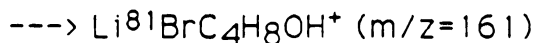
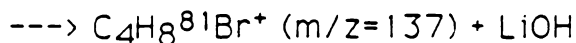
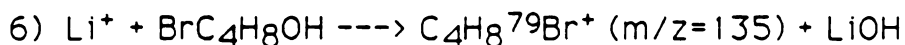
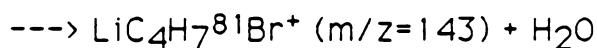
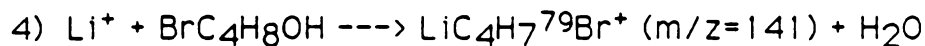
12) 4-Chlorobutanol

The chemistry of this compound is very interesting, as the products suggest. Dehydrohalogenation, dehydration, and a combination of both of these two reactions occur. Products where the OH^- is abstracted by the lithium ion are formed yielding a chloroalkyl cation.



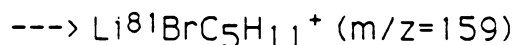
13) 4-Bromobutanol

The chemistry of this compound with the lithium ion is very similar to that observed for the 4-chloro-butanol.



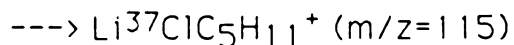
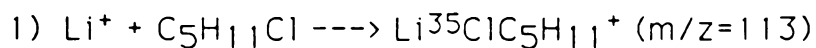
14) 1-Bromopentane

This compound adds to the lithium ion. Loss of HBr also occurs.



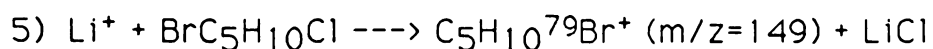
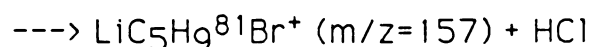
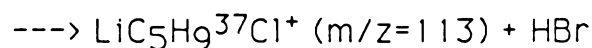
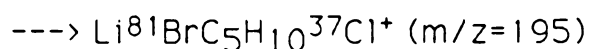
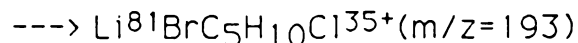
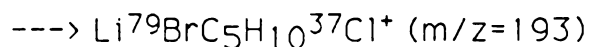
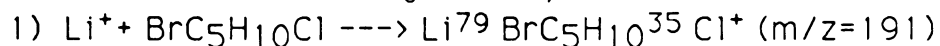
15) 1-Chloropentane

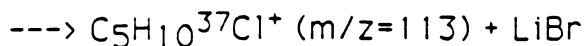
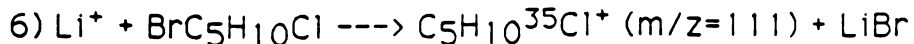
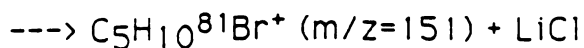
This compound adds to the lithium ion. Lithium ions also induce dehydrohalogenation of 1-chloropentane to eliminate HCl from the molecule.



16) 1-Bromo-5-Chloropentane

The chemistry that occurs with this compound when it reacts with the lithium ion is very similar with that observed for the 1-bromo-4-chlorobutane. Once again, alkyl ions are formed.





17) 3-Chloro-2-butanone

When lithium, and sodium ions were reacted with 3-chloro-2-butanone only addition products were observed. This compound was reacted with Li^+ with a prior suspicion that no reaction, i.e., dehydrohalogenation, would occur. This particular compound was chosen because it had a proton affinity greater than the proton affinity of LiCl . This compound was used to test the importance of the proton transfer step in determining whether product formation would occur. More will be explained about the function of this step in the mechanism in following sections.

18) Propylamine

Sodium and lithium ions showed addition products with propylamine. This compound was chosen to determine whether amines were reactive with Li^+ .

f. DISCUSSION OF MONOFUNCTIONAL COMPOUNDS WITH Li^+

The main focus of this work was to observe how bifunctional molecules react with Li^+ . The molecules studied varied in chain length from two to five carbons and had combinations of chlorine and a hydroxide group, chlorine and bromine, and bromine and a hydroxide group. As mentioned previously, it was hoped that the presence of the second functional group would stimulate chemistry not previously observed with only one functional group present. The logic behind this theory had to do with the possibility that extra energy would be available if the Li^+ could bind to both groups simultaneously, such that early barriers to the reaction might be surpassed.

Before the bifunctional molecules are discussed, it is important to understand how monofunctional molecules, such as the chloroalkanes, bromoalkanes, and alcohols react with Li^+ . This information will be useful in helping to interpret, and explain the more complex bifunctional molecules.

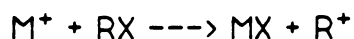
Appendix C contains a listing of the heats of formation for all the compounds used in this work, as well as the corresponding references.

g. CHEMISTRY OF Li^+ WITH CHLOROALKANES

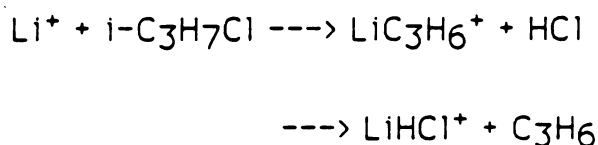
To begin the discussion, the chloroalkanes will be discussed, since a large portion of the work reported in the literature deals with how these molecules dehydrohalogenate when they react with Li^+ .

Two of the first published studies of work done with an alkali metal ion, lithium, and a chloroalkane were performed by Staley, and Beauchamp^{8,23}. Their purpose was to investigate the halide ion

transfer reaction between carbonium ions to determine the relative heterolytic bond energies of alkali halides to various carbonium ions as follows:

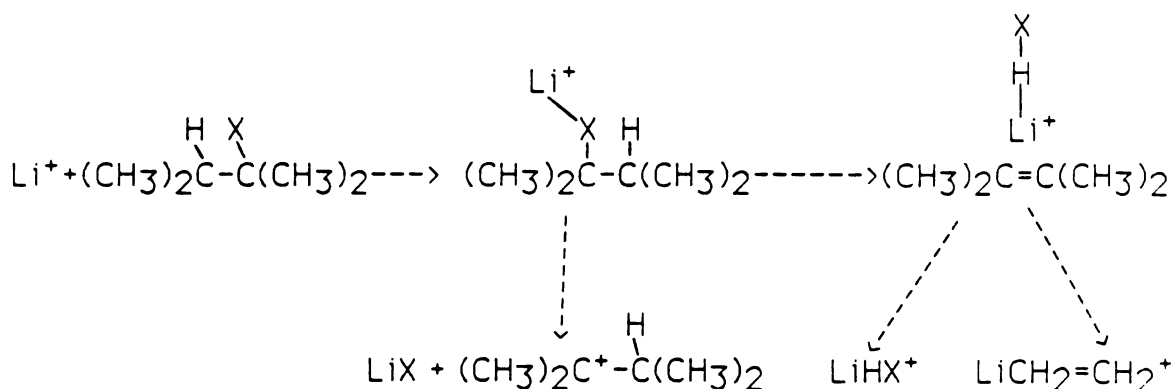


In their investigation isopropyl chloride was used, and the results were as follows:



They¹⁸ described the mechanism depicted in Scheme 2 as follows: the "association of an alkali ion and organic halide leads to the formation of a chemically activated species, which may dissociate to an alkali halide and carbonium ion. The intermediate may also eliminate HX to give an alkene, with the alkali ion remaining bound to either species in the products."

Scheme 2



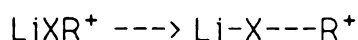
Note, that this interpretation of the mechanism provided by Staley and Beauchamp did not provide any mention of how the HX elimination occurred.

Allison and Ridge^{15,26} further studied how alkyl chlorides reacted with lithium ions to induce dehydrohalogenation. The chloroalkanes that were studied by Allison and Ridge are as follows: ethyl chloride, isopropyl chloride, n-butyl chloride, t-butyl chloride, benzyl chloride, 1-chloroadamantane, and t-amyl chloride.

Allison and Ridge found that the lithium ion was able to dehydrohalogenate t-butyl chloride, n-butyl chloride, t-amyl chloride, and isopropyl chloride, but not ethyl chloride.

Allison²⁶ discussed the mechanism of HX elimination from alkyl halides induced by the lithium ion, as first forming an electrostatic complex LiXR^+ . It was said that if the Li^+-X^- bond was sufficiently strong, that partial X^- transfer could occur, which would form HX and (R-H) from RX. To see if there was any correlation between the energy required for elimination of HX, and the reactivity of a compound with an alkyl metal ion, they evaluated the bond strengths for alkali halides with lithium, and some enthalpies of dehydrohalogenation for a number of compounds. No correlation existed.

Allison and Ridge then proposed a resonance structure for the LiXR^+ complex as follows:



This resonance structure suggests that charge generation could occur on the alkyl group. To see whether this resonance structure was plausible, Allison and Ridge evaluated the chloride affinities of the lithium ion vs. the alkyl cation, to indicate the stability of the resonance complex. The values are listed in Table 5.

The ethyl cation has a chloride affinity 31.2 kcal/mol greater than the chloride affinity of the lithium ion, and no reaction is observed to occur. This suggests that charge build-up on the halogenated carbon is necessary for the elimination of HCl to occur,

Table 5 Compilation of data for chlorine compounds

R ⁺	D(R ⁺ -Cl ⁻)kcal/mol	P.A.(R-H) kcal/mol
Li ⁺	155.10	(LiCl), 200.70
CH ₃ ⁺	220.62	196.70
C ₂ H ₅ ⁺	191.00	162.60
n-C ₃ H ₇ ⁺	188.30	179.80
s-C ₃ H ₇ ⁺	171.20	179.50
n-C ₄ H ₉ ⁺	179.70	194.90
t-C ₄ H ₉ ⁺	155.10	179.40
n-C ₅ H ₁₁ ⁺	170.50	179.00

All thermodynamic data were supplied by reference 35. It should be noted, that the P.A. of 1-pentene was approximated, to be 179.00, since all the other 1-ene compounds were calculated to be approximately 179 kcal/mol.

and did not occur with this molecule. Based on this observation, a general rule was proposed regarding the reactions of alkali metal ions with alkyl chlorides. If the $D(R^+-Cl^-)-D(M^+-Cl^-)$ is less than 30 kcal/mol, then HCl elimination will occur. It should however be noted, that this 30 kcal/mol was established by Allison and Ridge's results, and the true upper limit is somewhere between 24.7-31.2 kcal/mol. The unreactivity of ethyl chloride is consistent with these results.

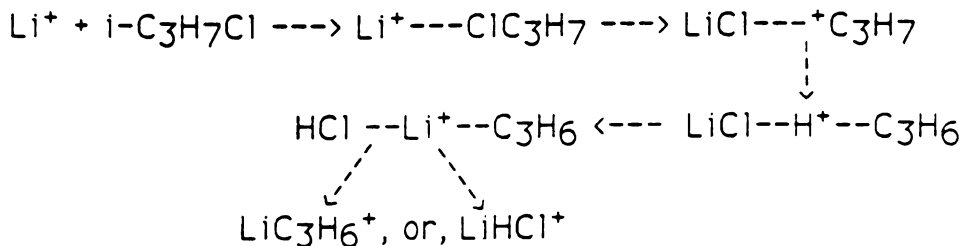
Allison and Ridge then suggest that the next step in the mechanism would be a β -H transfer as H^+ to eliminate HX. The energy of this step would depend on the proton affinity of the olefin formed by the loss of a β -hydrogen from R^+ . Since $LiHCl^+$ is formed in the reaction with isopropyl chloride, they suggested a limit on the heats of formation of this species, which was used to calculate a limit on the proton affinity of LiCl:

$$P.A. (LiCl) > 197 \text{ kcal/mol.}$$

Since the proton affinity of LiCl is greater than all the proton affinities for the compounds listed, the hydrogen shift is always exothermic. Once a hydrogen shift occurred, an $(olefin)Li^+(R-H)$ was the complex that resulted. This species fragmented by breaking the weakest bond to give the final products.

The mechanism Allison and Ridge proposed for the reaction of alkali metal ion with an alkyl halide, to be explained using isopropyl chloride, (and with alcohols to be seen later), is in Scheme 3 as follows:

Scheme 3

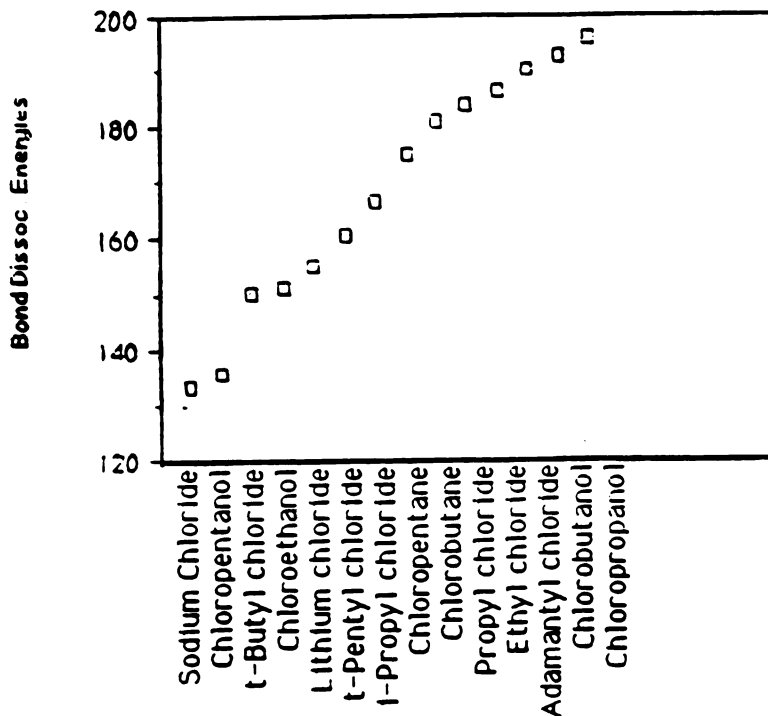


It should also be noted, that the compound n-pentyl chloride was studied in this work, since it deals with C₂ to C₅ molecules, and n-pentyl chloride has not been previously studied. It does dehydrohalogenate when it reacts with the lithium ion. The chloride affinity of the pentyl cation, and the proton affinity of 1-pentene are provided in Table 5.

Before continuing on with some cases where thermodynamic data has been experimentally determined for the reaction coordinate of the associated reactions, I would like to propose a means to predict whether the monofunctional molecules (i.e., chloroalkanes, bromoalkanes, and alcohols) and the bifunctional molecules (i.e., α,ω -chloro, bromo alkanes, α,ω -bromoalcohols, α,ω -chloroalcohols) to be considered in this work will undergo a reaction, when reacted with Li⁺. The compounds can be separated into three classes, those containing a chlorine, a bromine, and a hydroxyl group.

To consider the first case, observe Figure 19. Figure 19 is a plot of heterolytic bond dissociation energy for the various chloroalkanes to be discussed in this work. From Figure 19 it can be seen that the chloride affinity of Li⁺ is 155.10 kcal/mol. There are three compounds, chloroethanol, t-butylchloride, and chloropentanol, that have a chloride affinity less than 155.10 kcal/mol. Therefore, a possible reaction that may occur, when Li⁺ is reacted with these compounds, is the complete abstraction of Cl⁻ by Li⁺. The actual

Chloride Affinities



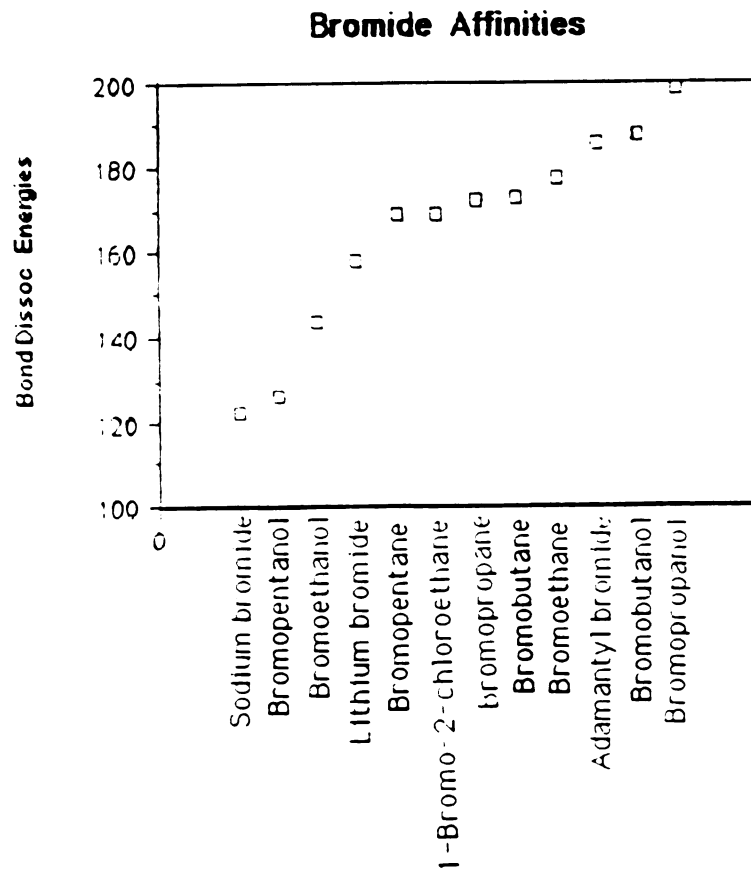
Compound	($R^+ - X^-$) (kcal/mol)
Sodium chloride	133.10
Chloropentanol	135.75
t-Butyl chloride	150.50
Chloroethanol	151.20
Lithium chloride	155.10
t-Pentyl chloride	160.76
i-Propyl chloride	166.70
Chloropentane	175.20
Chlorobutane	181.10
Propyl chloride	183.80
Ethyl chloride	186.50
Adamantyl chloride	190.20
Chlorobutanol	192.82
Chloropropanol	196.20

Figure 19 Chloride affinities

energy for this reaction is equal to ΔH_{ex} . It is known that when alkali metal ions react with alkyl halides, dehydrohalogenation results. Predicting whether dehydrohalogenation can occur is quite useful. It was determined by Allison²⁶ that if the $D(R^+-Cl^-)-D(M^+-Cl^-)$ was less than 30 kcal/mol, then a dehydrohalogenation reaction could occur. By observing Figure 19 it can be noted that Li^+ is able to induce dehydrohalogenation in all compounds with a bond dissociation energy less than 185.10 kcal/mol. This means of predicting reactions generally holds true for the monofunctional compounds discussed in this work, since the next step in the mechanism, as discussed previously, is the transfer of a proton, and the proton affinities of the monofunctional compounds under consideration were always less for the (R-H) than the proton affinities of (Li-Cl). This however is not necessarily the case for the bifunctional molecules. For bifunctional molecules this method of predicting if a reaction will occur can only be utilized when all other steps in the mechanism are exothermic after the transfer of the chlorine.

Figure 20 presents a similar situation. The bond dissociation energies are plotted for various compounds studied in this work containing bromine. It can be observed that the Li^+ can only completely abstract a Br^- from two compounds by the same logic used above. In order to predict if dehydrohalogenation should occur, it will be found in section i, that the $D(R^+-Br^-)-D(Li^+-Br^-)$ must be $< 31.8-34$ kcal/mol²⁶. Therefore, Li^+ should be able to induce dehydrohalogenation in all of the bromine compounds listed except bromopropanol. As mentioned above, this system works well for monofunctional compounds however, for bifunctional molecules in order for this method to be effective all other steps in the reaction must be thermodynamically "down hill", after the functional group is transferred.

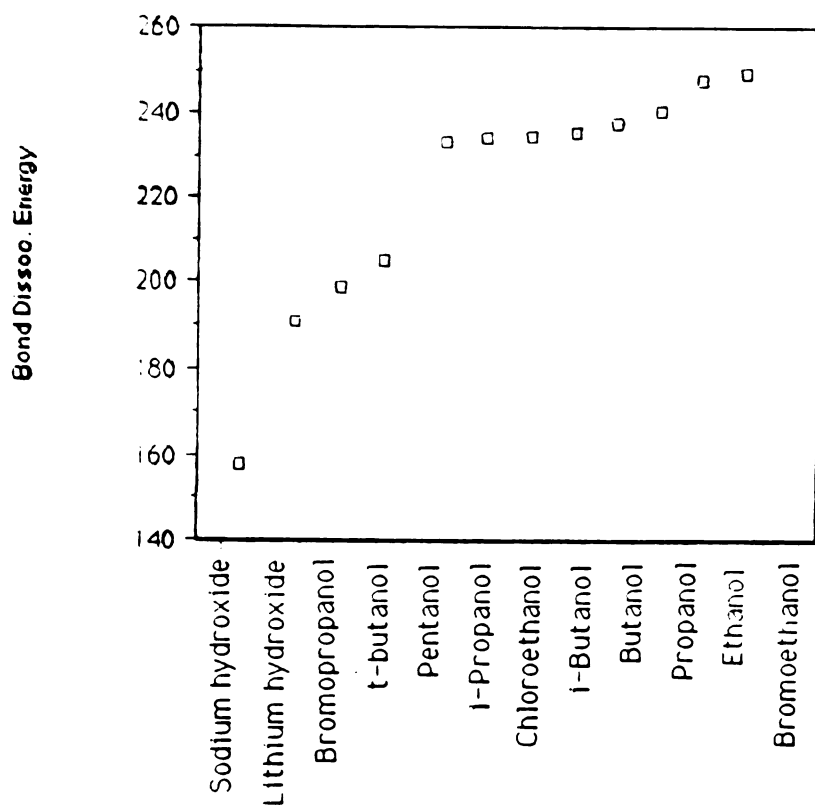
Figure 21 is a plot of bond dissociation energy versus the various alcohol compounds in this work. It can be observed that lithium ions can't abstract the hydroxide completely from any of the alcohols



Compound	($R^+ - X^-$) (kcal/mol)
Sodium bromide	122.40
Bromopentanol	126.65
Bromoethanol	144.00
Lithium bromide	153.90
Bromopentane	168.90
1-Bromo-2-chloroethane	169.10
Bromopropane	172.40
Bromobutane	172.70
Bromoethane	177.50
Adamantyl bromide	185.90
Bromobutanol	197.72
Bromopropanol	198.79

Figure 20 Bromide Affinities

Hydroxide Affinities



Compound	(R ⁺ - X ⁻) (kcal/mol)
Sodium hydroxide	159.93
Lithium hydroxide	188.60
Bromopropanol	198.74
t-Butanol	206.80
Pentanol	231.20
i-Propanol	231.90
Chloroethanol	232.30
i-Butanol	233.00
Butanol	235.00
Propanol	238.00
Ethanol	246.90
Bromoethanol	248.30

Figure 21 Hydroxide affinities

listed. Allison²⁶ suggests that a dehydration reaction will occur if $(R^+-OH^-)-(Li^+-OH^-) < 18.23 - 32.73$ kcal/mol. Therefore, it can be predicted that Li^+ can induce dehydration in bromobutanol, t-butanol, and pentanol. Once again, this method is sufficient for predicting if monofunctional compounds are going to react with Li^+ , however, for the bifunctional compounds all subsequent steps after the hydroxide is transferred to Li^+ must be exothermic.

Included in the tables were $(Na-X)$ affinities, where $X=Cl, Br,$ and OH , to show why only a few reactions are observed with Na^+ . The chloride affinity of Na^+ is 133.10 kcal/mol. Since none of the chlorine compounds listed have chloride affinities less than that reported for Na^+ , it can be assumed that Na^+ are unable to completely abstract a chlorine from any of the compounds. A similar situation exists for the other two cases. Since the bromide and hydroxide affinity of the Na^+ are sufficiently smaller, Na^+ are unable to completely abstract a bromide, or a hydroxide from any of the compounds listed in Figure 20, and 21.

For some time now, it has been known that the potential energy surface for an alkali metal ion reacting with an alkyl halide, or an alcohol, contains a double minima, as seen in Figure 18a.

In order to completely understand why some alkyl halides and alcohol react, and others do not, it is necessary to understand the energetics associated with the reaction. It was generally known, from the work of Allison and Ridge^{15,26} that the reaction would go to completion if a functional group could be transferred to the Li^+ . The energy required for this transfer to occur is E_b , the barrier to the reaction. See Figure 18a. If E_b is below the zero-line, the reaction will usually proceed to products. The zero-line corresponds to the energy available to the system based on the reactants. Until recently, this barrier height was only estimated, based on the difference in $D(R^+-X^-)-D(M^+-R^+)$, where M^+ is the lithium ion, and X^- is a halide, or a hydroxide group. However, work was conducted by Farrar and Creasy to estimate this barrier height for isopropyl

chloride³³. They suggested³³ that the barrier height depends on charge development on the alkyl group, and also involves the hydrogen atom migration to some extent.

In an effort to understand how alkyl chlorides react with lithium ions more fully, the energies for the isopropyl case will be calculated here. With the knowledge of how this system works, the information can be used to help explain the reactivity of bifunctional molecules containing a chloride. For the following discussion of isopropyl chloride and other chloroalkanes refer to Figure 22.

Beauchamp and Staley²³ estimated that the approximate binding energy of the lithium ion electrostatically bound to isopropyl chloride, E_b , is 30 kcal/mol. Their scale was relative to $D(\text{Li}^+-\text{H}_2\text{O}) = 34$ kcal/mol. As mentioned, to estimate E_b , one would generally consider the affinities of the lithium ion and the alkyl cation for the functional group to be transferred. If the affinity of the alkyl portion was greater than the affinity of the lithium ion it was assumed that no reaction would occur. Creasy and Farrar were able to approximate E_b to be 1.07 eV, or 24.7 kcal/mol. This data was provided by doing molecular beam experiments. This suggests that up to this point, where the chloride exchange occurs, the reaction is exothermic. The energy, E_b , could be roughly calculated if all the ΔH_f 's for the compounds were available, which they are not. The structure was assumed to be similar to $\text{LiCl}---\text{C}_3\text{H}_7^+$. The energy, E_b , could be calculated as follows:

$$E_b = D(\text{R}^+-\text{Cl}^-) + D(\text{Li}^+---\text{ClR}) - D(\text{Li}^+-\text{Cl}^-) - D(\text{LiCl}---\text{R}^+).$$

A closer look at the above expression for E_b will show that another way to represent the expression is $E_b = \Delta H_{ex} + D(\text{Li}^+ - \text{ClR}) - D(\text{R}^+ - \text{ClLi})$, where $\Delta H_{ex} = D(\text{R}^+-\text{Cl}^-) - D(\text{Li}^+-\text{Cl}^-)$. Since, it is known that $E_b = 24.7$ kcal/mol, and $\Delta H_{ex} = 15.8$ kcal/mol a rearrangement will show that $-D(\text{Li}^+-\text{RCl}) + D(\text{R}^+-\text{LiCl}) > 0$,

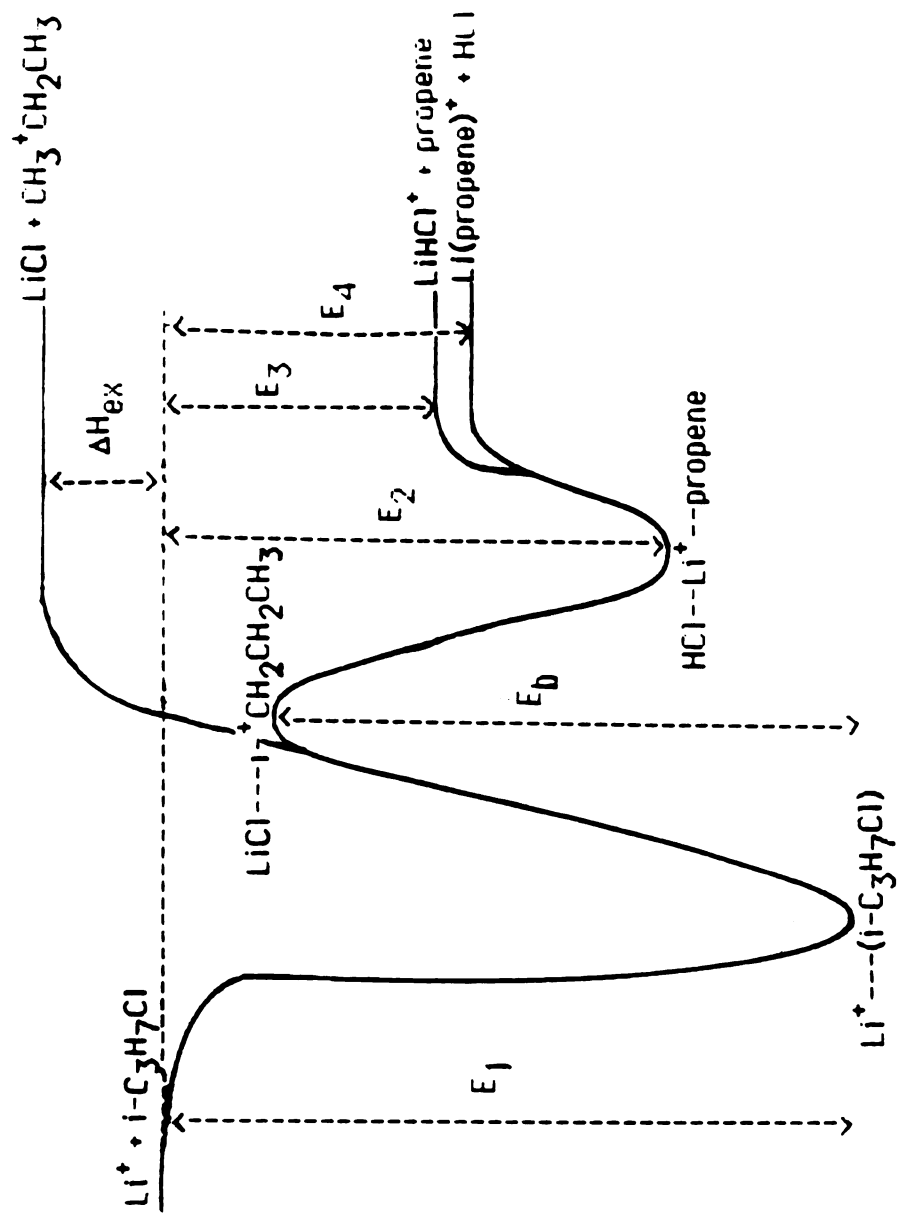


Figure 22 Potential energy diagram for Li^+ and isopropyl chloride

therefore, $D(R^+-LiCl) > D(Li^+-RCl)$. Since, $D(Li-RCl^+)=30$ kcal/mol, then the $D(R^+-LiCl) > 30$ kcal/mol. It should be noted, that $E_b > \Delta H_{ex}$, but $E_b < E_1$ so the reaction can proceed exothermically.

To calculate the energy, E_2 , a structure needs to be assumed. In order to get to Structure III, from Structure II, a hydrogen would need to be transferred. To determine if proton transfer from the alkyl cation is favorable, consider the P.A. of propene, and the P.A. of LiCl. Since the P.A. (LiCl) $>$ P.A. (propene), hydrogen transfer from the isopropyl cation, to yield propene, to the chloride to form HCl can occur. A good assumption for the resulting complex is $C_3H_6---Li^+---HCl$. To form this complex, the energy necessary, 17.3 kcal/mol, to form propene and HCl from isopropyl chloride, needs to be taken into account. Also, two bonds need to be formed. These include a bond formed between the lithium ion and propene, and the lithium ion and HCl. This process gives an energy of 42.2 kcal/mol to the system. Therefore, the net energy so far is calculated to be -24.9 kcal/mol. Note that this is not the correct energy, since the second bond to lithium is not as strong as the first one, so 10 kcal/mol need to be deducted to give a final E_2 of -14.9 kcal/mol³⁴. E_3 , and E_4 , the energies necessary to form products can be calculated from the heats of formation of the following reactions:

$$E_3 = \Delta H \quad Li^+ + \text{isopropyl chloride} \rightarrow HCl + Li(\text{propene})^+ = 1.15 \text{ kcal/mol} = .05 \text{ eV}$$

$$E_4 = \Delta H \quad Li^+ + \text{isopropyl chloride} \rightarrow LiHCl + (\text{propene})^+ = 5.07 \text{ kcal/mol} = .22 \text{ eV}$$

The products observed, and their associated branching ratios, depend on which ligand has the stronger affinity to the lithium ion.

The final energy value that needs to be calculated in Figure 22 is for the ΔH of dehydration as follows, in kcal/mol:

$i\text{-C}_3\text{H}_7\text{Cl}(-34.6) \rightarrow \text{HCl}(-22.1) + \text{C}_3\text{H}_6(4.8) \Rightarrow \Delta H_{\text{dehy}} = 17.3$
kcal/mol. This reaction is endothermic.

If the thermochemical data for ethyl chloride is compared to that of isopropyl chloride it can be understood why this small chloroalkane is unreactive. The ΔH_{ex} of ethyl chloride, which is 33.2 kcal/mol, is greater than the ΔH_{ex} for isopropyl chloride, which is 16.3 kcal/mol. Therefore, E_{b} is expected to be larger as well. Another hinderance to the reaction proceeding is that E_1 increases as the size of RX increases, where X=Cl, Br, and OH. So, E_1 is smaller for ethyl chloride than for isopropyl chloride. The intermediate II is therefore inaccessible due to the large value of E_{b} and smaller value for E_1 in the case of ethyl chloride.

h. MONOFUNCTIONAL ALCOHOLS REACTING WITH Li^+

The next monofunctional molecules to be discussed, as to how they react with Li^+ , are the alcohols. The alcohols present a different situation than the chloroalkanes, because their heterolytic bond strength, and therefore ΔH_{ex} , are substantially higher, and they are much less reactive. Most of the work previously reported on alcohols reacting with alkali metal ions has been done by Allison et al²⁶. In Allison's work, he proposes that the alkali metal ion, lithium, induces dehydration in alcohols, by the same mechanism as in the case of alkyl halides reacting with Li^+ , as seen in Scheme 3.

The alcohols that Allison studied include methanol, ethanol, n-propanol, isopropanol, n-butanol, and t-butanol. It should be noted, that the only compound that the lithium ion induced dehydrohalogenation in was t-butanol. Table 6 lists all of the alkyl cations, and the Li^+ , used by Allison, and their associated hydroxide affinities.

Based on the results of the experiments performed, Allison deduced a general rule that water elimination would occur only if the $D(\text{R}^+-\text{OH}^-)-D(\text{Li}^+-\text{OH}^-) < 18.23-32.73$ kcal/mol. Once again, the

Table 6 Compilation of data for alcohols

R ⁺	D(R ⁺ -OH ⁻)kcal/mol	P.A.(R-H) kcal/mol
Li ⁺	188.60±4 ^b	(LiOH), 241.00
CH ₃ ⁺	276.53	96.70
C ₂ H ₅ ⁺	238.03	162.60
n-C ₃ H ₇ ⁺	238.23	179.80
s-C ₃ H ₇ ⁺	222.33	179.50
n-C ₄ H ₉ ⁺	235.03	194.90
t-C ₄ H ₉ ⁺	206.83	179.40

All thermodynamic data were supplied by reference 35, except the value marked with a "b", which came from reference 36.

importance of charge development on the carbon with the hydroxide is stressed as being important in the elimination reaction mechanism.

To understand why dehydration did not occur in the isopropyl complex, Allison and Ridge looked at the bond strength of the Li^+ -isopropyl complex. They wanted to make sure that it was less than the hydroxide affinities, since no reaction occurred. Although the bond strength of $\text{D}(i\text{-C}_3\text{H}_7\text{OH-Li}^+)$ was not known, the $\text{D}(\text{CH}_3\text{OH-Li}^+)$ was known to be 38 kcal/mol. The hydroxide affinity difference is 32.73 kcal/mol and therefore, a reaction should have been observed. Since no reaction was observed, this compound was used to set the upper bound to the general rule. As for the other alcohols studied, it was assumed that they were unreactive based on the general rule proposed by Allison and Ridge. These results suggested that $\text{D}(\text{ROH-Li}^+)$ might play an analogous role in alcohols, as the $\text{D}(\text{RX-Li}^+)$ does in the alkyl halides rule.

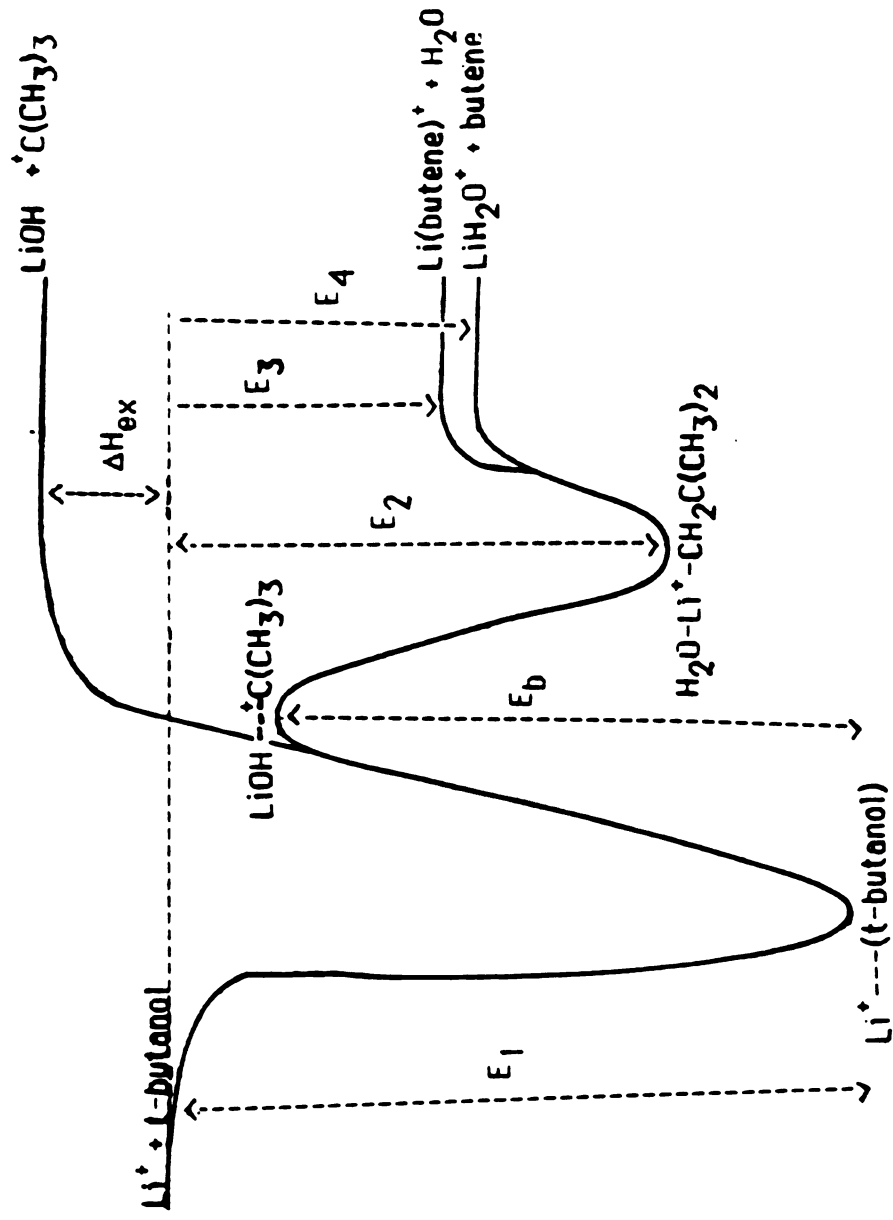
If the proton affinities are considered in Table 6, it can be seen that H^+ transfer to make H_2O is not a problem since the $\text{P.A.}(\text{Li-OH}) \gg \text{P.A.}(\text{R-H})$ in all cases. Since LiHOH^+ is formed in the reaction of t-butyl alcohol, Allison placed a limit on the heat of formation of this species, and therefore a limit can be placed on the proton affinity of LiOH :

$$\text{P.A.}(\text{Li-OH}) > 218.9 \text{ kcal/mol.}$$

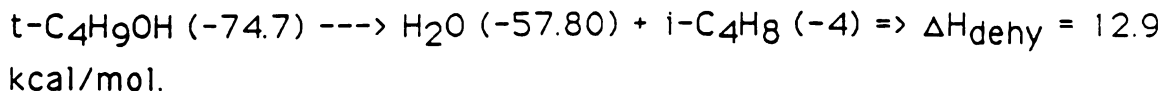
Farrar and Creasy also did some work with the lithium ion, and t-butanol^{37,38}. They were able to estimate the $\text{D}(\text{Li}^+\text{-HOC}_4\text{H}_9)$ of this complex to be 2.0 eV, which corresponds to 46.12 kcal/mol. They were also able to estimate the heats of formation of LiH_2O^+ (-17.99 kcal/mol), and $\text{Li}(\text{butene})^+$ (-11.99 kcal/mol), the two products in a dehydration reaction of t-butanol. They also estimated the $\text{D}(\text{Li}^+\text{-H}_2\text{O})$ to be 28.83 kcal/mol, and the $\text{D}(\text{Li}^+\text{-butene})$ to be 34.13 kcal/mol.

Based on the information that has been provided, it is now possible to look at the energetics involved when Li^+ reacts with t-butanol to get an idea of how the system reacts. Once this information is understood, it will be helpful in understanding, and interpreting what is occurring in bifunctional systems that contain an alcohol. See Figure 23. The energy, E_1 , has been provided by Farrar to be -46.1 kcal/mol ^{37,38}. The energy, E_b , has also been estimated by Farrar³³ to be 36.9 kcal/mol . It is known that $E_b = D(\text{Li}^+-\text{t-butanol}) - D(\text{LiOH}-\text{t-C}_4\text{H}_9^+) - D(\text{Li}^+-\text{OH}^-) + D(\text{OH}^--\text{t-C}_4\text{H}_9^+)$. Since the heat of exchange, $\Delta H_{\text{ex}} = -D(\text{t-C}_4\text{H}_9^+-\text{OH}^-) - D(\text{Li}^+-\text{OH}^-)$, E_b can be written as $E_b = \Delta H_{\text{ex}} - D(\text{LiOH}-\text{t-C}_4\text{H}_9^+) + D(\text{Li}^+-\text{HOC}_4\text{H}_9)$, therefore, $E_b > \Delta H_{\text{ex}}$. If this reaction is rearranged, the $-D(\text{LiOH}-\text{t-C}_4\text{H}_9^+) + D(\text{Li}^+-\text{HOC}_4\text{H}_9) > 0$, so it can be deduced, that the $D(\text{Li}^+-\text{HOC}_4\text{H}_9) > D(\text{LiOH}-\text{t-C}_4\text{H}_9^+)$. Once again, ΔH_{ex} , 22 kcal/mol , and E_b are less than E_1 and the reaction can proceed as in the case of isopropyl chloride and Li^+ .

To go from the intermediate II to the complex III, a proton transfer will need to occur. A proton transfer is plausible if the $\text{P.A.}(\text{LiOH}) > \text{P.A.}(\text{i-C}_4\text{H}_8)$, which it is. The energy of the second well on the potential surface, E_2 , can also be calculated as follows: $E_2 = -D(\text{Li-butene}) - D(\text{Li-HOH}) - \Delta H(\text{t-butanol} \rightarrow \text{H}_2\text{O} + \text{butene}) - 10 = -28.83 - 34.113 + 12.9 + 10 = -40.06 \text{ kcal/mol}$. The addition of 10 kcal/mol is used to take into account, that the Li^+ does not form as strong of a bond to the second ligand. The number, 10 kcal/mol , arose from a paper by Keese and Castleman³⁴, who provides thermochemical data on gas/phase ion/molecule associations, and clustering reactions. The energy that it takes to make products from reactants, E_3 , and E_4 , can be calculated using the heats of formation for the reaction. $E_3 = \Delta H = (\text{Li}^+ + \text{t-butanol} \rightarrow \text{Li-butene}^+ + \text{HCl}) = -162.4 - (-74.7) + 40.90 + 57.8 = -11 \text{ kcal/mol}$. $E_4 = \Delta H = (\text{Li}^+ + \text{t-butanol} \rightarrow \text{LiH}_2\text{O}^+ + \text{butene}) = -162.4 - (-74.7) + 69 + .1 = -18.6 \text{ kcal/mol}$.

Figure 23 Potential energy diagram for Li^+ and *t*-butanol

Finally, the ΔH of dehydration can be calculated as follows, in kcal/mol:



It is not unreasonable that the straight chain alcohols were unreactive, because the molecules have a larger $D(\text{R}^+-\text{OH}^-)$, for ethanol to butanol, of 242 to 236 kcal/mol, respectively. This large heterolytic bond strength leads to larger ΔH_{ex} 's, which contribute to larger E_b s, which prohibits a conversion of complex I to intermediate II. This is prohibited because charge generation on the alkyl group is limited. Another point that needs to be reinforced before going on is the importance of the reaction barrier. Consider Li^+ reacting with isopropyl chloride and isopropanol. In the former case the products are formed exothermically, and the ΔH of dehydration is 12.1 kcal/mol, which implies that less energy is required to form propene from the alcohol than from the chloroalkane. However, in the case involving the alcohol, ΔH_{ex} is sufficiently large, such that the intermediate II is inaccessible from the energy available due to the formation of the initial complex, thus reactions for the alcohol does not occur.

i. CHEMISTRY OF Li^+ WITH BROMOALKANES

The last class of monofunctional alkanes are the bromoalkanes. These compounds were studied in this work to establish a limit on the difference in bond strength between the alkyl bromide, and lithium bromide, $D(\text{R}^+-\text{Br}^-) - D(\text{Li}^+-\text{Br}^-)$, where dehydrohalogenation would be observed. Also, to establish a limit on the proton affinity of LiBr , and to observe if it was in experimental agreement with the value provided by Farrar and Creasy³³. It was supposed that the alkyl bromides would follow the mechanism depicted in Scheme 3 for the dehydrohalogenation of alkyl chlorides by lithium

ions through charge build-up on the alkyl group. Based on the results, this was the case.

The bromide compounds studied in this work include the ethyl bromide, n-propyl bromide, isopropyl bromide, n-butyl bromide, and n-pentyl bromide. The results showed, that the lithium ion was able to dehydrohalogenate all of the alkyl bromides except ethyl bromide. Table 7 lists the various alkyl cations and the lithium ion, and their various bromide affinities.

Based on the results of the experiments performed, it was deduced that HBr elimination would occur only if the $D(R^+-Br^-) - D(Li^+-Br^-) < 31.8-34.0 \text{ kcal/mol}$. Bromoethane was assumed to be unreactive since charge generation did not occur on the halogenated carbon. To set a limit on the P.A. of lithium bromides, the results of the reactions were observed. The proton affinity can be noted in Table 7. Since HBr elimination was observed in n-butyl bromide, (i.e., this compound has the highest P.A. in Table 7), it can be said that the proton affinity of LiBr $> 194.9 \text{ kcal/mol}$. Based on work done by Creasy and Farrar, who provided the $\Delta H(LiHBr^+)$ to be 134.3 kcal/mol , the proton affinity could be calculated to be 195 kcal/mol . This value is in good agreement with the estimated proton affinity from the results obtained, therefore, the $P.A.(LiBr) = 195 \text{ kcal/mol}$.

Work has also been reported where Li^+ was reacted with isopropyl bromide by Creasy, and Farrar, who approximated the barrier height of E_b , in Figure 22³³. The barrier height that they reported was 27.67 kcal/mol . They also reported some significant numbers relating to the $D(Li^+-HBr)$, 20.29 kcal/mol , and $D(Li^+-propene)$, 23.06 kcal/mol . Staley and Beauchamp^{18,23} reported an approximate number of E_1 in kcal/mol for the $D(Li^+ - \text{isopropyl bromide})$. This corresponds to the E_1 on the potential energy surface in Figure 24. Since most of the thermochemical data have been provided for the isopropyl bromide system, and this compound

Table 7 Compilation of data for bromine compounds

R ⁺	D(R ⁺ -Br ⁻)kcal/mol	P.A.(R-H) kcal/mol
Li ⁺	148.50	(LiBr), 194.40
CH ₃ ⁺	219.50	196.70
C ₂ H ₅ ⁺	182.50	162.60
n-C ₃ H ₇ ⁺	180.30	179.80
s-C ₃ H ₇ ⁺	163.40	179.50
n-C ₄ H ₉ ⁺	177.70	194.90
t-C ₄ H ₉ ⁺	146.90	179.40
n-C ₅ H ₁₁ ⁺	170.50	153.0

All thermodynamic data were supplied from reference 35.

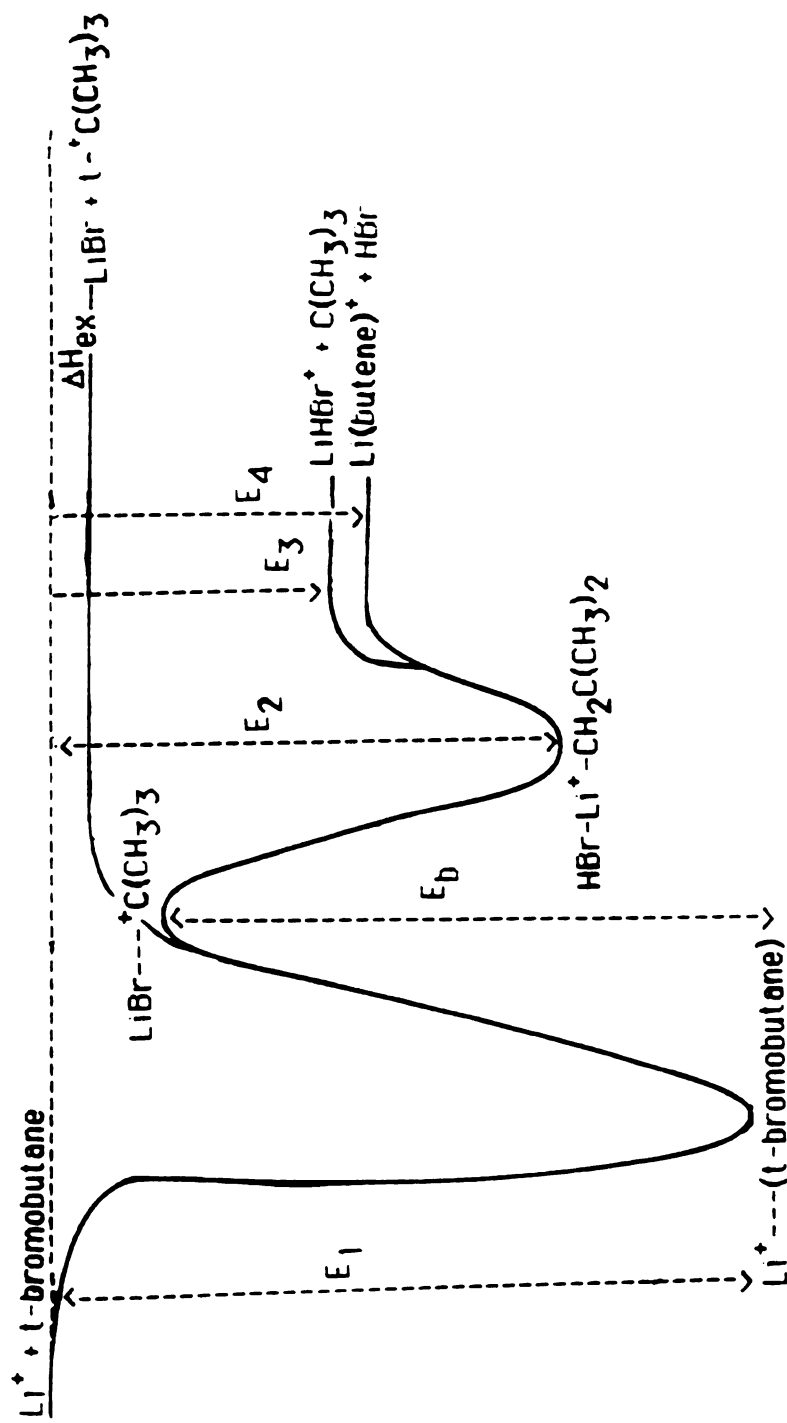


Figure 24 Potential energy diagram for Li^+ and isopropyl bromide

is known to eliminate HBr when induced by Li^+ , this systems energetics will be studied to help explain bifunctional system's containing a bromide.

As mentioned previously, $E_1 = 31$ kcal/mol, and $E_b = 27.67$ kcal/mol. Since $E_1 > E_b$ the reaction to the intermediate II proceeds. Note also, that $E_b > \Delta H_{\text{ex}}$ so the reaction is exothermic. The proton transfer from intermediate II to complex III can occur easily since the P.A.(LiBr), 195 kcal/mol, is greater than the P.A.(C_3H_6), which is 159.5 kcal/mol. The energy, E_2 , can be calculated as follows: $E_2 = \Delta H(\text{i-C}_3\text{H}_7\text{Br} \rightarrow \text{HBr} + \text{propene}) - D(\text{Li}^+\text{-propene}) - D(\text{Li}^+\text{-HBr}) + 10 = 19.2 - 20.3 - 23.06 + 10 = -14.16$ kcal/mol.

To calculate the energy required to form products, E_3 , and E_4 , from the reactants, the heats of formations are employed. The numbers utilized were from data provided by Creasy and Farrar³³. The calculations are as follows:

$$E_3 = \Delta H (\text{Li}^+ + \text{i-C}_3\text{H}_7\text{Br} \rightarrow \text{LiHBr}^+ + \text{propene}) = -0.9 \text{ kcal/mol.}$$

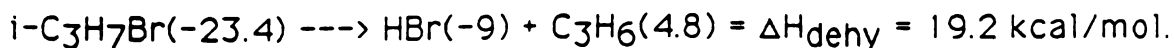
$$E_4 = \Delta H (\text{Li}^+ + \text{i-C}_3\text{H}_7\text{Br} \rightarrow \text{Li-propene}^+ + \text{HBr}) = -3.7 \text{ kcal/mol.}$$

It should be noted, that the ΔH_{ex} , the energy required to form an alkyl cation and LiBr is as follows:

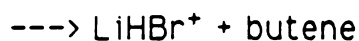
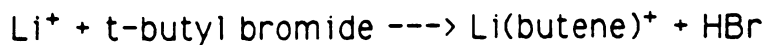
$$\Delta H_{\text{ex}} (\text{Li}^+ + \text{i-C}_3\text{H}_7\text{Br} \rightarrow \text{LiBr} + \text{i-C}_3\text{H}_7^+) = -162.4 - (-23.4) + (-37) + 190.9 = 14.9 \text{ kcal/mol.}$$

This reaction is endothermic, so there is no likelihood that the lithium ion will abstract a bromide, with the initial energy available to the system.

To calculate the ΔH of dehydrohalogenation, the following reaction in kcal/mol can be used:



Weiting, Staley, and Beauchamp²⁴ also studied how t-butyl bromide reacts with the lithium ion. Their results were as follows:



These results prove to be very interesting, since the formation of butene and LiBr are observed because the exchange energy, ΔH_{ex} , is negative. No other monofunctional compounds have shown a negative exchange energy. This is an important example, since a negative exchange energy will be observed often with the reactions of bifunctional molecules with the lithium ion. Therefore, the thermochemical information should be considered for this reaction. See Figure 25.

The energy, E_1 , for the initial interaction complex has been estimated to be greater than 31 kcal/mol, since isopropyl bromide was found to be 31 kcal/mol. Based on work done by Staley and Beauchamp²³ it can be observed that $D(\text{Li}^+ \text{--propene}) < D(\text{Li}^+ \text{--butene})$. Therefore, it will be assumed that this trend would hold true if a bromide were added, such that the $D(\text{Li}^+ \text{--}i\text{C}_3\text{H}_7\text{Br}) < D(\text{Li}^+ \text{--}t\text{-C}_4\text{H}_9\text{Br})$.

Since no information has been provided for E_b , it can only be assumed that it is a negative number, less than that for the initial interaction complex, or no reaction would be observed, therefore, $E_b < E_1$.

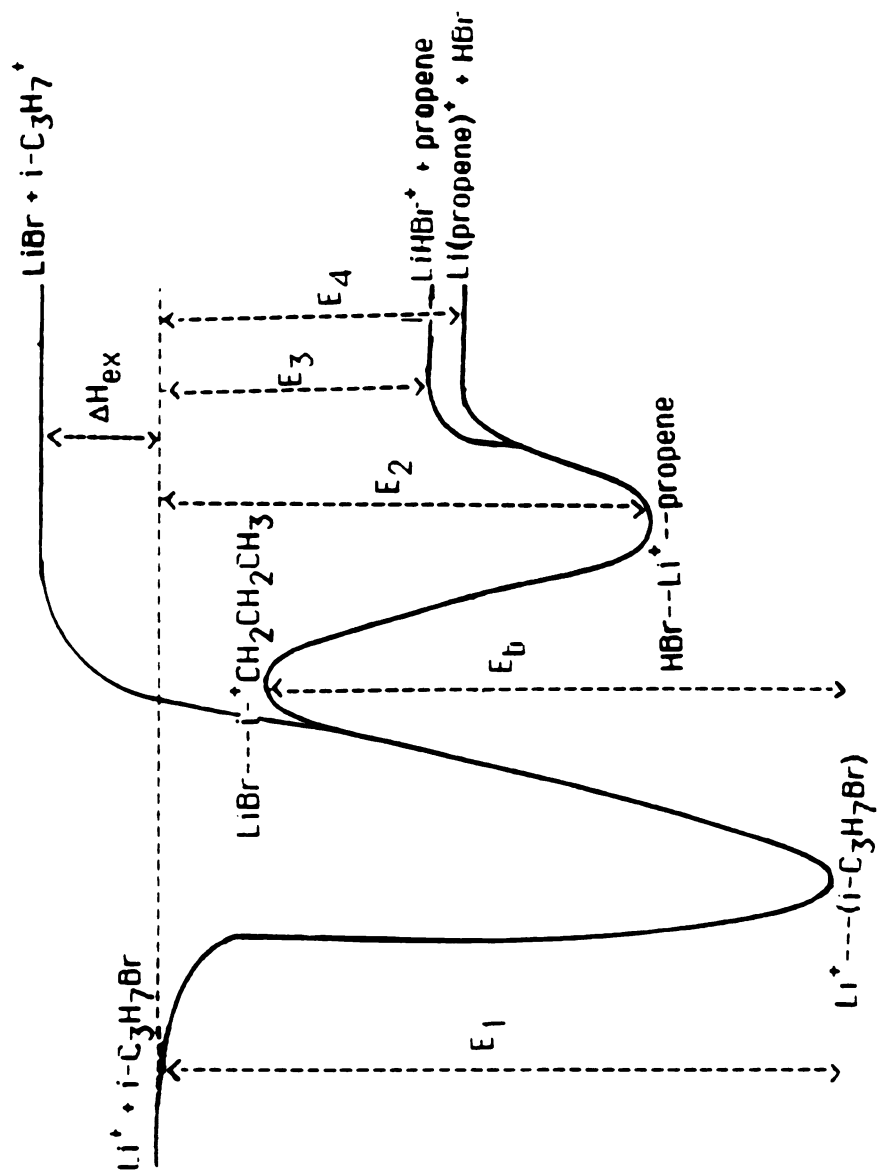


Figure 25 Potential energy diagram for Li^+ and *t*-butyl bromide

The energy, E_2 , for the reaction where a β -Hydrogen on the t-butyl cation is shifted onto the bromide to form the complex $\text{HBr} \cdots \text{Li}^+ \cdots \text{butene}$, can be calculated as follows:

$$E_2 = \Delta H (\text{t-butyl bromide} \rightarrow \text{butene} + \text{HBr}) - D(\text{Li}^+ \cdots \text{butene}) - D(\text{Li}^+ \cdots \text{HBr}) + 10.$$

$$E_2 = 19.0 - 19.1 - 28.3 + 10 = 18.1 \text{ kcal/mol.}$$

Once again, the 10 kcal/mol was estimated based on experiments by Keesee and Castleman to account for a weaker bond being formed to the lithium ion by the second ligand³⁴.

To calculate the position of the products on the potential energy surface, ΔH_{ex} , E_3 , and E_4 , the heats of formation for the respective reactions are utilized, and are as follows:

$$\Delta H_{\text{ex}} (\text{Li}^+ + \text{t-butyl bromide} \rightarrow \text{LiBr} + \text{i-C}_4\text{H}_9^+) = -162.4 - (-32) - 37 + 165.8 = -1.6 \text{ kcal/mol.}$$

$$E_3 = (\text{Li}^+ + \text{t-butyl bromide} \rightarrow \text{LiHBr}^+ + \text{butene}) = -162.4 - (-32) + 134.3 - 5.2 = -1.3 \text{ kcal/mol.}$$

$$E_4 = (\text{Li}^+ + \text{t-butyl bromide} \rightarrow \text{Li}(\text{butene})^+ + \text{HBr}) = -162.4 - (-32) + 129.57 - 9 = -9.8 \text{ kcal/mol.}$$

Since the proton affinity of LiBr is approximately equal to the proton affinity of i-C₄H₈, proton transfer occurs via $\text{LiBr} \cdots \text{H}^+ \cdots \text{C}_4\text{H}_8$, and this intermediate can dissociate at competitive rates to yield [LiBr and C₄H₉⁺] or [LiHBr⁺ and butene], or [Li(butene⁺) and HBr].

j. Chemistry of Li^+ With Bifunctional Molecules

After reviewing the chemistry of Li^+ with the monofunctional alkanes, now the real focus of this work, the bifunctional molecules reacting with Li^+ , will be discussed. To observe if the reactivity of bifunctional molecules with Li^+ are similar to that of the monofunctional molecules, some information should be kept in mind. The reactivity of Li^+ with R^+X^- , where $\text{X}=\text{Cl}$, Br , and OH , parallels the heterolytic bond strength of RX , such that, as the RX bond increases, reactivity decreases as seen in the case of monofunctional alcohols. Also, barrier height was important, in predicting reactivity and was found to relate to the magnitude of ΔH_{ex} . As ΔH_{ex} increased, so did the barrier height. Recall, that ΔH_{ex} expresses the difference in the affinities of Li^+ and R^+ for the anion X^- . The ΔH_{ex} was found to be positive for most chloroalkanes, and alcohols, which indicates that the alkyl group has a greater affinity for the anion and complete functional group abstraction by Li^+ will not occur exothermically. Cases have been observed with monofunctional compounds where $\Delta H_{\text{ex}} < 0$. The reactions were as follows: $\text{M}^+ + \text{RX} \rightarrow \text{MX} + \text{R}^+$, where $\text{M}^+ = \text{Li}^+, \text{Na}^+, \text{Cs}^+, \text{Li}^+$ and $\text{RX} = t\text{-C}_4\text{H}_8\text{Br}^{24}$, $(\text{CH}_3)_2\text{BrC}-\text{C}(\text{CH}_3)_2\text{Br}^{24}$, $\text{C}_6\text{H}_5\text{CH}_2\text{Cl}^{25}$, and 1-chloroadamantane¹⁵ respectively. By observing the ΔH_{ex} values of monofunctional molecules which react with Li^+ , and those which did not, it appears that the reactive systems had small positive, or negative values of ΔH_{ex} . These situations exist when $D(\text{M}^+-\text{X}^-)$ is large, or when $D(\text{R}^+-\text{X}^-)$ is small. Since $D(\text{M}^+-\text{X}^-)$ decreases as the size of the metal increases, this correlates well with the reactivity of the alkali ions $\text{Li}^+ > \text{Na}^+ > \text{K}^+ > \text{Cs}^+$, for $\text{X} = \text{Cl}$, Br , and OH .

The previous work on bifunctional compounds was conducted by Staley, Weiting, and Beauchamp²⁴, who observed the reactions of various organic dibromides containing four to six carbons with Na^+ , and K^+ . A compilation of this work can be found in Table 8.

Table 8 Previous work with bifunctional molecules, and alkali metal ions

Reaction	Observed reactivity ^a
$\text{Li}^+ + (\text{CH}_3)_2\text{CHBr} \begin{cases} \xrightarrow{<1\%} (\text{CH}_3)_2\text{CH}^+ + \text{LiBr} \\ \xrightarrow{100\%} [\text{C}_2\text{H}_5]\text{Li}^+ + \text{HBr} \end{cases}$	Not observed Fast
$\text{Li}^+ + \text{CH}_3\text{COBr} \rightarrow \text{CH}_2\text{CO}^+ + \text{LiBr}$	Not observed
$\text{Li}^+ + (\text{CH}_3)_3\text{CBr} \begin{cases} \xrightarrow{6\%} (\text{CH}_3)_3\text{C}^+ + \text{LiBr} \\ \xrightarrow{80\%} [\text{C}_2\text{H}_5]\text{Li}^+ + \text{HBr} \\ \xrightarrow{1\%} \text{HBrLi}^+ + \text{C}_2\text{H}_5 \end{cases}$	Slow Fast Slow
$\text{Li}^+ + \text{CH}_3\text{CH}_2\text{COBr} \begin{cases} \xrightarrow{60\%} \text{CH}_3\text{CH}_2\text{CO}^+ + \text{LiBr} \\ \xrightarrow{37\%} [\text{CH}_3\text{CHCO}]\text{Li}^+ + \text{HBr} \end{cases}$	Fast Fast
$\text{Na}^+ + \text{Br}-\text{C}_5\text{H}_9-\text{Br} \rightarrow \text{C}_5\text{H}_9\text{Br}^+ + \text{NaBr}$	Not observed
$\text{Na}^+ + \text{Br}-\text{C}_5\text{H}_9-\text{Br} \rightarrow \text{C}_5\text{H}_9\text{Br}^+ + \text{NaBr}$	Not observed
$\text{Na}^+ + \text{Br}-\text{C}_5\text{H}_9-\text{Br} \rightarrow \text{C}_5\text{H}_9\text{Br}^+ + \text{NaBr}$	Not observed
$\text{Na}^+ + \text{Br}-\text{C}_{10}\text{H}_{16}-\text{Br} \rightarrow \text{C}_{10}\text{H}_{16}\text{Br}^+ + \text{NaBr}$	Not observed
$\text{Na}^+ + \text{Br}-\text{C}_6\text{H}_8-\text{Br} \rightarrow \text{C}_6\text{H}_8\text{Br}^+ + \text{NaBr}$	Not observed
$\text{Na}^+ + \text{Br}-\text{C}_6\text{H}_8-\text{Br} \rightarrow \text{C}_6\text{H}_8\text{Br}^+ + \text{NaBr}$	Fast
$\text{K}^+ + \text{Br}-\text{C}_6\text{H}_8-\text{Br} \rightarrow \text{C}_6\text{H}_8\text{Br}^+ + \text{KBr}$	Not observed

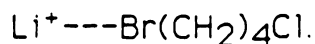
This work deals with many α,ω -bisubstituted compounds composed of chlorines and bromides, chlorines and hydroxides, and bromines and hydroxides, and how they react with Li^+ . The discussion will explain why two monofunctional compounds such as ethanol, and chloroethane are unreactive, yet their bifunctional analog, 1-chloro-2-ethanol, reacts with Li^+ . To understand the type of reactions that are observed when Li^+ react with bifunctionals, the α,ω -bromo, chloro compounds will be examined first.

k. Chemistry of Li^+ With α,ω -bromo, chloroalkanes

To start the discussion of the work reported in this study, see Table 4 for a summary of the reactions observed when Li^+ reacts with α,ω -bromo, chloro compounds. By considering the branching ratios in Table 4 some general observations can be noted. It can be observed, that, in all cases, the loss of HCl is much greater than the loss of HBr , and the loss of LiCl is much greater than the loss of LiBr . Therefore, the chlorine substituent reacts to a greater extent with Li^+ than the bromine end. Also, for longer chains, alkyl cations are formed where they were not observed for their monofunctional analogues.

Since most of the information on the heats of formation can be approximated for the $\text{Cl}(\text{CH}_2)_4\text{Br}$ system, the energetics for this case will be discussed. The potential energy surface that will be used to explain the mechanism is a triple minimum curve, see Figure 26. The proposed mechanism for the reaction, and the associated energies will be discussed.

If the initial interaction complex is considered, three possibilities arise as to how the lithium ion could approach the molecule. The Li^+ could approach the bromine end of the molecule to form this complex:



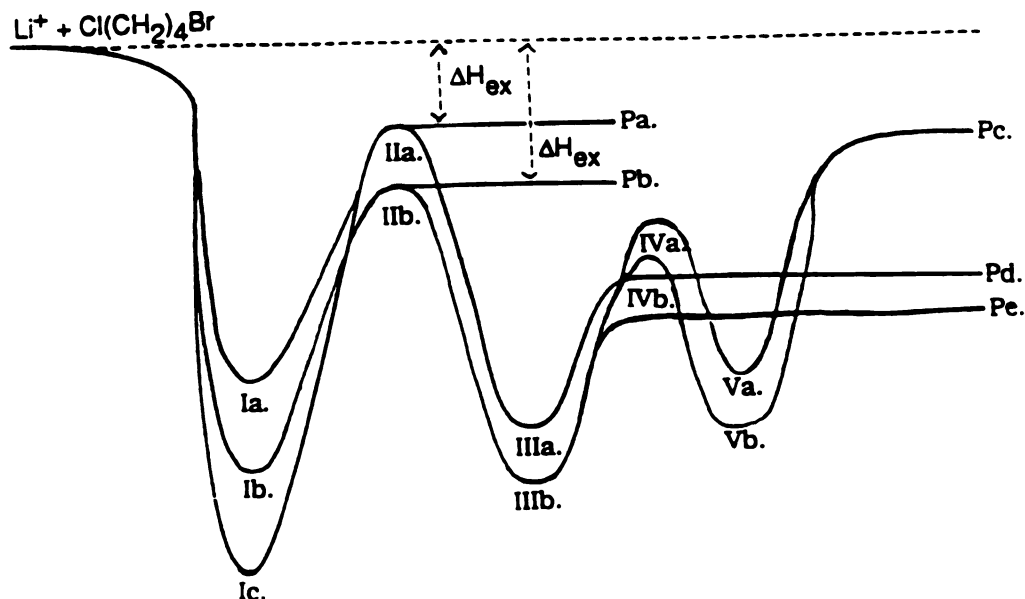
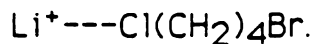


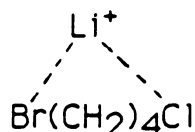
Figure 26 Potential energy diagram for Li^+ , and α,ω -chloro, bromobutane

- | | | | |
|-------|---|------|---|
| Ia. | $\text{Li}^+ \cdots (\text{Cl}(\text{CH}_2)_4\text{Br})$ | IVb. | $\text{LiCl} \cdots {}^+\text{CH}_2\text{CH}_2\text{CHCH}_2$ |
| Ib. | $\text{Li}^+ \cdots (\text{Br}(\text{CH}_2)_4\text{Cl})$ | Va. | $\text{HBr} \cdots \text{Li}^+ \cdots \text{CH}_2\text{CHCHCH}_2$ |
| Ic. | $\text{cyclo}(\text{Li}^+(\text{Cl}(\text{CH}_2)_4\text{Br}))$ | Vb. | $\text{HCl} \cdots \text{Li}^+ \cdots \text{CH}_2\text{CHCHCH}_2$ |
| IIa. | $\text{LiBr} \cdots \text{cyclo}((\text{CH}_2)_4\text{Cl}^+)$ | Pa. | $\text{LiBr} + \text{cyclo}((\text{CH}_2)_4\text{Cl}^+)$ |
| IIb. | $\text{LiCl} \cdots \text{cyclo}((\text{CH}_2)_4\text{Br}^+)$ | Pb. | $\text{LiCl} + \text{cyclo}((\text{CH}_2)_4\text{Br}^+)$ |
| IIIa. | $\text{HBr} \cdots \text{Li} \cdots {}^+\text{CH}_2\text{CH}_2\text{CHCH}_2\text{Cl}$ | Pc. | $\text{Li}(\text{CH}_2\text{CHCHCH}_2)^+ + \text{HCl} + \text{HBr}$ |
| IIIb. | $\text{HCl} \cdots \text{Li} \cdots {}^+\text{CH}_2\text{CH}_2\text{CHCH}_2\text{Br}$ | Pd. | $\text{Li}(\text{ClCH}_2\text{CH}_2\text{CHCH}_2)^+ + \text{HBr}$ |
| IVa. | $\text{LiBr} \cdots {}^+\text{CH}_2\text{CH}_2\text{CHCH}_2$ | Pe. | $\text{Li}(\text{BrCH}_2\text{CH}_2\text{CHCH}_2)^+ + \text{HCl}$ |

Another possibility would be that the Li^+ approached the chlorine end of the molecule to form:



The final possibility, would be where the lithium ion binds simultaneously to both the chlorine, and the bromine as follows:



Since no work has been done to measure the interaction of this molecule with the lithium ion, the energy released by these three interactions will need to be approximated. For the first case, a list of binding energies to Li^+ provided by Staley, and Beauchamp will be used²³. This list shows, that $D(\text{Li}^+ \text{-} i\text{-C}_3\text{H}_7\text{Br})$ is approximately 31 kcal/mol. Also, it can be seen that as the chain length is increased the binding energies increase, therefore, by using values provided in their table, it will be assumed that the $D(\text{Li}^+ \text{-} \text{Br}(\text{CH}_2)_4\text{Cl}) = E_1 > 31$ kcal/mol.

For the second case, where the chlorine end of the molecule is interacting with the Li^+ the same data provided by Beauchamp, and Staley, as used in the prior case, can be employed. However, from the list of the binding energies²³, it can be seen that Li^+ has a lower binding energy to molecules with chlorine, than to molecules with bromine, by about 1 kcal/mol. Therefore, the $D(\text{Li}^+ \text{-} \text{Cl}(\text{CH}_2)_4\text{Br}) = E_2$ is about 30 kcal/mol.

For the third case, the energy of the first two cases are not additive. At least 10 kcal/mol should be removed to account for the fact that lithium does not form as strong of a bond to the second ligand³⁴. Therefore, E_3 is approximately 51 kcal/mol.

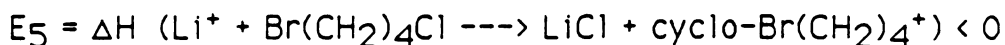
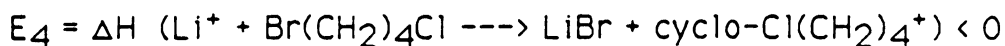
When trying to envision the early stages of the reaction, three possible scenarios were proposed, and their associated energies were estimated. At this point it is advantageous to know where, and how the chloride versus bromide affinity reveals itself. By observing the binding energies of bromide and chloride to Li^+ , it would appear that the bromine end of the molecule bound to Li^+ is more stable, than when the Li^+ is bound to the chlorine end.

The next step in the mechanism is the transfer of the functional group to the lithium ion. There are two complexes which can be formed, since a bromide or a chloride could be transferred. In the case where the Li^+ binds to both functional groups a Li-Cl bond, or a Li-Br bond will need to be broken. The resulting complexes are represented as follows:

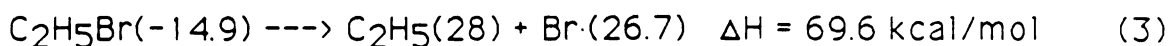
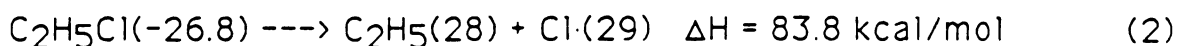
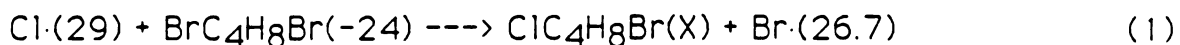


Since no work has been done to estimate the barrier height of these complexes, it can only be assumed that they are numbers smaller than E_1 , since the overall reactions are exothermic. At this point these two complexes can do one of two things. The first, is that the bond can be broken between the LiX and the rest of the complex to form products. This energy is the heat of exchange. The ΔH_{ex} of both reactions is positive therefore, this dissociation would be unexpected. The next step expected, if the monofunctional analogs are considered, would be a hydrogen shift. However, if charge generation on the alkyl group allows for the formation of a cyclic halonium ion, then the exchange reaction can proceed exothermically, and the Li^+ can completely abstract a halogen. This situation was reported in the case of the Li^+ reacting with $t\text{-C}_4\text{H}_8\text{OH}$, where a negative heat of exchange was observed. A negative heat of exchange has resulted because of the stability of the cyclic halonium ions. The stability of cyclic halonium ions increase as the size of the ring increases, to the point where the ΔH_{ex} becomes negative and halide abstraction occurs when $n \geq 4$. The

data in Table 4 reveal that $\text{LiCl} \cdots \text{cycloC}_4\text{H}_8\text{Br}^+$ is more stable than $\text{LiBr} \cdots \text{cycloC}_4\text{H}_8\text{Cl}^+$. This can also be concluded by calculating the ΔH_{ex} for the two complexes. The ΔH_{ex} of the former is less than the latter, therefore ΔH_{ex} values predict that chlorine transfer will occur to a greater extent than the bromine transfer. See Figure 27 for the various ways that the early stages just discussed can be represented. The equations that are used to express the energy of the cyclic products that result from halide abstraction by Li^+ , E_4 , and E_5 , can not be solved for since all the thermochemical information of the reactants and products are not available. However, the missing thermochemical information the $\Delta H_f(\text{ClC}_4\text{H}_8\text{Br})$, $\Delta H_f(\text{cyclo-Cl}(\text{CH}_2)_4^+)$, and the $\Delta H_f(\text{cyclo-Br}(\text{CH}_2)_4^+)$, in E_4 , and E_5 , will be approximated.



To estimate $\Delta H_f(\text{ClC}_4\text{H}_8\text{Br})$, reaction 1 will be used. Before reaction 1 can be used, reactions 2, and 3 are needed to estimate the ΔH for the overall reaction in reaction 1. Reactions 2 and 3 are used to calculate the difference in the bond strength between a C-Cl, and a C-Br bond, whose difference is the ΔH for reaction 1.



The difference between the ΔH 's of reaction 2, and 3 is -14.2 kcal/mol. Therefore, -14.2 kcal/mol can be used as the ΔH for the overall reaction represented in reaction 1. With this information, the $\Delta H_f(\text{ClC}_4\text{H}_8\text{Br})$ can be found to be -35.9 kcal/mol.

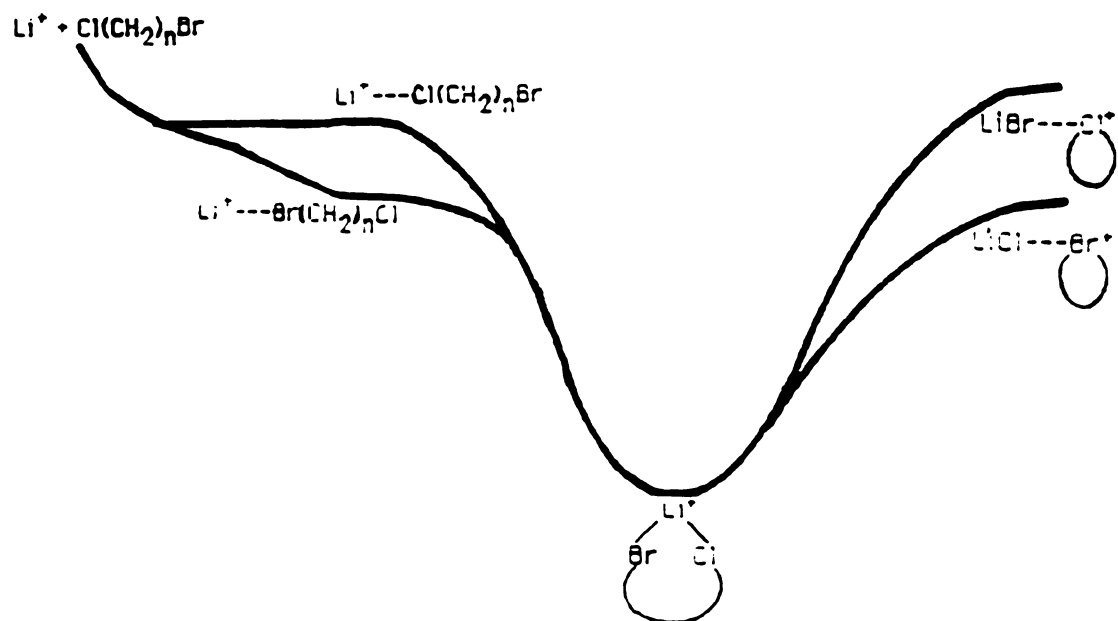
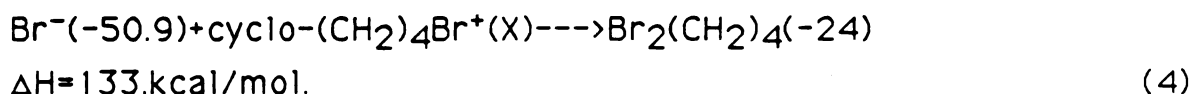


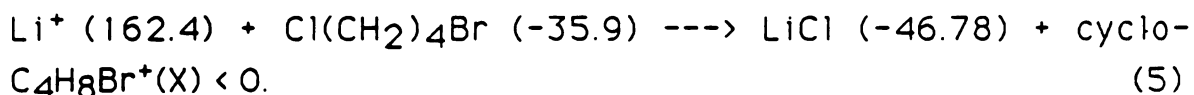
Figure 27 Various ways to represent the early stages of a reaction

To calculate the $\Delta H_f(\text{cyclo}-(\text{CH}_2)_4\text{Br}^+)$, data on the bromide affinity of $\text{cyclo}-(\text{CH}_2)_4\text{Br}^+$ provided by Staley, Beauchamp, and Weiting²⁴ will be used. They reported that the $D(\text{Br}^- \cdots \text{cyclo}-(\text{CH}_2)_4\text{Br}^+) = 133.6 \text{ kcal/mol}$. With this information, the $\Delta H_f(\text{cyclo}-(\text{CH}_2)_4\text{Br}^+)$ can be solved for as follows, by reaction 4.



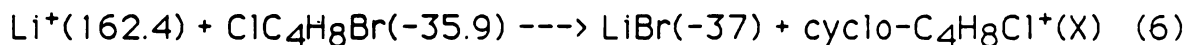
Therefore "X", the $\Delta H_f(\text{cyclo}-(\text{CH}_2)_4\text{Br}^+)$ is 160.5 kcal/mol.

This value is in agreement with the results found in this work. This work allowed the calculation of an upper limit on the $\Delta H_f(\text{cyclo}-\text{C}_4\text{H}_8\text{Br}^+)$ by considering reaction 5.



Therefore, $\Delta H_f(\text{cyclo}-\text{C}_4\text{H}_8\text{Br}^+) < 173.28 \text{ kcal/mol}$.

In order to solve for the $\Delta H_f(\text{cyclo}-\text{Cl}(\text{CH}_2)_4^+)$, the fact that the reaction is exothermic will need to be used. Consider reaction 6:



By assuming $\Delta H_{rxn} < 0$ for (6), it is found that the $\Delta H_f(\text{cyclo}-\text{Cl}(\text{CH}_2)_4^+) < 163.5 \text{ kcal/mol}$. This value is in good agreement with the $\Delta H_f(\text{cyclo}-\text{Cl}(\text{CH}_2)_4^+)$ of 160.3 kcal/mol calculated theoretically by McManus and Worley³⁹.

The second situation that could occur, is that the reaction can proceed by transferring a β -hydrogen, as in the mechanism for the alkyl halides and alcohols reacting with Li^+ . The complexes that would result are as follows:

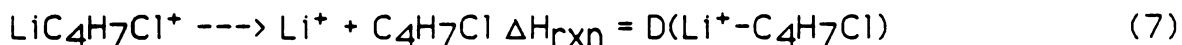


By considering the expression for the energies E_6 , and E_7 below to form these intermediates from reactants, some thermochemical information can be obtained.

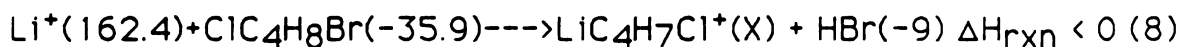
$$E_6 = \Delta H (\text{Cl}(\text{CH}_2)_4\text{Br} \longrightarrow \text{HCl} + \text{CH}(\text{CH}_2)_3\text{Br}) - D(\text{Li}^+ - \text{HCl}) - D(\text{Li}^+ - \text{CH}_2\text{CH}(\text{CH}_2)_2\text{Br}) - 10$$

$$E_7 = \Delta H (\text{Cl}(\text{CH}_2)_4\text{Br} \longrightarrow \text{HBr} + \text{CH}(\text{CH}_2)_3\text{Cl}) - D(\text{Li}^+ - \text{HBr}) - D(\text{Li}^+ - \text{CH}_2\text{CH}(\text{CH}_2)_2\text{Cl}) - 10$$

The $D(\text{Li}^+ - \text{C}_4\text{H}_7\text{Cl})$ and the $D(\text{Li}^+ - \text{C}_4\text{H}_7\text{Br})$ can be approximated, as well as the $\Delta H_f(\text{C}_4\text{H}_7\text{Cl})$, and the $\Delta H_f(\text{C}_4\text{H}_7\text{Br})$. To calculate the $D(\text{Li}^+ - \text{C}_4\text{H}_7\text{Cl})$ consider the following reaction.



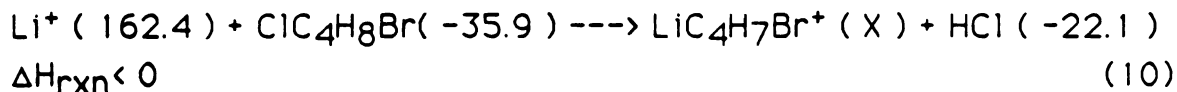
Before the ΔH for reaction 7 can be calculated, an upper bound for the ΔH_f of $\text{LiC}_4\text{H}_7\text{Cl}^+$ needs to be calculated from reaction 8, as follows:



Therefore, the $\Delta H_f(\text{LiC}_4\text{H}_7\text{Cl}^+) < 135.5$ kcal/mol. By inserting this value into reaction 7 the $D(\text{Li}^+ - \text{C}_4\text{H}_7\text{Cl}^-)$ is found to be > 37.3 kcal/mol. To calculate the $D(\text{Li}^+ - \text{C}_4\text{H}_7\text{Br})$ consider the following reaction:

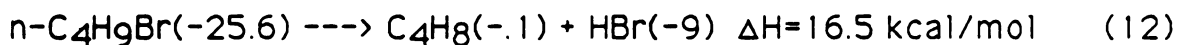


Before the ΔH for reaction 9 can be calculated, an upper bound for the ΔH_f of $\text{LiC}_4\text{H}_7\text{Br}^+$ needs to be calculated by reaction 10, as follows:

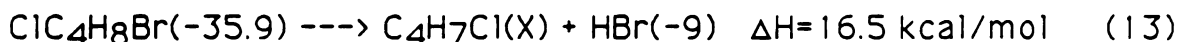


Therefore, $\Delta H_f(\text{LiC}_4\text{H}_7\text{Br}^+) < 148.6$ kcal/mol. By inserting this value into reaction 9 the $D(\text{Li}^+ - \text{C}_4\text{H}_7\text{Cl}^-)$ is found to be > 14.7 kcal/mol.

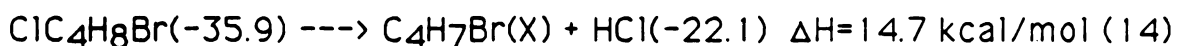
To calculate the $\Delta H_f(\text{C}_4\text{H}_7\text{Cl})$ and the $\Delta H_f(\text{C}_4\text{H}_7\text{Br})$ consider the following reactions:



The ΔH 's for reactions 11, and 12 provide an approximation for the energy necessary to break a C-Cl, and a C-Br bond. These values can be used to calculate the $\Delta H_f(\text{C}_4\text{H}_8\text{Cl})$, and $\Delta H_f(\text{C}_4\text{H}_8\text{Br})$ in reaction 13, and 14.

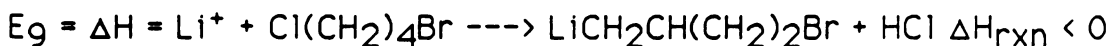


Therefore, $\Delta H_f(\text{C}_4\text{H}_7\text{Cl}) = 10.4$ kcal/mol.



Therefore, $\Delta H_f(\text{C}_4\text{H}_7\text{Br}) = -.9$ kcal/mol.

At this point, these complexes can go to products, by the loss of HX, and their associated energies are represented as follows:



Another possibility is that these complexes, $\text{LiC}_4\text{H}_7\text{Cl}$ and $\text{LiC}_4\text{H}_7\text{Br}$ could undergo a further reaction, refer to Figure 26, by transferring a halide to form the following complexes:



The C_4H_7 cation can then transfer a β -hydrogen to the chlorine to form:



This double dehydrohalogenation occurs when $n \geq 4$. Proton transfer always occurs at this point because the P.A.(butadiene), $<$ P.A.(LiX). From here, products are formed by the loss of HBr, and HCl, with a $\text{Li}(\text{butadiene})^+$ complex resulting. Branching ratios in Table 4 show that this pathway is minor. To conclude with this example, the energy, E_{10} , of the final product for this reaction pathway can be expressed by the reaction as follows:

$$E_{10} = \Delta H_{rxn} \text{ for } (\text{Li}^+ + \text{ClC}_4\text{H}_8\text{Br} \cdots \rightarrow \text{Li}(\text{butadiene})^+ + \text{HCl} + \text{HBr}) < 0.$$

Some thermochemical implications of the above reactions should be noted before moving on. In order for reaction 15 to occur, it requires 31 kcal/mol.



Therefore, $D(\text{Li}^+ \cdots \text{butadiene})$ must be greater than 31 kcal/mol, which is close to a value reported by Farrar and Creasy. They³⁷ suggest that the $D(\text{Li}^+ \cdots \text{butadiene})$ was 28 kcal/mol.

Before proceeding to the next case, a comment should be made about why products were observed from both halonium ions, and its isomeric haloalkyl cation. It has been reported by McManus and Worley⁴⁰ that an equilibrium exists between the halonium ions and

its isomeric haloalkyl cation. If a situation such as this occurs, then $\text{cyclo}(\text{C}_4\text{H}_8\text{X}^+) \longleftrightarrow {}^+\text{CH}_2(\text{CH}_2)_3\text{X}$.

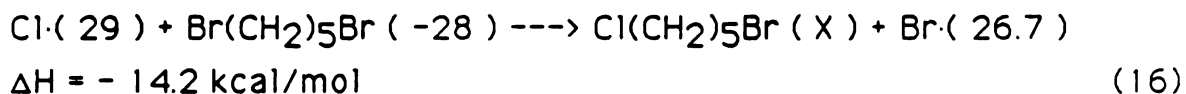
If the structure of the $\text{LiX} \cdots \text{cyclo}(\text{CH}_2)_n\text{Y}^+$, where X, and Y, are chlorine and bromine, and $n=4$, and 5, is considered, the question must be asked, can cyclic halonium ions transfer a proton? Proton transfer would be possible if the charge resided on a carbon center that could yield a hydrogen. Theoretical calculations show that there is no substantial positive charge located on the halogen, of the cyclic halonium structures, but on a methylene closest to the halogen^{40,41}. Calculations can prove that it takes more energy to transfer a proton from a cyclic halonium ion, than from its straight chain analogue, and the latter is the only one that can protonate LiX. A possibility is that there is a dynamic sampling of the cyclic and acyclic structures, and when the acyclic is present, proton transfer can occur. Experimental data shows that the cyclic complex is more stable. If the configuration of $\text{C}_4\text{H}_8\text{X}^+$ is cyclic, then the products $\text{LiX} + \text{cyclo}(\text{C}_4\text{H}_8\text{X}^+)$ are observed. If on the other hand $\text{C}_4\text{H}_8\text{X}^+$ has the configuration ${}^+\text{CH}_2(\text{CH}_2)_3\text{X}$, then the reaction proceeds by a β -hydrogen transfer, and then the loss of HX, and $\text{Li}(\text{CH}_2)\text{CH}(\text{CH}_2)_2\text{X}$ are formed as products.

McManus and Worley also reported⁴⁰ that the equilibrium would be shifted towards the halonium ion dramatically in the absence of solvent, i.e. the gas phase. In support of this statement, if the branching ratios are observed in Table 4, it can be seen that the loss of LiBr and LiCl have a higher probability of occurring, than the loss of HBr, and HCl that occur when the haloalkyl cation is the configuration. Therefore, experimental data shows that the cyclic complex is more stable.

Since 1-bromo-5-chloro-pentane yields the products observed by the same mechanisms as proposed when Li^+ are reacted with 1-bromo-4-chloro-butane, see Table 4, not much discussion is necessary. The potential energy surface used to represent how all of

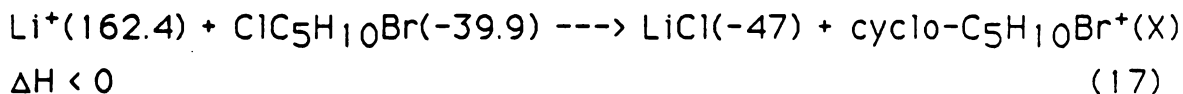
the products are formed is the same as in Figure 26. To gain insight into the stability of the cyclic products, the ΔH_f 's of cyclo- $C_5H_{10}Br^+$, and cyclo- $C_5H_{10}Cl^+$ will be approximated. This information will be useful later in this work.

The reaction of Li^+ with this compound is exothermic therefore the ΔH of the reaction is less than zero. Since the $\Delta H_f(ClC_5H_{10}Br)$, and the $\Delta H_f(\text{cyclo-}C_5H_{10}Br^+)$ are not in the literature, they will need to be approximated. Consider reaction 16.

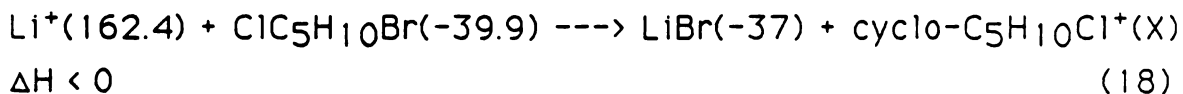


The ΔH for the reaction, -14.2 kcal/mol , was found previously in reactions (2) and (3) where the difference in the difference in bond strength between a C-Cl, and a C-Br was determined. If "X" is solved for, then $\Delta H(Cl(CH_2)_5Br) = -39.9 \text{ kcal/mol}$.

If reactions 17, and 18 are utilized, the $\Delta H_f(\text{cyclo-}C_5H_{10}Br^+)$ and the $\Delta H_f(\text{cyclo-}C_5H_{10}Cl^+)$ can be approximated, based on the fact that the reactions were exothermic.

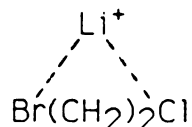


Therefore, " X " = $\Delta H_f(\text{cyclo-}C_5H_{10}Br^+) < 169.5 \text{ kcal/mol}$. This value can not be compared to another, since this value has not been reported in the literature.



Therefore, " X " = $\Delta H_f(\text{cyclo-}C_5H_{10}Cl^+) < 159.5 \text{ kcal/mol}$. This value is consistent with a value of 151.7 kcal/mol , derived by McManus, Worley, and Beaty by means of a MINDO calculation⁴⁰.

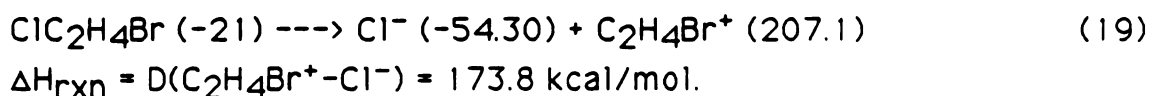
To continue the discussion of the α,ω -bromo, chloro compounds with Li^+ , the next molecule to be discussed is 1-bromo-2-chloroethane. When reacted with Li^+ , it was hoped that one of two situations would occur. To consider the first possibility, it was hoped that the initial interaction showed that the Li^+ preferred one functional group over the other, resulting in dehydrohalogenation of this functional group, but this was not observed. The second scenario was that the Li^+ was not necessarily forced to choose one functional group over the other, since the chain was so small, so when the Li^+ comes up to the bromoethanol molecule, the following type of interaction, where the Li^+ was attached to both functional groups may occur:



It was hoped, that this initial interaction with two functional groups would provide more energy to the reaction to observe chemistry not before observed, such as the loss of ClBr , but this was not the case. No reactions were observed. By observing the ΔH_{ex} for these reactions, i.e. the complete abstraction of a halogen by Li^+ , they are endothermic and it can therefore be predicted that no reaction will occur. To propose a reason for these results, it is possible that since the bromide affinity to the Li^+ and the chloride affinity to the Li^+ are so close, that the Li^+ ion does not prefer one group over the other, and the two halogens compete to transfer. In this case partial cationic character would exist on the carbons adjacent to the two halogens and the complex would dissociate back to reactants, and dehydrohalogenation of neither group occurs. Therefore, dehydrohalogenation of neither group is preferred.

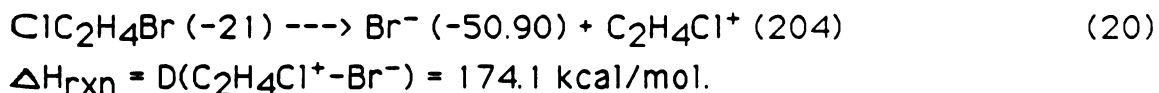
To reinforce the reason provided for why no reactions were observed, it is necessary to observe the individual steps in the reactions to note if perhaps there was a barrier to the reaction in another part of the mechanism, that had nothing to do with the

initial interactions. Let's assume that the initial interaction involved the Li^+ being attached to both functional groups. In order to form products either the C-Cl, or the C-Br bond would need to be broken. To consider if a halide transfer is the limiting step, the chloride affinity of the Li^+ , $D(\text{Li}^+-\text{Cl}^-)$, and the bromide affinity of the Li^+ , $D(\text{Li}^+-\text{Br}^-)$, need to be compared to the $D(\text{C}_2\text{H}_4\text{Br}^+-\text{Cl}^-)$, and $D(\text{C}_2\text{H}_4\text{Cl}^+-\text{Br}^-)$ respectively. To consider the first case, the chloride affinity of the lithium ion is 155.1 kcal/mol. To calculate the chloride affinity of $\text{C}_2\text{H}_4\text{Br}^+$, consider reaction 19.



Since the $D(\text{Cl}^--\text{C}_2\text{H}_4\text{Br}^+) > D(\text{Li}^+-\text{Cl}^-)$ by 18.7 kcal/mol, the chloride group can be transferred to the lithium ion, therefore the reaction should proceed.

To look at the second case, the $D(\text{Li}^+-\text{Br}^-)$ is 148.5 kcal/mol. To calculate the bromide affinity of $\text{C}_2\text{H}_4\text{Cl}$, consider reaction 20.



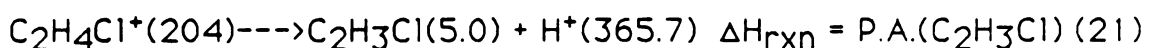
It can be observed, that the $D(\text{Br}^--\text{C}_2\text{H}_4\text{Cl}^+) > D(\text{Li}^+-\text{Br}^-)$ by 19.0 kcal/mol, so the bromide group can be transferred to the lithium ion, therefore the reaction is not inhibited by the halide transfer step.

Since both situations can occur, and the following complexes are formed:



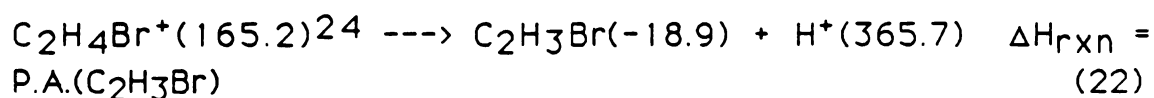
The next step is a β -hydrogen transfer. To see if this step can occur, it is necessary to compare the P.A. of LiCl, to the P.A. of $\text{C}_2\text{H}_3\text{Br}$, and the P.A. of LiBr to the P.A. of $\text{C}_2\text{H}_3\text{Cl}$.

To calculate the P.A. of C_2H_3Cl the ΔH of the following reaction needs to be calculated.



The ΔH of the reaction, which is the proton affinity of C_2H_3Cl is 166.7 kcal/mol. The P.A. C_2H_3Cl (166.7 kcal/mol) < P.A. LiBr (194 kcal/mol).

To calculate the P.A. of C_2H_3Br the ΔH of the following reaction needs to be calculated.

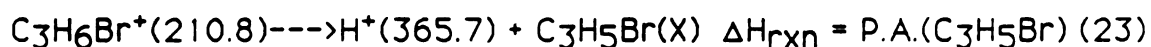


The ΔH of the reaction, which is the proton affinity of C_2H_3Br is 181.6 kcal/mol. The P.A. C_2H_3Br (181.6 kcal/mol) < P.A. LiCl (197 kcal/mol), therefore, the reaction is not inhibited at this point, and product formation is not obstructed by the hydrogen transfer step of the mechanism.

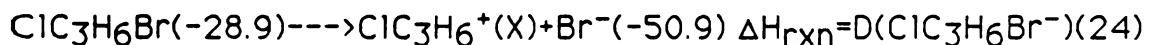
The final compound in this series to be discussed is 1-bromo-3-chloro-propane. When this compound reacts with the Li^+ , only the elimination of HCl is observed. See Table 4. This suggests that the Li^+ either prefers to bind with the chlorine over the bromine, or that some other step in the mechanism is inhibited in the case where the Li^+ is bound to the bromine end of the molecule.

Since the bromide affinity to the lithium ion, 148.5 kcal/mol, and the chloride affinity to the Li^+ , 155.1 kcal/mol, are so close in energy, let's consider the next case, since no preference can be assumed.

Let's assume that the $\text{LiBr} \cdots \text{C}_2\text{H}_4\text{Cl}$ complex is formed, whether it arose from the Li^+ approaching the bromine end of the molecule, or from a Li-Cl bond breaking after the initial complex is formed where the Li^+ is attached to both functional groups. The next step in the mechanism is a β -hydrogen shift on to the bromine. To see whether or not this step is exothermic, or endothermic, the P.A. of LiBr, and the P.A. of $\text{C}_3\text{H}_5\text{Cl}$ will need to be considered. To calculate the proton affinity of $\text{C}_3\text{H}_5\text{Br}$ consider reaction 23.



To estimate the $\Delta H_f(\text{C}_3\text{H}_5\text{Br})$ consider the following information. It is known from Table 4 that $\text{Li}^+ + \text{HO}(\text{CH}_2)_3\text{Br}$ does not form $\text{LiOH} + \text{C}_3\text{H}_5\text{Br}^+$, $\Delta H > 0$. Therefore, $\Delta H_f(\text{C}_3\text{H}_5\text{Br}) > 210.8 \text{ kcal/mol}$. If the $\Delta H_f(\text{C}_3\text{H}_5\text{Br})$ is inserted into reaction 23 it can be found that the P.A. ($\text{C}_3\text{H}_5\text{Br}$) = 164.9 kcal/mol. Since the P.A. ($\text{C}_3\text{H}_5\text{Br}$) < P.A.(LiBr), 194.4 kcal/mol, then this step is not the barrier to the reaction for the elimination of HBr. Once again, as in the case of 1-bromo-2-chloroethane, it is necessary to go back and look at the bromide affinity between Li^+ , and $\text{C}_3\text{H}_6\text{Cl}^+$. The $D(\text{Li}^+-\text{Br}^-)$ is 148.5 kcal/mol. To calculate the $D(\text{ClC}_3\text{H}_6^+-\text{Br}^-)$ consider reaction 24.



Note, that reaction 24 can not be calculated due to the fact that the $\Delta H_f(\text{ClC}_3\text{H}_6^+)$ is not known. However, the $D(\text{ClC}_3\text{H}_6^+-\text{Br}^-)$ will be assumed to be less than 148.5 kcal/mol, since the reaction is endothermic.

1. Chemistry of Li^+ With α,ω -bromo-alcohols

The next class of compounds to be discussed are the α,ω -bromo-alcohol compounds. The results when these compounds are reacted with Li^+ are found in Table 4.

Before going on to a discussion of the actual reaction that occurred, some general observations need to be made about the difference between the α,ω -bromo-chloro compounds and the α,ω -halo-alcohol compounds. First, there is a major chemical difference that exists between the bromide and the hydroxide groups, that did not exist with the chemically similar chlorine and bromine, so the chemistry when these compounds are reacted with Li^+ should be different. Also, the binding energies of Li^+ to alcohols is much greater than for the alkyl halides, which was seen from the monofunctional analog. Therefore, there should be a definite preference of the α,ω -bromo-alcohols to react as the monofunctional alcohol analogs, rather than bromoalkanes. This suggests that the complex $\text{Li}^+ \cdots \text{HO} \cdots (\text{CH}_2)_4 \text{Br}$ is more stable than $\text{Li}^+ \cdots \text{Br} \cdots (\text{CH}_2)_n \text{OH}$, where $n=2$ to 4.

To begin the discussion of how Li^+ reacts with 1-bromo-2-ethanol, consider the ΔH_{ex} values for the abstraction of the two functional groups by Li^+ . The ΔH_{ex} value for the bromide abstraction by Li^+ is approximately 18 kcal/mol. The value of 18 kcal/mol is less than the ΔH_{ex} 's for the n-bromo alkanes which reacted, and therefore, E_b should also be smaller so the reaction is expected to proceed. The value of ΔH_{ex} for hydroxide abstraction by Li^+ is 40 kcal/mol. This value is greater than the ΔH_{ex} of isopropanol which was unreactive, and since it is known that as ΔH_{ex} increases, E_b increases, E_b will be assumed to be sufficiently large to prohibit this reaction at the HO-end of this molecule. Even if this first step was not the inhibiting step, a proton transfer from a halonium ion is

unlikely, and this too would inhibit the formation of products. In the reaction of Li^+ with 1-bromo-2-ethanol, we note that Li^+ only induces dehydrohalogenation products. No dehydration products, typical when Li^+ reacts with alcohols, are observed.

To explain the formation of these products, consider the initial interaction complexes that could result. The Li^+ can bind to the bromine end of the molecule or to the hydroxide end of the molecule to form the following complexes:



We propose that the former is less stable than the later. This is suggested since Beauchamp reported that the $D(\text{Li}^+ \text{---} \text{HOR}) > D(\text{Li}^+ \text{---} \text{BrR})$. Therefore, the Li^+ prefers being bonded to the alcohol end of the molecule. This will be discussed in more detail when the reactions of Li^+ with 1-bromo-4-butanol are discussed. When the Li^+ does bond to the bromine end of the molecule, the classical mechanism proposed for how an alkyl halide molecule react with Li^+ , depicted in Scheme 3, occurs. The bromide is transferred to the Li^+ which results in a build up of charge on the carbon. From here, a hydrogen is transferred to the bromide by a protonated oxirane which is capable of transferring a proton, unlike cyclic halonium ions. This occurs because the P.A.(cyclo- $\text{CH}_2\text{CH}_2\text{O}$) is 187.9 kcal/mol, and the P.A.(LiBr) is 195 kcal/mol. The proton transfer leads to the dehydrohalogenation products.

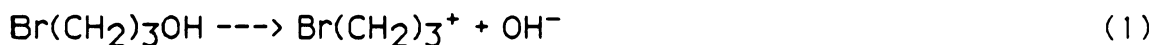
If the second complex is considered, where the hydroxide end is attached to the Li^+ , a different scenario occurs here. The initial interaction complex can not proceed by OH^- transfer as is the case with a monofunctional alcohols reacting with Li^+ . Also, transferring a proton to LiOH from a cyclic halonium ion is unlikely, and therefore formation of the products (H_2O , and $\text{LiC}_2\text{H}_3\text{Br}^+$) will not occur.

Consider the initial interaction complex as follows:

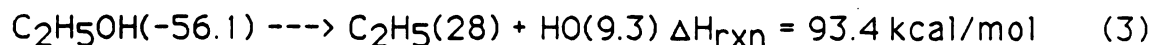
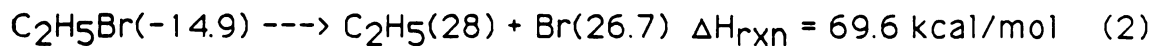


To thermodynamically explain why no reaction is observed, the hydroxide affinity of the Li^+ should be compared to the hydroxide affinity of $(\text{CH}_2)_2\text{Br}^+$ to determine if the functional group transfer step can occur. It can be determined, that the hydroxide affinity of Li^+ is approximately 186 kcal/mol, and the hydroxide affinity of $\text{C}_2\text{H}_4\text{Br}^+$ is about 226 kcal/mol. Therefore, although the Li^+ prefers to be bound to the hydroxide portion of the molecule, rather than the bromine portion, there is not a strong enough interaction to extract the hydroxide from BrC_2H_4^+ , and the reaction is obstructed at this point.

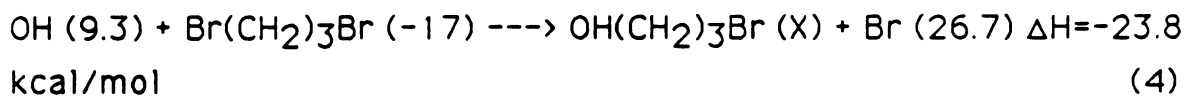
The same situation is occurring when 1-bromo-3-propanol reacts with Li^+ . Only the dehydrohalogenation is occurring, to form products. The dehydration reaction is once again inhibited because the hydroxide affinity of the Li^+ , 186 kcal/mol, is not large enough to remove the hydroxide from $\text{C}_3\text{H}_6\text{Br}^+$. The hydroxide affinity can be calculated as follows in reaction 1.



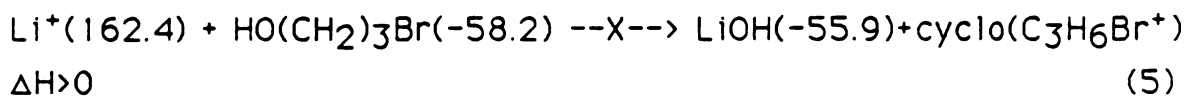
Before ΔH for reaction 1 can be evaluated, the $\Delta H_f(\text{Br}(\text{CH}_2)_3\text{OH})$ needs to be calculated as follows. Reactions 2 and 3 are used to determine the difference in the bond strength between a C-Br, and a C-OH bond.



The difference between reactions 2, and 3 is 23.8 kcal/mol. With this information the $\Delta H_f(\text{Br}(\text{CH}_2)_3\text{OH})$ can be calculated by reaction 4.

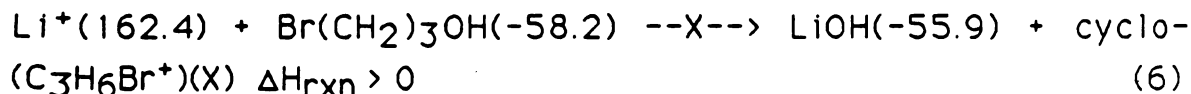


Also, before reaction 1 can be evaluated, a value of $\Delta H_f(\text{cyclo-C}_3\text{H}_6\text{Br}^+)$ can be approximated by reaction 5.

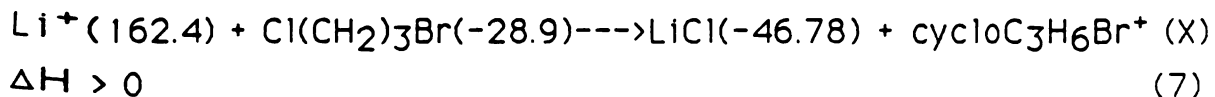


If the $\Delta H_f(\text{Br}(\text{CH}_2)_3\text{OH}) = -58.20 \text{ kcal/mol}$, found in reaction 4, and the $\Delta H_f(\text{cyclo-C}_3\text{H}_6\text{Br}^+) > 160.1 \text{ kcal/mol}$ then reaction 1, can be employed to show, that the hydroxide affinity of $\text{C}_3\text{H}_6\text{Br}^+$ is found to be $> 185.2 \text{ kcal/mol}$. Therefore, the hydroxide affinity of Li^+ is not sufficiently large to remove the hydroxide from $\text{C}_3\text{H}_6\text{Br}^+$.

An experimental estimate for the heat of formation of $\text{cyclo-C}_3\text{H}_6\text{Br}^+$ has not been determined. It is known that reaction 6, is endothermic, and is not observed.



Being that the reaction is endothermic, a lower bound can be estimated for the $\Delta H_f(\text{cyclo-C}_3\text{H}_6\text{Br}^+) > 160.1 \text{ kcal/mol}$. However, a more significant lower bound can be set if reaction 7, is evaluated, from the proceeding section:



Since reaction 7 is observed, we can conclude $\Delta H_f(\text{cyclo-C}_3\text{H}_6\text{Br}^+) > 180.3 \text{ kcal/mol}$.

The last case to be discussed is 1-bromo-4-butanol reacting with Li^+ . The potential energy diagram in Figure 28 can be used to show the mechanisms for the products formed for this case.

It has been reported by Beauchamp, and Schilling³² that the most important step when dealing with organic molecules reacting with atomic metal ions is the first step. The first step would be the initial interaction of the Li^+ with the alcohol molecule. Beauchamp reported that the $D(\text{Li}^+-\text{HOR}) > D(\text{Li}^+-\text{BrR})$, where $\text{R}=\text{H}$. He reported that the $D(\text{Li}^+-\text{H}_2\text{O})$ is 34 kcal/mol, and the $D(\text{Li}^+-\text{HBr})$ is 20.29 kcal/mol.

If the Li^+ prefers to be bound to the OH group, then the functional group transfer will be assumed to lead to $\text{LiOH}-\text{C}_4\text{H}_8\text{Br}^+$. It is known that the $^+\text{C}_4\text{H}_8\text{Br}$ group would form $\text{cyclo-}^+\text{C}_4\text{H}_8\text{Br}$, due to the stability of rings. It is unlikely that this stable cyclic ion could act as a protonating agent. To reinforce this Hehre, and Hiberty⁴¹ describe these cyclic halonium compounds as follows: "very little of the positive charge is actually borne by the halogen itself. Rather it is delocalized through out the molecular framework." Therefore, if the interaction is $\text{LiOH}--\text{cyclo}(\text{C}_4\text{H}_8\text{Br})^+$ the products, would be LiOH and $\text{cyclo}(\text{C}_4\text{H}_8\text{Br})^+$. This mechanism was discussed first since the branching ratios in Table 4 show that these are the most stable products.

In contrast to what was occurring in the case where the Li^+ was reacting with 1-bromo-2-ethanol, and 1-bromo-3-propanol, the hydroxide affinity of the lithium ion, 186 kcal/mol, is finally as large as than the hydroxide affinity of the $(\text{CH}_2)_n\text{Br}^+$ portion of the molecule. In this case, the hydroxide affinity of $\text{C}_4\text{H}_8\text{Br}^+$ is reported to be 186 kcal/mol. It can be seen from the branching ratios in Table 4, that the loss of LiOH gives the dominant product, $\text{cyclo}(\text{C}_4\text{H}_8\text{Br}^+)$, and the dehydrohalogenation mechanism produces only a minor product.

Another situation would be if the Li^+ first became bound to the bromine end of the molecule. See Figure 28. If the initial interaction formed is $\text{LiBr}--\text{cyclo}(\text{C}_4\text{H}_8\text{OH})^+$, the cyclic ion would make a better protonating reagent where a proton could be

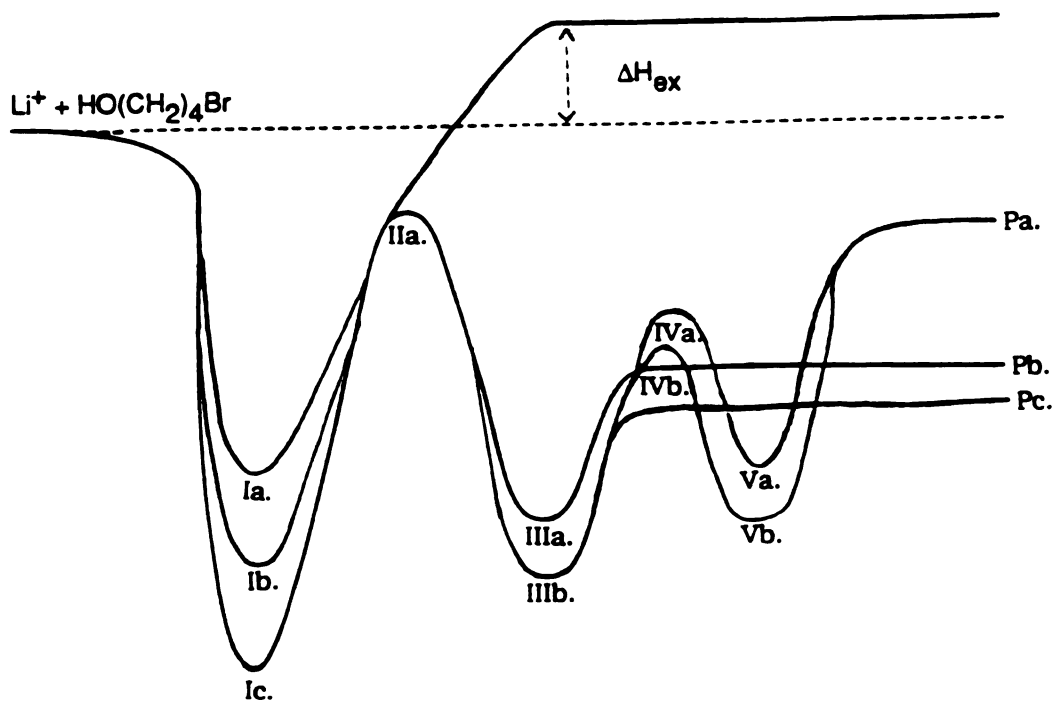
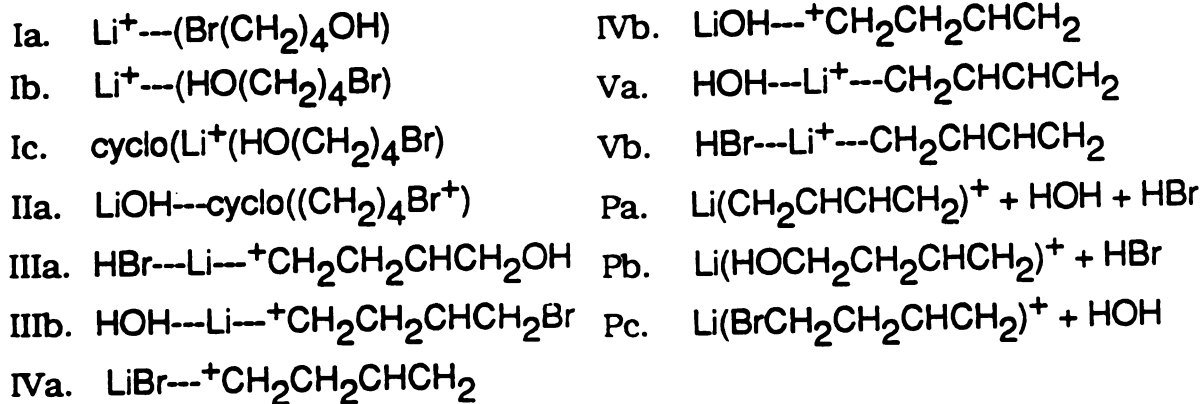
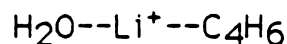


Figure 28 Potential energy diagram for Li^+ , and α,ω -bromobutanol

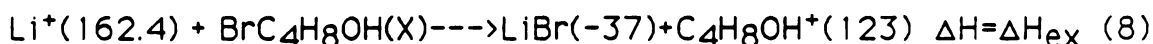


transferred to make $\text{HBr} \cdots \text{Li}^+ \cdots \text{C}_4\text{H}_8\text{O}$. From here, the loss of HBr could occur leaving $\text{Li}^+ \cdots \text{C}_4\text{H}_8\text{O}$. At this point, since it is known that the Li^+ prefers to be bound to the OH group another proton transfer could occur to form:

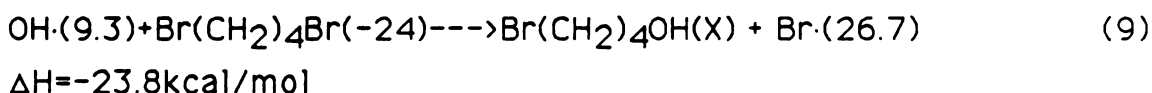


This complex could then lose H_2O leaving the Li^+ (butadiene) complex.

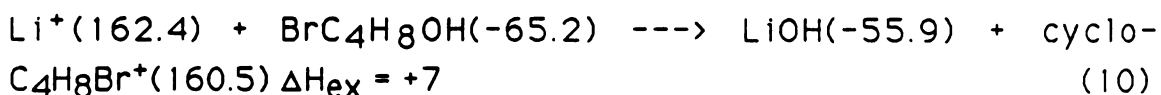
If the ΔH_{ex} values are observed for this case, by observing the products that result, the abstraction of bromide, and of hydroxide, by Li^+ must be exothermic. To calculate the ΔH_{ex} for the abstraction of bromide, consider reaction 8.



In order to calculate the ΔH_{ex} , the $\Delta H_f(\text{BrC}_4\text{H}_8\text{OH})$ can be calculated by reaction 9, if it is recalled that the difference in the bond strength between a C-Br , and a C-OH is -23.8 kcal/mol.

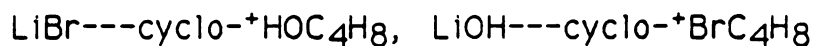


Therefore, the $\Delta H_f(\text{Br}(\text{CH}_2)_4\text{OH}) = -65.2$ kcal/mol. With this value the ΔH_{ex} is approximately -11 kcal/mol. The ΔH_{ex} value for the hydroxide abstraction by Li^+ must also be exothermic since a reaction occurs. However, if reaction 10 is observed, the ΔH_{ex} is positive.

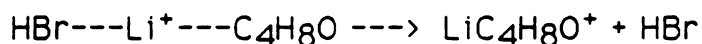


To comment on this value, the bond strength of $(\text{R}^+ \cdots \text{OH}^-)$, where $\text{R}^+ = \text{cyclo-C}_4\text{H}_8$, was calculated with a value reported by Staley, Beauchamp, and Weiting²⁴, to within ± 10 kcal/mol. Thus, this

heterolytic bondstrength may be as much as 7, or 8 kcal/mol higher than listed in the table. It is curious then, why this abstraction reaction by lithium ions is favored over the abstraction of the bromide by Li^+ , when the latter reaction is more exothermic. To explain this observation, the initial interaction where the Li^+ is attached to the hydroxide end of the molecule is sufficiently different from the Li^+ being attracted to the bromine end, that it is this initial interaction that determines which products result. Therefore, both ends of the molecule react to produce the following intermediates:



As noted in the previous example, only the first intermediate has a mobile proton, therefore proton transfer can occur and the resulting products are a result of dehydrohalogenation as follows:

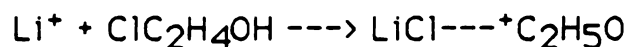


In contrast, the intermediate, $\text{LiOH} \cdots \text{cyclo-}^+\text{BrC}_4\text{H}_8$ can not rapidly transfer a proton, since no mobile protons are available. Therefore, this compound dissociates to form the products LiOH , and $\text{cyclo}(\text{C}_4\text{H}_8\text{Br}^+)$. This process is favored. Branching ratios in Table 4 show that this product is the most abundant.

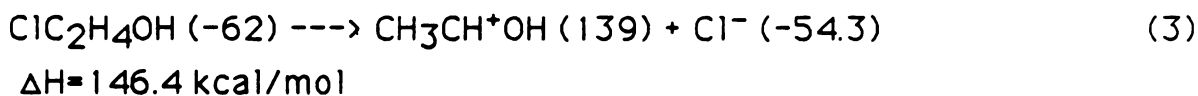
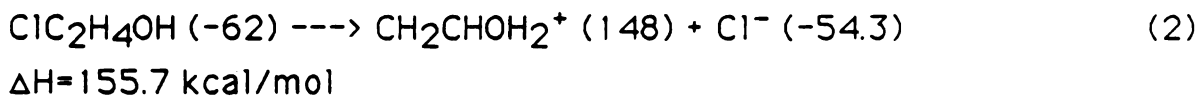
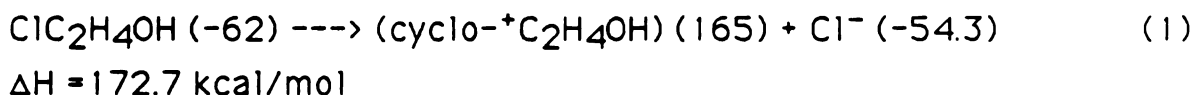
m. Chemistry of Li^+ With α,ω -chloro-alcohols

The last class of compounds to be studied in regard to how they react with Li^+ are the α,ω -chloro-alcohol compounds. Table 4 contains a listing of the compounds and the observed reaction products as well as the branching ratios for the products. By observing the branching ratios in Table 4, it can be noted, that the loss of HCl is much greater than the loss of H_2O . Also, LiOH is a product of the exchange reaction, but LiCl is not. These two observations were also made for the α,ω -bromo-alcohol compounds.

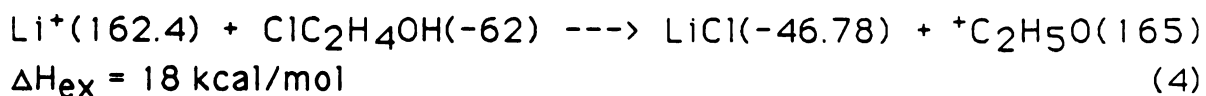
To start the discussion, observe how Li^+ reacts with 1-chloro-2-ethanol. The only reaction products observed was from the loss of HCl. The lithium ion was not able to induce dehydration in this compound. The same situation that was occurring with the α,ω -bromo-alcohols is occurring here. Dehydrohalogenation of HCl is induced by Li^+ by the same mechanism as Li^+ reacting with alkyl halides depicted in Scheme 3. After the chloride is transferred to the Li^+ , the following structure can be implied:



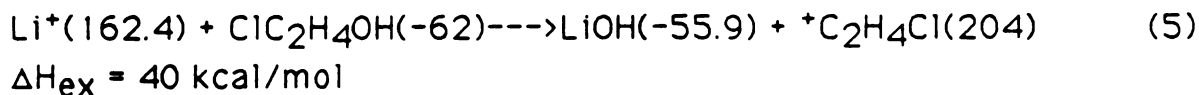
This structure can be assumed if the various ΔH 's for the reaction 1 to 3 are considered. The ΔH 's of the following reactions represent the chloride affinities of $\text{C}_2\text{H}_5\text{O}^+$ for the possible structures.



The $\Delta\text{H}_{\text{ex}}$ value can be calculated for the abstraction of chlorine by the Li^+ in reaction 4, in kcal/mol.

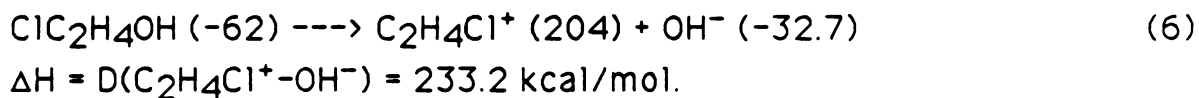


The $\Delta\text{H}_{\text{ex}}$ is 18 kcal/mol. If the $\Delta\text{H}_{\text{ex}}$ for the abstraction of the hydroxide group by Li^+ is calculated, this value is substantially higher. Observe reaction 5.



This ΔH_{ex} value is larger than other ΔH_{ex} values for alcohols that do not react. Therefore, the value for E_b would also be expected to be sufficient large to prohibit the exchange of the hydroxide. Do to the large values of E_b , and ΔH_{ex} for the abstraction of hydroxide, the α,ω -chloro-alcohol would be expected to react as a chloroalkane, and not an alcohol. It will not be until the alkyl chain is at least four carbons in length that the reactions show alcohol-like products.

Dehydration of this compound does not occur because the hydroxide affinity of Li^+ , 192 kcal/mol, is sufficiently less than the hydroxide affinity of $\text{C}_2\text{H}_4\text{Cl}^+$. The hydroxide affinity of $\text{C}_2\text{H}_4\text{Cl}^+$ is calculated in reaction 6.



Since the $D(\text{C}_2\text{H}_2\text{Cl}^+-\text{OH}^-) > D(\text{Li}^+-\text{OH}^-)$ by 41.2 kcal/mol, the reaction is prohibited to proceed after the first electrostatic complex is formed because the hydroxide group can not be transferred with the Li^+ . Recall, as mentioned in Section h, that if the $D(\text{R}^+-\text{OH}^-)-D(\text{Li}^+-\text{OH}^-) > 18.23 - 32.73$ kcal/mol, the H_2O elimination would not occur.

These similar circumstances exist with 1-chloro-3-propanol. Dehydrohalogenation is induced by Li^+ , but dehydration is not. Once again, dehydration is inhibited because the Li^+ does not have a hydroxide affinity which is sufficiently larger than that of $\text{C}_3\text{H}_6\text{Cl}^+$.

In the case of 1-chloro-4-butanol, many reaction products result. Figure 29 contains the potential energy diagram to explain this system. This compound reacting with the Li^+ is very similar to how 1-bromo-4-butanol reacted with Li^+ .

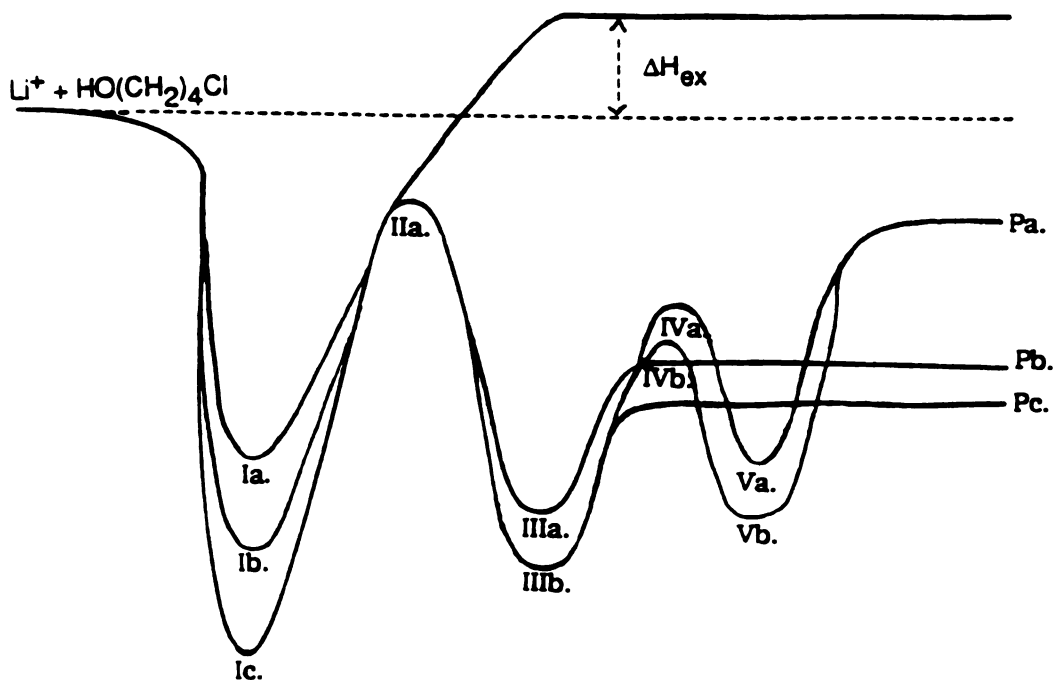
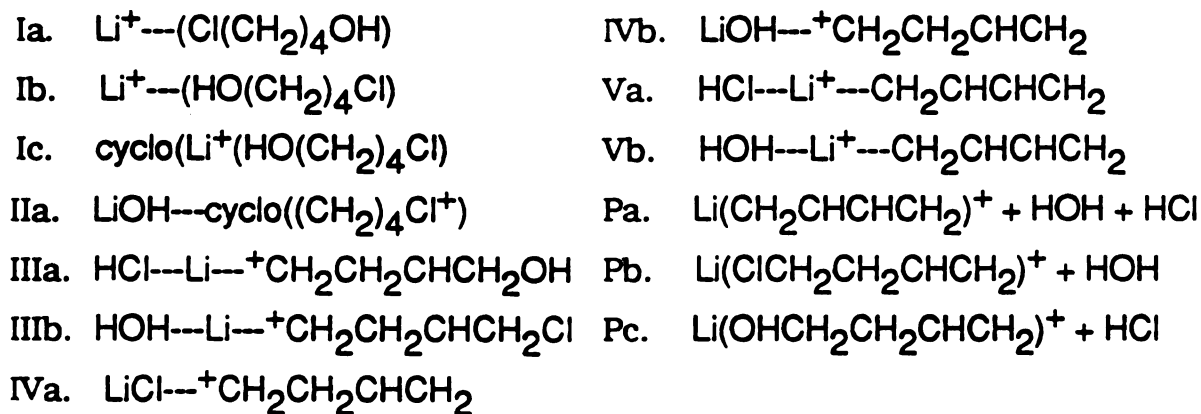
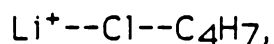


Figure 29 Potential energy diagram for Li^+ and α,ω -chlorobutanol



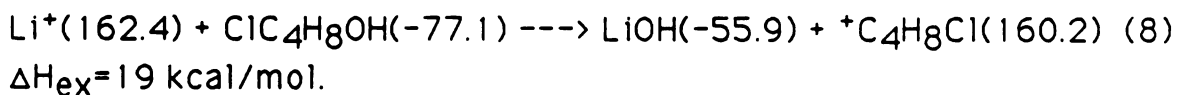
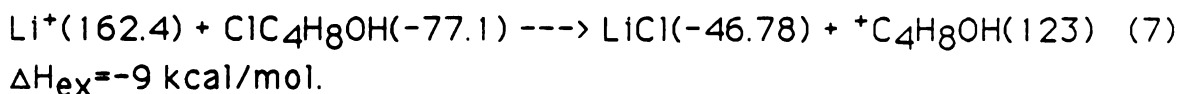
If the initial interaction occurs where the Li^+ is bound to the chlorine end of the molecule, then dehydrohalogenation will occur by transferring a functional group, charge building up on the halogenated carbon, hydrogen transfer to the chlorine, and product formation.

If, on the other hand, the initial interaction occurs where the Li^+ is bound to the hydroxide end of the molecule, then finally, with this compound, of the series studied, is the hydroxide affinity of Li^+ sufficiently large so that it can transfer a hydroxide from $\text{C}_4\text{H}_8\text{Cl}^+$. Recall also, that the reaction shuts down at this point since $(\text{CH}_2)_n\text{Cl}^+$, where $n=2$, and 3, can act as protonating agents and therefore, no reaction products are observed. Therefore, up until now, where $n=4$, the molecules reacted like their monofunctional analogs, the chloroalkanes. When $n=4$, this compound, $\text{C}_4\text{H}_8\text{Cl}^+$ is able to transfer a proton after the hydroxide group is transferred, such that the mechanism proceeds, and the loss of H_2O is observed. The product complex can now rearrange such that the following complex results:

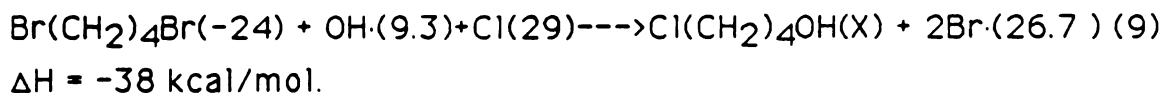


where the chlorine end of the molecule is complexed to the Li^+ . The reaction can now proceed as in the case of other alkyl halides reacting with Li^+ , to result in dehydrohalogenation of HCl to form a $\text{Li}^+(\text{butadiene})$ complex.

The ΔH_{ex} values are calculated for 1-chloro-4-butanol by reactions 7, and 8.



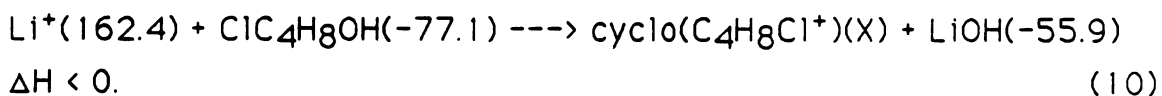
The $\Delta H_f(\text{ClC}_4\text{H}_8\text{OH})$ was estimated by reaction 9 as follows:



Therefore, it is assumed that, in order to calculate $\Delta H_f(\text{Cl}(\text{CH}_2)_4\text{OH})$, that the energy required to break two C-Br bonds needed to be considered, as well as the energy gained by forming a C-Cl, and a C-OH bond. In section k, equation 3, it was found that it requires 69.6 kcal/mol to break a C-Br bond. In section k, equation 2, that 83.8 kcal/mol of energy is gained upon the formation of a C-Cl bond. Also, in section, equation 3 it was calculated that 93.4 kcal/mol of energy is gained upon the formation of a C-OH bond. Therefore, by calculating the net energy of equation 9, the heat of the reaction is -38 kcal/mol. Therefore, the $\Delta H_f(\text{Cl}(\text{CH}_2)_4\text{OH}) = -77.1 \text{ kcal/mol}$.

Recall that the heat of exchange for isopropanol is 37 kcal/mol. Isopropanol is known not to react with Li^+ . However, t-butanol is known to react with Li^+ , and the heat of exchange for this reaction is 22 kcal/mol. Since reaction 8 has a ΔH_{ex} of 19 kcal/mol, and this value is less than the ΔH_{ex} value reported for t-butanol, 1-chloro-4-butanol can be expected to exhibit reactions from both functional groups.

Table 4 also suggests that Li^+ reacts with 1-chloro-4-butanol to form $\text{cyclo-C}_4\text{H}_8\text{Cl}^+$, as a minor product. In all other cases, when the halonium ions were formed, they were formed as a dominant product. Thus, it should be noted, that this product is probably due to an impurity reacting with Li^+ , instead of 1-chloro-4-butanol. In proof of this statement, the heat of formation can be calculated in reaction 10, for $\text{cyclo-C}_4\text{H}_8\text{Cl}^+$, in kcal/mol.

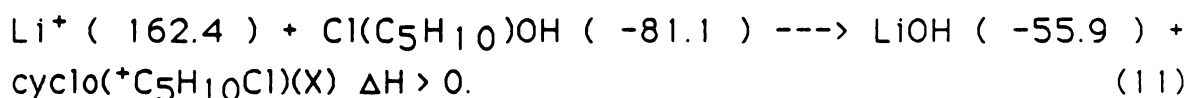


Reaction 10 implies that the $\Delta H_f(\text{cyclo-C}_4\text{H}_8\text{Cl}^+)$ is less than 141.2 kcal/mol. This value is low when compared to other ΔH_f values of

cyclo-(CH₂)_nCl⁺. This value is also not in agreement with a reported literature value of 160.3 kcal/mol. This latter value was calculated by theoretical MINDO calculations^{39,40}.

The same situation exists in the case of 1-chloro-5-pentanol reacting with Li⁺ as in the proceeding section, except, the loss of LiOH to form a cyclic((CH₂)₅Cl⁺) does not occur.

In section k, it was suggested, that the upper bound for the $\Delta H_f(\text{cyclo-C}_5\text{H}_{10}\text{Cl}^+)$ was less than 159.3 kcal/mol. Since the reaction to form this cyclic product is endothermic, a lower bound can be set by reaction 11 for the $\Delta H_f(\text{cyclo-C}_5\text{H}_{10}\text{Cl})$, as follows:



The $\Delta H_f(\text{Cl}(\text{CH}_2)_5\text{OH})$ was calculated in the same manner as described for the $\Delta H_f(\text{Cl}(\text{CH}_2)_4\text{OH})$. Therefore, the $\Delta H_f(\text{cyclo-C}_5\text{H}_{10}\text{Cl}^+)$ is greater than 137.2 kcal/mol. If the value is approximated to be midway between the two values suggested, we can suggest that the $\Delta H_f(\text{cyclo-C}_5\text{H}_{10}\text{Cl}^+)$ is 148 ± 11 kcal/mol. This value is in good agreement with a theoretical value of 151.7 kcal/mol provided by MINDO calculations^{39,40}.

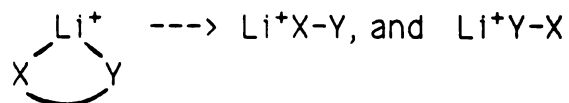
n. CONCLUSIONS

This work has shown that for the chloride, bromide, and hydroxide groups, α,ω -bifunctional alkanes show more chemistry than their monofunctional analogues.

For the monofunctional molecules, like the alcohols, and the haloalkanes, there is a transfer of the functional group, when the ΔH_{ex} is low. It was also observed that a sufficiently small value for ΔH_{ex} will also predict that the reaction E_b will be small such that the reaction can proceed. The next step involves the transferring of a proton. This steps occurrence is consistent with the proton affinity of LiX, where X=Cl, Br, and OH. If the P.A.(LiX) > P.A.(R-H) then products result from dehydrohalogenation, or dehydration.

For bifunctional molecules the initial interaction complex transfers a functional group. If this intermediate, $^+CH_2(CH_2)_nX$, where n=3, or 4, is sufficiently long-lived, it can take on a cyclic structure. If X=hydroxide, then the cyclic structure appears as a protonated cyclic ether, which can readily transfer a proton. The products that result are due to the loss of LiY, where Y= Cl, or Br. If X=halogen, then this cyclic structure can not readily transfer a proton, and this complex may dissociate to yield a cyclic organic ion that does not contain Li.

Preference for one of the functional groups over the other was always exhibited. This is not so difficult to imagine after so much emphasis was put on the initial interaction complex. It can be recalled, that the initial interaction of the molecule with Li^+ can involve both single, and multiple interactions as follows:



When X, and Y have similar affinities to Li^+ , for example, when X, and Y are chlorine, and bromine, then the equilibrium is shifted to the left. This complex will then dissociate to form the intermediate. However, when X, and Y are not similar for example, a halogen, and a hydroxide, then the equilibrium will be shifted to the right, and a preference for one functional group over another is definite.

If we further look at the early stages of a reaction involving bifunctional molecules with Li^+ , it can be found that the initial binding energy produced when an ion, and a molecule form a complex is important since it will help in predicting if reaction barriers can be overcome \times . Therefore, when a compound has two functional groups a large bonding energy is expected to Li^+ . This does not appear to be as important here in terms of increasing reactivity, as it is with transition metals, since the charge stays on the transition metal. In the case with the alkali ions, charge migration is the key component. Therefore, a second functional group provides stability to the cyclic halonium ion that is formed so a reaction can proceed.

APPENDICES

APPENDIX A

PROGRAM LISTINGS of SIRESS, DOUBRES, and SCANNER

The following contains a line by line explanation of the programs "siress", "doubres", and "scanner".

The purpose of the program "siress" is to add eight spectra collected repeatedly in an effort to increase the resolution, and the peak shapes. The spectra were displayed on the monitor to make sure that the spectrum being added were actually superimposable, and the experiment was functioning properly.

Listing of Siress

10-45 Dimensions all necessary variables.

50 This opens the file holding the MacAdios routine ("calls"). Also, communication is started between the Macintosh and the MacAdios.

60 This MacAdios call initializes four parameters for an internal digital synchronized signal.

70-80 These two lines wait for the analogue input to reach the desired voltage before the program proceeds.

90 Collects 9000 points in the array "specy". This is the first array collected, and the first array collected is always offset from later arrays collected, and therefore not utilized later.

120-150 Repeats 60-90, only the points are saved in an array "spec".

155 Plot displays the collected spectrum "spec" on the monitor. This is to insure that the arrays are not offset from one another, and that the program is functioning properly.

160-190 Repeats 60-90, only the points are saved in an array "spoc".

200 Displays the collected spectrum "spoc" on the monitor.

210 Add takes the points in the array "spec", and "spoc", and creates a new nine thousand point array in "spec".

220 This saves the array "spec" so that it can be viewed by MacManager.

230-260 Repeats 60-90. Collected data is stored in the array "spec".

270 A plot of "spocy" is displayed on the monitor.

280-310 Repeats 60-90. Data points are stored in the array "spac".

320 The contents of the array "spacy" is added to the data in the array "spac".

330 The data in the array "spacy" is added to the data in the array "spuc". and the resultant data is in the array "spuc".

340 The data in array "spuc" is added to the data in the array "spec", and the resultant data is in the array "spec".

Sires

```

10 DIM spec$(9000),specy$(9000):ar% = 0
20 DIM sires$(9000),specy$(9000)
30 DIM spec$(9000),specy$(9000),sires$(9000)
40 DIM spec$(9000),specy$(9000)
45 DIM spec$(9000),specy$(9000)
50 LIBRARY "MacAries Calls":CALL msmt
60 CALL msmt(254,254,1000,1)
70 CALL ewait (1,0,25)
80 CALL ewait(1,1,25)
90 CALL ewait(0,0,9000,VARPTR(ar%),VARPTR(spec$(0)),0,0,0,0,0,0)
120 CALL msmt(254,254,1000,1)
130 CALL ewait (1,0,25)
140 CALL ewait(1,1,25)
150 CALL sires(0,0,9000,VARPTR(ar%),VARPTR(spec$(0)),0,0,0,0,0,0)
155 CALL plot(0.20,220,60,VARPTR(spec$(0)),500,0,5000,10,2,1,0)
160 CALL msmt(254,254,1000,1)
170 CALL ewait (1,0,25)
180 CALL ewait(1,1,25)
190 CALL sires(0,0,9000,VARPTR(ar%),VARPTR(spec$(0)),0,0,0,0,0,0)
200 CALL plot(0.20,220,60,VARPTR(spec$(0)),500,0,5000,10,2,1,0)
210 CALL add (VARPTR(spec$(0)),VARPTR(spec$(0)),0,9000,0)
220 CALL bsave("SoftAries", "spec",VARPTR(spec$(0)),2,9000)
230 CALL msmt(254,254,1000,1)
240 CALL ewait (1,0,25)
250 CALL ewait(1,1,25)
260 CALL sires(0,0,9000,VARPTR(ar%),VARPTR(specy$(0)),0,0,0,0,0,0)
270 CALL plot(0.20,220,60,VARPTR(specy$(0)),500,0,5000,10,2,1,0)
280 CALL msmt(254,254,1000,1)
290 CALL ewait (1,0,25)
300 CALL ewait(1,1,25)
310 CALL sires(0,0,9000,VARPTR(ar%),VARPTR(spec$(0)),0,0,0,0,0,0)
320 CALL plot(0.20,220,60,VARPTR(spec$(0)),500,0,5000,10,2,1,0)
330 CALL add (VARPTR(spec$(0)),VARPTR(specy$(0)),0,9000,0)
340 CALL add (VARPTR(spec$(0)),VARPTR(spec$(0)),0,9000,0)
350 CALL bsave("SoftAries", "spec",VARPTR(spec$(0)),2,9000)
230 CALL msmt(254,254,1000,1)
240 CALL ewait (1,0,25)
250 CALL ewait(1,1,25)
260 CALL sires(0,0,9000,VARPTR(ar%),VARPTR(specy$(0)),0,0,0,0,0,0)
270 CALL plot(0.20,220,60,VARPTR(specy$(0)),500,0,5000,10,2,1,0)
280 CALL msmt(254,254,1000,1)
290 CALL ewait (1,0,25)
300 CALL ewait(1,1,25)
310 CALL sires(0,0,9000,VARPTR(ar%),VARPTR(spec$(0)),0,0,0,0,0,0)
320 CALL plot(0.20,220,60,VARPTR(spec$(0)),500,0,5000,10,2,1,0)
330 CALL add (VARPTR(spec$(0)),VARPTR(specy$(0)),0,9000,0)
340 CALL add (VARPTR(spec$(0)),VARPTR(spec$(0)),0,9000,0)
350 CALL bsave("SoftAries", "spec",VARPTR(spec$(0)),2,9000)
360 CALL msmt(254,254,1000,1)
370 CALL ewait (1,0,25)
380 CALL ewait(1,1,25)
390 CALL sires(0,0,9000,VARPTR(ar%),VARPTR(spec$(0)),0,0,0,0,0,0)
400 CALL plot(0.20,220,60,VARPTR(spec$(0)),500,0,5000,10,2,1,0)
410 CALL msmt(254,254,1000,1)
420 CALL ewait (1,0,25)
430 CALL ewait(1,1,25)
440 CALL sires(0,0,9000,VARPTR(ar%),VARPTR(specy$(0)),0,0,0,0,0,0)
450 CALL plot(0.20,220,60,VARPTR(specy$(0)),500,0,5000,10,2,1,0)
460 CALL add (VARPTR(spec$(0)),VARPTR(specy$(0)),0,9000,0)
470 CALL add (VARPTR(spec$(0)),VARPTR(spec$(0)),0,9000,0)
480 CALL bsave("SoftAries", "spec",VARPTR(spec$(0)),2,9000)
490 BEEP

```


This is a listing for the program "doubres".

Doubres is a double resonance program that takes a resultant spectrum, from two spectra that were added together, and subtracts it from the resultant irradiated spectra, obtained by adding two irradiated spectra, and displays the subtracted spectra. Spectra were added to increase the resolution of the spectra, and improve the peak shapes.

Listing of Doubres

10 Dimensions variables

20 Dimensions variables

30 Opens the file holding the MacAdios routines("calls"). Starts communication between the MacAdios and the Macintosh.

40 MacAdios call which initializes four parameters for an internal digital synchronized signal.

50 MacAdios calls which waits for the analogue input to reach the desired voltage before the program proceeds.

60 Repeats 50.

70 Nine thousand points are input into the array "specy". This is the first array collected, and it appears to be offset from arrays collected later, therefore, this array is not utilized.

80-110 Repeat of 40-70.

120 This command tells the Wavetek to turn on the rf power at the desired frequency so that double resonance can be conducted.

130-150 Same as 40-60.

160 Nine thousand points are collected in an array called "irrad." These points were collected when ions of a chosen frequency were being irradiated (i.e. ejected from the cell).

170 This command triggers the Wavetek to turn itself off so ions are no longer irradiated and only a single resonance spectrum is obtained.

180 The wave from the array "specy" is saved as "spec". This allows the array to be examined using the MacManager.

190 The wave from the array "irrad" is saved as "irrad". This allows the information to be examined using the MacManager.

200-220 Repeats 50-70, and the points are collected in the array "spacy". Since this array is offset from the others, this array is not saved or utilized when arrays are added.

230-260 Repeats 40-70, and the points are collected in the array "spac".

270 This command plots the array "spac" on the monitor. This insures that the data being collected are not offset from one another, and that the program is functioning properly.

280 This is a repeat of 120, where the Wavetek is triggered on to irradiate ions of a chosen frequency.

290-320 Repeats 40-70. The 9000 points collected as the ions of a designated frequency are placed in the array "irrid".

330 Plots the array "irrid" onto the screen.

340 Turns the Wavetek off so that ions are no longer irradiated.

350 This add command takes the points in the array "spec", and "spoc", and adds them together to make a new 9000 point array which will be "spec".

360 Adds the 9000 points in "irrad" to the 9000 points in "irrid" to make a new 9000 point array "irrad".

370 Bsave will save the array "spec" so that it can be examined by the graphics program in the MacManager.

380 Bsave will save the array "irrid" so that it can be viewed in MacManager.

390 Subi is a MacAdios call that will subtract two spectra. The spectrum obtained when the ions were irradiated "irrad" is subtracted from the single resonance spectrum "spec". The resultant spectrum is saved in the array "irrad".

400 Bsave will take the array irrad, and save it in an array "subby", which can be viewed by MacManager.

410 Signifies that the program has reached completion.

Doubres

```

10 DIM spec%(9000),irrad%(9000),specy%(9000),irrady%(9000),subby%(9000):er%=0
20 DIM spec%(9000),irrad%(9000),specy%(9000),irrady%(9000),addy%(9000)
30 LIBRARY "macAdios Calls":CALL mainit
40 CALL mainit(254,254,1000,1)
50 CALL await (1,0,25)
60 CALL await (1,1,25)
70 CALL ainx (0,0,9000,VARPTR(er%),VARPTR(specy%(0)),0,0,0,0,0,0,0)
80 CALL msinit(254,254,1000,1)
90 CALL await(1,0,25)
100 CALL await(1,1,25)
110 CALL ainx(0,0,9000,VARPTR(er%),VARPTR(spec%(0)),0,0,0,0,0,0,0)
120 CALL aout(0,0,5000,0)
130 CALL msinit(254,254,1000,1)
140 CALL await(1,0,25)
150 CALL await(1,1,25)
160 CALL ainx(0,0,9000,VARPTR(er%),VARPTR(irrad%(0)),0,0,0,0,0,0,0)
170 CALL aout(0,0,0,0)
180 CALL bsave("softadios","spec",VARPTR(spec%(0)),2,9000)
190 CALL bsave ("SoftAdios","irrad",VARPTR(irrad%(0)),2,9000)
200 CALL await(1,0,25)
210 CALL await(1,1,25)
220 CALL ainx(0,0,9000,VARPTR(er%),VARPTR(specy%(0)),0,0,0,0,0,0,0)
230 CALL msinit (254,254,1000,1)
240 CALL await(1,0,25)
250 CALL await(1,1,25)
260 CALL ainx(0,0,9000,VARPTR(er%),VARPTR(spec%(0)),0,0,0,0,0,0,0)
270 CALL plot(0,20,220,60,VARPTR(spec%(0)),500,0,5000,10,2,1,0)
280 CALL aout(0,0,5000,0)
290 CALL msinit(254,254,1000,1)
300 CALL await(1,0,25)
310 CALL await(1,1,25)
320 CALL ainx(0,0,9000,VARPTR(er%),VARPTR(irrad%(0)),0,0,0,0,0,0,0)
330 CALL plot(0,20,220,60,VARPTR(irrad%(0)),500,0,9000,10,2,1,0)
340 CALL aout(0,0,0,0)
350 CALL add(VARPTR(spec%(0)),VARPTR(spec%(0)),0,9000,0)
360 CALL add(VARPTR(irrad%(0)),VARPTR(irrad%(0)),0,9000,0)
370 CALL bsave("softadios","spec",VARPTR(spec%(0)),2,9000)
380 CALL bsave("softadios","irrad",VARPTR(irrad%(0)),2,9000)
390 CALL subi(VARPTR(irrad%(0)),VARPTR(spec%(0)),0,9000,0)
400 CALL bsave("softAdios","subby",VARPTR(irrad%(0)),2,9000)
410 BEEP

```

SCANNER Remarks:

- 1 Dimensions all necessary variables.
- 2 Opens the file holding the MacADIOS routines ("calls").
Starts communication between the MacADIOS and the Macintosh.
- 10 Starts the first loop which will collect 3150 data points. The ramp starts at negative value so that a more of the allowable output range is used.
- 20 At each step, 12 points are input into the array "spec%".
- 30 The counter value i% is multiplied by 4.88, so that the ramp is incremented by 1 step. This value for j% is output through aout0. The ramp is incremented as soon as possible after collecting data. This allows the maximum time for the ion signal to stabilize before data is collected. The aout command also sends a 5 volt signal out aout1, which is used to gate the Wavetek FG signal on. Then, 1101 is added to the counter value; k% will be used to label points in the array irradi%, which must have positive values.
- 40 The points in array spec%, are added together (integrated) and saved as x!, a single precision variable.
- 50 The current point of the array irradi% is loaded with x!.
- 60 Returns the loop to line 10.
- 70 Displays the first collected spectrum so that the user can see if things are working correctly.
- 100-160 Repeats the loop 10-60 exactly, with two exceptions. In line 130, the gate signal to the Wavetek is zero, so no double resonance rf voltage goes to the cell. Since the ions are not receiving double resonance, this spectrum is saved as noirrad%.
- 200-210 The two collected waves are convoluted by a step

- function, smooth%. This removes much of the undesired noise.
- 220 The convolution step also multiplies the signal, so this scaling step reduces the wave's values to the original, preconvoluted, values.
- 230 The waves are saved as irrado% and noirrado%. This allows the information to be examined using the Macintosh Manager.
- 240 Noirrado% is subtracted from the wave irrado% and the result is stored in the array irrado%.
- 250 The subtracted spectrum is saved as the array "back".
- 260 The beep alerts the user that the program is finished (almost).
- 270 This resets the ramp to the starting voltage and thus the Tektronix FG to the starting frequency.

SCANNER

```

1  DIM irrad%(3150),noirrad%(3150),irrado%(3150),noirrado%
    (3150),spec%(20),smooth%(5):x!=0:er%=0:smooth%(0)=1:
    smooth%(1)=1:smooth%(2)=1:smooth% (3)=1:smooth%(4)=1
2  LIBRARY "MacADIOS Calls": CALL mainit
10  FOR i%=-1101 TO 2047
20  CALL ainx(0,0,11,VARPTR(er%),VARPTR(spec%(0)),0,0,0,0,0,0)
30  j%=i%*4.88:CALL aout(j%,5000,0,0):k%=i%+1101
40  CALL integ(VARPTR(spec%(0)),1,11,VARPTR(x!),-2)
50  irrad%(k%)=x!
60  NEXT i%
70  CALL plot(0,20,220,60,VARPTR(irrad%(0)),1000,0,3150,10,2,1,)
110  FOR i%=-1101 TO 2047
120  CALL ainx(0,0,11,VARPTR(er%),VARPTR(spec%(0)),0,0,0,0,0,0)
130  j%=i%*4.88: CALL aout(j%,0,0,0):k%=i%+1101
140  CALL integ(VARPTR(spec%(0)),1,11,VARPTR(x!),-2)
150  noirrad%(k%)=x!
160  NEXT i%
200  CALL convolve(VARPTR(irrad%(0)),VARPTR(smooth%(0)),
    VARPTR(irrado%(0)),3130,3,0)
210  CALL convolve(VARPTR(noirrad%(0)),VARPTR(smooth%(0)),
    VARPTR(noirrado%(0)),3130,3,0)
220  CALL scale(VARPTR(irrado%(0)),3130,0,1,4,2):CALLscale
    (VARPTR(noirrado%(0)),3130,0,1,4,2)
230  CALL bsave("ICDR","irrad",VARPTR(irrado%(0)),2,6280):
    CALL bsave("ICDR","noirrad",VARPTR(noirrado%(0)),2,6280)
240  CALL subi(VARPTR(irrado%(0)),
    VARPTR(noirrado%(0)),0,6280,0)
250  CALL bsave("ICDR","back",VARPTR(irrado%(0)),2,6280)
260  BEEP
270  CALL aout(-5372,0,0,0)

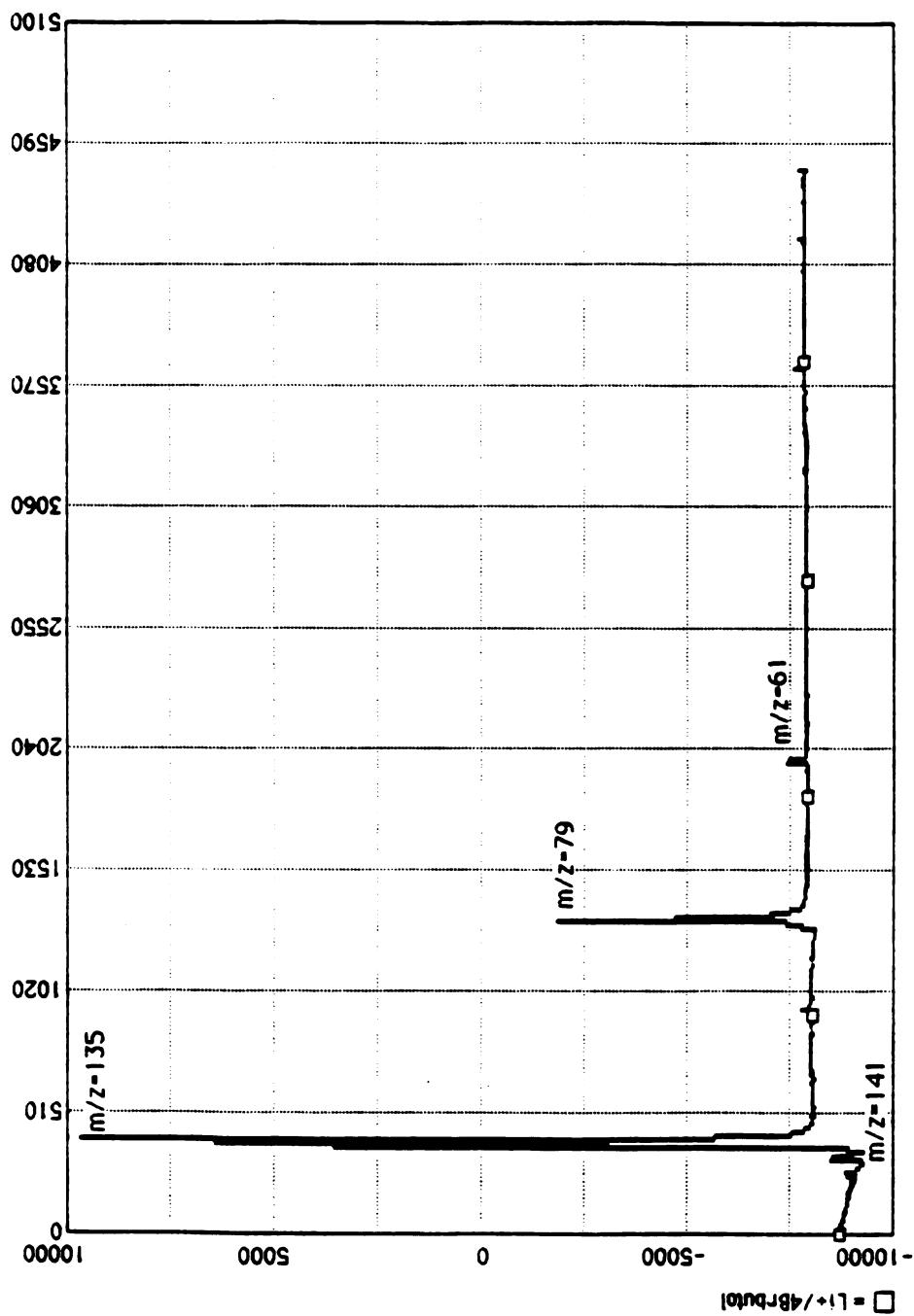
```

APPENDIX B

BRANCHING RATIOS

The following is an example to show how the branching ratios provided in Table 4 were calculated. The example chosen is Li^+ reacting with 4-bromo-1-butanol. The products resulting from this reaction was due to the loss of HBr, H_2O , LiOH, and (HBr + H_2O). Refer to Table 4, and the spectra provided in Figure 30 for more details.

When calculating the branching ratios, only product ions and their isotopes are considered. Parent ions, and reactant ions are ignored. Therefore, $m/z=61$, $m/z=79$, $m/z=135$, and $m/z=141$ as well as their isotopes were of interest in calculating the branching ratios for this example. The next step is to add the heights for all of the peaks of interest. To do this, I used the change in intensity from the top of a peak to the baseline for all peaks under consideration. This step was done on the computer where the graph could be amplified to obtain exact readings. The total intensity was found to be 33,350. The relative amount of $m/z=61$ can be obtained by adding the

Figure 30 Spectra of Li^+ and 4-bromo-1-butanol

intensity of this peak, and its isotope. This value was found to be 667. To calculate the branching ratio relative to 100%, the following equation was used: $(33,350/100\%)=(667/X\%)$. This calculation showed that $m/z=61$ was 2% of the total products formed. The same procedure is repeated for the other three product ions. The results can be found tabulated in Table 4.

APPENDIX C

COMPILATION of HEATS of FORMATION

Formula	ΔH_f (kcal/mol)	Reference
Li ⁺	162.4	35
OH ⁻	-32.7	35
OH	9.3	35
HOH	-57.8	35
Br ⁻	-50.9	35
H ⁺	365.7	35
Cl ⁻	-54.3	35
LiOH	-55.9	42
LiBr	-36.8	42
LiCl	-46.7	42
HCl	-22.1	35
Cl·	29.0	35
HBr	-9.0	35
Br·	26.7	35
C ₂ H ₅	28.0	35
C ₂ H ₄ Cl ⁺	204.0	35
C ₂ H ₄ Br ⁺	207.1	35
C ₂ H ₃ Br	-18.9	35

C_2H_3Cl	5.0	35
C_2H_5Cl	-26.8	35
C_2H_5Br	-14.9	35
C_2H_5OH	-56.1	35
ClC_2H_4OH	-62.0	35
ClC_2H_4Br	-21.0	35
$+C_2H_4OH$	165.0	35
$+CH_2CHOH_2$	148.0	35
CH_3CH^+OH	139.0	35
$C_2H_5O^+$	165.0	35
C_3H_6	4.8	35
$i-C_3H_7Br$	-23.4	35
$i-C_3H_7Cl$	-34.6	35
$C_3H_5Br^+$	>210.8	eqn. 23, Sect. k
$C_3H_6Br^+$	210.8	35
BrC_3H_6Br	-17	35
ClC_3H_6Br	-28.9	35
C_4H_8	-0.1	35
$n-C_4H_9Br$	-25.9	35
C_4H_6	38.7	42
$n-C_4H_9Cl$	-36.9	35
$+C_4H_8OH$	123.0	35
BrC_4H_8Br	-24.0	35
$+C_4H_8Cl$	160.2	35
$t-C_4H_9Br$	-32.0	35

i-C ₄ H ₉ ⁺	165.8	35
BrC ₄ H ₈ Br	-24.0	35
BrC ₅ H ₁₀	-28.0	35
ClC ₅ H ₁₀ OH	-81.1	35
C ₄ H ₇ Cl	10.4	Eqn. 13, Sect. k
C ₄ H ₇ Br	-.9	Eqn. 14, Sect. k
(cyclo- ⁺ C ₄ H ₈ Cl)	160.3	39
(cyclo- ⁺ C ₄ H ₈ Br)	160.5	Eqn. 4, Sect. k
(cyclo- ⁺ C ₅ H ₁₀ Cl)	151.7	39,40
BrC ₃ H ₆ OH	-58.2	Eqn. 4, Sect. l
(cyclo- ⁺ C ₃ H ₆ Br)	>180.3	Eqn. 7, Sect. l
t-C ₄ H ₈ OH	-74.7	35
i-C ₄ H ₉ ⁺	165.8	35
LiC ₄ H ₇ Br ⁺	<148.6	Eqn. 10, Sect. k
LiC ₄ H ₇ Cl ⁺	<135.5	Eqn. 8, Sect. k
ClC ₄ H ₈ OH	-77.1	Eqn. 9, Sect. m
ClC ₄ H ₈ Br	-35.9	Eqn. 1, Sect. k
BrC ₄ H ₈ OH	-65.2	Eqn. 8, Sect. l
(cyclo- ⁺ C ₅ H ₁₀ Br)	<169.5	Eqn. 17, Sect. k
ClC ₅ H ₁₀ Br	-39.9	Eqn. 16, Sect. k

APPENDIX D

ICR OPERATING MANUAL

This information is a brief description of the electronic components of the ICR at MSU. The parameters that the units are typically operated at are also provided.

Magnet The Varian Field dial magnet control can be operated either in a sweep mode, or at a constant field. Normal operation of the magnet is at a constant field of 18.80 kG. The magnet has a range of 0 to 23kG. The magnet is cooled from distilled water by a Haskris heat exchanger. The power supply to the magnet is also water cooled.

Magnet Power Supply The V-7X00/E-7X00 regulated Magnet Power Supplies are designed for spectrometers requiring stable magnetic fields. The supply delivers controlled dc power into a 1-ohm load such as a V-7000 electromagnet. The magnetic field is indicated in kilogauss by the field-set controls. This power supply is water cooled, and can be regulated to within 1 ppm of the set field or 5 mG.

The field ranges applicable with this power supply range from 0 kG to 23 kG.

Haskris Heat Exchanger The heat exchanger is used to cool the magnet and its power supply. The magnet system is tap water cooled, and normally operates in the temperature range of 16° to 27°C.

Emission Current Controller This unit controls the amount of current that passes through the filament, or the emitter, which are used for ionization.

When operating with the filament, the front panel bias connector is provided so the filament may be floated to 100V dc off ground. Generally, this current controller is run on "EM" mode which constantly monitors the amount of current that is being generated, by means of a feedback circuit. Current information is sent to the Keithley picoammeter which puts out a voltage proportional to this current, and sends a voltage to the back of the current controller. This feedback circuit insures that a constant current is being supplied to the filament. The initial amount of current applied to the filament wire is controlled by a current knob. The current dialed in can be read from the meter above the knob. On "FIL" mode, there is no longer a feedback process occurring. Instead, current is sent to the ionizing filament but the amount, and whether it remains constant is unknown. Prior to operating this unit, the picoammeter,

the magnet and its power supply, and the heat exchanger must first be operating. The filament switch located on the little box needs to be turned on, as well as the switch on the current controller panel. The picoammeter should now read .3 on the 100 μ A scale. The current knob is then turned to the amount of current, required to heat the filament to generate electrons, which is generally 1-3 amperes. If the current knob is turned and the current remains at zero, this indicates that the filament is burned out and is unable to allow the current to flow. If this scenario occurs it should be replaced.

This panel is also used to control the amount of current that is passed through the emitter. Generally .9-2.5 Amperes is sufficient current to heat the emitter and observe the alkali ion of the emitter employed. When the emitter is operated, the switch is placed on "Fil" mode, instead of "EM" mode. Also, with the emitter, the bias needs to be slightly positive, and generally 0-4 volts of bias voltage is enough voltage to cause the alkali ions to come off the emitter.

Little Box This box is located on top of the vacuum feedthrough, between the polecaps of the magnet. The filament on/off switch is mounted on the outside of this box. Coming into this box are the voltages to manipulate the eight plates of the cell, the second frequency source to do double resonance experiments, and the filament current. Also, the emission current obtained from the electron collector is measured here.

This box is also used to pass current through the alkali emitter, which results in the formation of alkali ions.

Textronix PG 505 Pulse Generator This unit functions to provide -70 volts to the emission current controller bias. This occurs when the unit is operated in the "locked on" mode, while the filament is used. Also, The pulse generator provides approximately 0-5 Volts to the emission current controller bias, when the emitter is operated.

Textronix FG 504 40MHz Function Generator This unit provides the means to conduct a frequency sweep over a specified range. The frequency range chosen is related to the mass range of interest, and can be set with the start and stop knobs on the frequency dial. A typical frequency range is .073 kHz to .73 kHz which corresponds to a mass range of 39 a.m.u. to 394 a.m.u. at a field of 18.80 kG. The rf output is sent to a 503 counter and to an rf attenuator. This function generator puts out a 10 V ramp from the "lin sweep output", which is sent to channel B of the oscilloscope to drive the horizontal axis. Each frequency sweep corresponds to 1 ramp. To insure that the frequency scan always starts at the same spot for the data being acquired by the computer, a voltage of .025 volts from the linear sweep output is used to trigger the computer to start collecting data. Also, "trig output" is used as a frequency reference for the phase sensitive detector by putting out a 0-5 V square wave that is 90° shifted from the rf signal. This 90° phase shift helps account for the phase shift in the bridge detector's components.

Textronix DC 503 Universal Counter The counter will display the frequency sweep of the rf signal that is provided by the 504 function generator.

Radio Frequency Attenuator This module acts like a voltage divider. It reduces the rf signal being output from the function generator. Normally, a scan speed of .1s (i.e. the speed used for viewing the scan on the oscilloscope) requires -25 db's to maximize the signal's size. When the scan speed is slowed to 10 s (i.e. the speed used for data collection) more power needs to be taken out and generally -35 to -45 db's prove useful. The attenuation should be checked and set each time a spectrum is collected to maximize the spectrum.

Signal Summer This unit takes an rf signal and splits it into two sine waves of equal intensity, and 180° phase shifted. One of these components is sent to the excitation plates of the ICR cell, and the other signal is sent to the balance capacitor to serve as a reference.

Balance Capacitor The capacitance of the balance capacitor should equal that of the ICR's analyzer plates. When this is maladjusted, the baseline observed on the oscilloscope is non-linear. Since the balance capacitor is made up of high quality tunable capacitors the problem of a non-linear baseline is easily adjusted by tuning the capacitors until the baseline is straight. The capacitance of this unit is approximately .047 picofarads. The balance capacitor can be

found mounted on a "T" BNC to the vacuum flange that houses the cell. The vacuum side is attached to the drift bottom analyzer plate and the top is hooked to the signal summer and the preamplifier.

Preamplifier This amplifier, as well as its power supply, is part of the detection system. The preamplifier receives the d.c. bias voltage from the drift bottom analyzer, and the signal. To the incoming signal, the preamplifier provides an amplification of 101 times, and then sends this signal to the detector.

Phase Sensitive Detector This part of the detection system takes the ion signal from the preamplifier, and compares it to the reference square wave that it obtains from the 504 function generator. If the PSD receives an out of phase signal when compared with the reference this signal is rejected. The switch on the outside of the box can either be set to TTL or 50 ohms.

Keithley Electrometer This serves as a voltage amplifier for the signal coming out of the phase sensitive detector. This is typically set on .1 with the gain dial and "Volts" on the main dial. To prevent the needle from obtaining any damage, the meter is left off, but the power remains on.

Oscilloscope When a fast scan speed of .1 seconds is provided by the function generator, the resultant spectrum is displayed on the oscilloscope. Channel A's input is the ion signal from the Keithley

Electrometer. Channel B's input is the 15 volt ramp from the function generator's "lin sweep output".

Buffer An LF 356 op-amp serves as a buffer to prevent feedback from the MacAdios that occurs when data is analyzed. The buffer is located on the control panel, between the MacAdios, and the Keithley Amplifier.

Filter This homemade device is a low-pass RC filter designed to filter out high frequency noise that is generated from the amplifier. It is composed of a 100 k Ω resistor, and a 10⁴ picofarad capacitor.

Wavetek 144 Function Generator This provides a second rf source required to do double resonance experiments. This rf signal is sent from the 50 Ω output to the source region of the ICR's cell. Typical operating parameters have the frequency set to 100 kHz, the mode is on gated, the signal source is set to the sine wave, and the output attenuation is set to -20 db's. This unit also allows for the determination of the masses of ions of interest. The frequency dial can be changed until the frequency indicator, a blip, lines up with the ion of interest. Since the frequency can then be known exactly, the mass can be determined.

Control Panel This homebuilt unit provides the means to manipulate the voltages applied to the eight plates of the ICR cell, as well as the sign (+,-) of the plate.

MacAdios 411 This digital to analog converter is used for data acquisition and control. This unit communicates with a Macintosh Computer via a 500,000 bit per second serial link to the MODEM port. This converter contains many input and output connectors to facilitate data collection. Programs can either be written in C, MicroSoft Basic, or MacAdios Manager. When data is being acquired the "tsfr" light flashes. Looking to observe that this light is flashing is a helpful indication as to whether data is actually being collected, or if something is malfunctioning.

Macintosh Plus Computer This computer is compatible with the MacAdios, and is a powerful, graphics-oriented workstation which when combined with the MacAdios provides a useful laboratory tool.

LIST OF REFERENCES

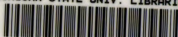
LIST OF REFERENCES

1. H. Sommer, H. A. Thomas, and J. A. Hipple, *Phy. Rev.* 82, 697 (1975).
2. J. L. Beauchamp, *Ann. Rev. Phys. Chem.* 22, 527 (1971).
3. G. C. Goode, R. M. O'Malley, A. J. Ferrer-Correia, and K. R. Jennings, *Nature* 227, 1093 (1970).
4. J. D. Baldeschwieler and S. S. Woodgate, *Acc. Chem. Rev.*, 4, 114, (1971).
5. K. P. Wanczek, *Int. J. Mass Spectrom. Ion Proc.*, 60, 11 (1984).
6. G. C. Goode, R. M. O'Malley, A. J. Ferrer-Correia, and K. R. Jennings, *Adv. Mass Spectrom.*, 5, 195 (1971).
7. T. C. O'Haver, *J. Chem. Educ.* 49,A131 (1972).
8. *Ann. Rev. Chem.*, 22, 527 (1971).
9. A. Tsarbopoulos and J. Allison *Organometallics* 1984, 3 (1986).
10. J. Allison and D. P. Ridge, *J. Am. Chem. Soc.* 101, 4998 (1979).
11. R. M. Stepnowski, Ph.D. Thesis, Michigan State University (1988).
12. D.C. Hartman, and J.S. Winn, *J.Chem. Phys.*, 68, 2990 (1978).

13. T.A. Lehman, and M.M. Bursy, "Ion Cyclotron Resonance Spectroscopy," 1 (1976).
14. C. J. Cassady, B. S. Freiser, S. W. McElvany and J. Allison, *J. Am. Chem. Soc.*, 106, 6125 (1984).
15. J. Allison and D. P. Ridge, *J. Am. Chem. Soc.*, 101, 4998 (1979).
16. J. Allison and D. P. Ridge, *J. Am. Chem. Soc.*, 7445 (1979).
17. R. L. Woodlin and J. L. Beauchamp, *J. Am. Chem. Soc.*, 100, 5 (1978).
18. R. D. Wieting, R. H. Staley, and J. L. Beauchamp, *J. Am. Chem. Soc.*, 97, 924 (1975).
19. G. H. Weddle, J. Allison, and D. P. Ridge, *J. Am. Chem. Soc.*, 99, 105 (1977).
20. I. Dzidic and P. Kebarle, *J. Phys. Chem.*, 74, 1466 (1970).
21. B. S. Freiser, R. H. Staley, and J. L. Beauchamp, *Chem. Phys. Lett.*, 39, 49 (1976).
22. G. D. Miller and S. A. Safron, *J. Chem. Phys.*, 64, 5065 (1976).
23. R. H. Staley and J. L. Beauchamp, *J. Am. Chem. Soc.*, 97, 5920 (1975).
24. R. H. Staley and R. D. Wieting, and J. L. Beauchamp, *J. Am. Chem. Soc.*, 99, 5964 (1977).
25. S. A. Safron, G. D. Miller, F. A. Rideout, and R. C. Howat, *J. Chem. Phys.*, 64, 5051 (1976).
26. J. Allison, Ph.D. Thesis, University of Delaware (1978).
27. Lit Mass spec
28. R.V. Hodges, P.B. Armentrout, and J.L. Beauchamp, *Int. J. Mass. Spectrom. Ion. Phys.*, 29, 375 (1979).
29. M.M. Kappes, and R.H. Staley, *J. Phys. Chem.*, 85, 942 (1981).

30. J.A. Rutherford, and D.A. Vroom, *J. Chem. Phys.*, 65, 4445 (1976).
31. J.S. Uppal, and R.H. Staley, *J. Am. Chem. Soc.*, 104, 1229 (1982).
32. J.B. Schilling, and J.L. Beauchamp, *J. Am. Chem. Soc.*, 110, 15 (1988).
33. W.R. Creasy, and J.M. Farrar, *J. Chem. Phys.*, 87, (9), 5280 (1987).
34. R.G. Keesee, and A.W. Castleman Jr., *J. Phys. Chem.*, 15, 1011 (1988).
35. S. G. Lias, J. E. Bartmess, J. F. Liebman, J. L. Holmes, R. D. Levin and W.G. Mallard, *J. Phys. Chem. Ref. Data*, Vol. 17, Suppl. 1 (1988).
36. J.L. Franklin, J.G. Dillard, H.M. Rosenstock, J.T. Herron, K. Draxl, and F.H. Field, Ionization Potentials, Appearance Potentials, and Heats of Formation of Gaseous Positive Ions, NSRDS-NBS, 26, National Bureau of Standards, Washington, D.C. (1969).
37. W.R. Creasy, and J.M. Farrar, *J. Chem. Phys.*, 89, 3952 (1985).
38. W.R. Creasy, and J.M. Farrar, *J. Chem. Phys.*, 85, 162 (1986).
39. S.P. McManus, S.D. Worley, *Tet. Lett.*, 6, 555 (1977).
40. S.D. Beatty, S.D. Worley, S.P. McManus, *J. Am. Chem. Soc.*, 100, 4254 (1978).
41. W.J. Hehre, and D.C. Hiberty, *J. Am. Chem. Soc.*, 96, 2665, (1974).
42. M.W. Chase, Jr., C.A. Davies, J.R. Downey, Jr., D.J. Erurip, R.A. McDonald, A.N. 5, *J. Phys. Chem. Ref. Data* 14, Suppl #1, (1985), JANAF Thermochemical Tables, Third Ed.

MICHIGAN STATE UNIV. LIBRARIES



31293008973178